RUSSIAN GEOGRAPHICAL SOCIETY

FACULTY OF GEOGRAPHY,
LOMONOSOV MOSCOW STATE UNIVERSITY

INSTITUTE OF GEOGRAPHY,
RUSSIAN ACADEMY OF SCIENCE

Vol. 11 2018 No. 03

GEOGRAPHY ENVIRONMENT SUSTAINABILITY

EDITORIAL BOARD

CONTENTS

CONTENTS

SUSTAINABILITY

Aleksey Yu. Sidorchuk[1]
[1]Faculty of Geography, Lomonosov Moscow State University, Moscow, Russia
*** Corresponding author:** fluvial05@gmail.com

THE FLUVIAL SYSTEM ON THE EAST EUROPEAN PLAIN: SEDIMENT SOURCE AND SINK

ABSTRACT. The modern fluvial system on the lowland East European Plain is of depositional type. Sediment transport to the seas is only a few percent of the total erosion, and the main part of eroded material is accumulated in the channels. The recent deposition of suspended sediments is caused by accelerated soil erosion on the arable slopes, which led to a high rate of lateral sediment input and deposition at the river headwaters and on the floodplains. The process of accumulation is facilitated by the unfilled "negative" volume of the net of dry valleys formed during the Late Glacial catastrophic erosion event. Such events of catastrophic erosion of the sediments deposited in the lowland fluvial systems occur with a frequency of 100-120 thousand years. In the conditions of both scarce vegetation and extremal surface runoff, the entire fluvial systems become the area of intensive erosion, with the deep incision of gullies and of the river channels. Therefore, despite the modern intensive deposition, delivery ratio for the fluvial systems on this lowland territory is close to one in the long-term perspective.

KEY WORDS: The fluvial system, delivery ratio, recent accelerated erosion, sediment deposition, Late Glacial catastrophic erosion event, East European Plain

CITATION: Aleksey Yu. Sidorchuk (2018) The fluvial system on the East European plain: sediment source and sink. Geography, Environment, Sustainability, Vol.11, No 3, p. 5-20
DOI-10.24057/2071-9388-2018-11-3-05-20

INTRODUCTION

A fluvial system is the cascade of connected or disconnected linear depressions (channels) with catchments, formed by modern and ancient water flows, having long history of morphological evolution (Makkaveev 1955; Schumm 1977). These flows, generally directed by the gravity force from upper to lower reaches, interact with the surface layer of the lithosphere, being one of the main denudation agents.

The erosion and deposition in the fluvial systems are well investigated (Gregory and Walling 1976; Schumm 1977; Meade 1996 etc.). Erosion by water produces sediments – particles of different size and weight. These sediments can be transported through the fluvial system only when and where transport capacity of the flow is higher than sediment load. The ability of the fluvial system to deliver sediments to the lowermost point is well described by the ratio between the amount of sediments arriving at the outlet of a fluvial system and the total eroded sediments within the catchment, i.e. delivery ratio *Dr*. The fluvial system can be of erosive type, when delivery ratio is high and of depositional type, with low delivery ratio. The boundary can be appointed at *Dr*=50% (Sidorchuk 2015).

The modern global fluvial system delivers annually to ocean and internal seas about 19 10^9 ton of sediment particles (Milliman and Farnsworth 2011). This is only a part of the global relief destruction by erosion. Annual soil erosion by water only from the global farmland (about 10% of the global terrestrial area) is estimated in a broad range from 172.1 10^9 (Ito 2007) to 22.2 10^9 ton (van Oost et al. 2007). In any case, the modern global delivery ratio is lower than one, and sediment sink in the fluvial systems (mostly at the lowlands) is one of the significant geomorphological processes. The alluvial and non-alluvial sediments, deposited in the fluvial systems, together with channel morphology, represent the memory of the system (Knighton 1984).

The Late Glacial period was characterized by extremal surface runoff, typical at least for the Northern Hemisphere (Dury 1965; Volkov 1963; Sidorchuk 2003). However, for this period the type of the fluvial systems on the lowlands, erosional or depositional. is not well investigated. The main goal of this paper is to show the differences, as well as the similarities, in the processes of the fluvial systems on the East European plain during these two highly contrasting periods of erosion: the period, dominated by human-induced accelerated erosion, lasted about 300 years, and the Late-glacial period about 2-3 thousand years long, with the natural extremal erosion.

The rivers of the East European Plain

The East European plain is a large lowland covering an area of about 4.0 10^6 km^2 (Alayev et al. 1990). The largest European rivers: Volga, Don, Dnieper, drain its southern megaslopes. The headwaters of these rivers on the main water-divide of the plain have maximum altitudes of about 250-300 m. Therefore, the inclinations of the main rivers 1900-2700 km long are not more than 0.13-0.14$‰_0$. The inclinations and lengths of river basin slopes vary in the broad range with highly negatively asymmetrical distributions. The multiple values of the *LS* factor of USLE (Wischmeier and Smith 1978), calculated on the field scale using slope length and inclination, are typically less than 7 with 80% in the range of 0.1-1.0 (see Fig. 2.14 in Litvin 2002).

The drainage density of the modern permanent rivers and streams with the length more than 1 km on the southern megaslope of the East European plain is 0.36 km/km^2: 150717 rivers totally 574414 km long belong to the Volga River basin (1360000 km^2), 13012 rivers totally 90416 km long belong to the Don River basin (422000 km^2) and 31954 rivers totally 163467 km long belong to the Dnieper River basin (504000 km^2) (Domanitskiy et al. 1971). This is only the part of the fluvial system within the study area. The net of dry valleys with a density of 0.4-0.6 km/km^2 dominates the physiography of the erosion landscape (Fig. 1). These dry valleys (called "balka" or "sukhodol") typically have lengths of 1-10 km. These systems drain water mostly during snow thaw period or after intensive rain. Dense vegetation usually cover their bottoms and slopes, so the modern erosion here is negligible in the pristine conditions. The bottom width of dry valleys is much larger than the width of the flows in these valleys, and the ratio of these two width increases with basin area decrease. The same effect is typical for small and median river valleys. Dokuchaev (1878) was the first describing this phenomenon and addressing it to the history of fluvial system evolution.

The Late-glacial period of extreme erosion

Climate-induced episodes of accelerated erosion occurred repeatedly during periods of deglaciation of the continental ice-sheets (Vandenberghe 1995). The large rivers of the Late Glacial time were formed during these episodes of high surface runoff and were first described by G. Dury (1965) and I. Volkov (1963). The reconstructed mean annual surface runoff was 2-4 times greater on the East European plain for the Late Glacial time about 16-18 ka ago, and the maximum discharges were 5-6 times greater (Sidorchuk et al. 2001, 2008). The river channels were then wider than the modern ones, long and deep gullies dissected slopes of the valleys, and the permanent watercourse net was

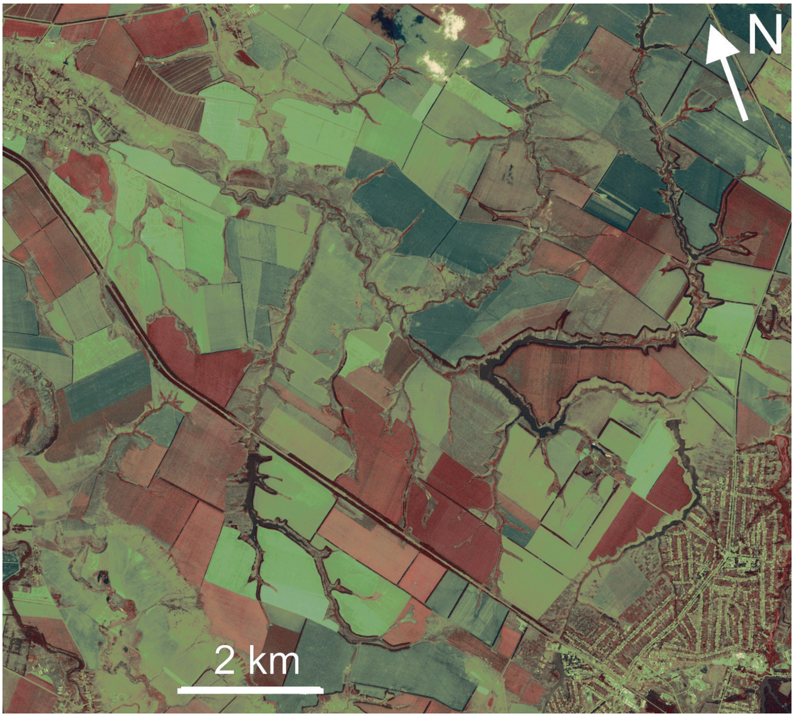

Fig. 1. The dry valley net at the Khoper River basin. The part of SPOT image ID 5 119-246 07/07/30 08:26:01 2 J, central point lat. 51.5° N, lon. 41.92° E (provided by MSU Geoportal)

much denser. The volume of the linear erosion during this geologically rather short episode (2-3 thousand years) was extremely high.

For example, the Khoper River basin (the tributary of the Don River) with an area of 61,100 km^2 has a recent total length of the permanent flows and dry valleys of 36,000 km. The permanent river net (267 rivers with the total length of 9000 km) consists of the streams equal and more than 10 km long. The dry valleys (some of them with permanent springs) are shorter than app. 10 km length and form the erosion net with a total length of 27000 km, which dissects the basin slopes.

The "negative" volume of these dry valleys can be estimated from the valley volumes with known number of the valleys. The negative volume of a dry valley V_b (km^3) depends on its length L (km) and the difference between the upper and lower points of its longitudinal profile H_0 (km). Measurements in the Khoper River basin led to the relationship:

$$V_b = 0.007 H_0 L^2 \quad (1)$$

H_0 vary in the Khoper River basin in the range of 20 to 85 m with a mean value of 45 m.

The number of dry valleys with the length less than 10 km can be estimated from the data on the structure of the fluvial network. This structure is well described by the magnitude – frequency function (Fig. 2). It is convenient to use the length of the dry valley L as the magnitude, and the sum of the lengths of the valleys ΣL with the length greater than $\boldsymbol{L}$ as the frequency:

$$\sum L = ML^{1-D} \quad (2)$$

The variables in formula (2) correspond to the terms of the fractal approach. The exponent D can be called the fractal dimension of the valley network, and the coefficient M is a measure of the structure of the network, equal to the total length of all valleys with the length more than 1 km. The formula (2) is empirical and dimensional. therefore all lengths in formulas (1)-(6) are in the same units (km).

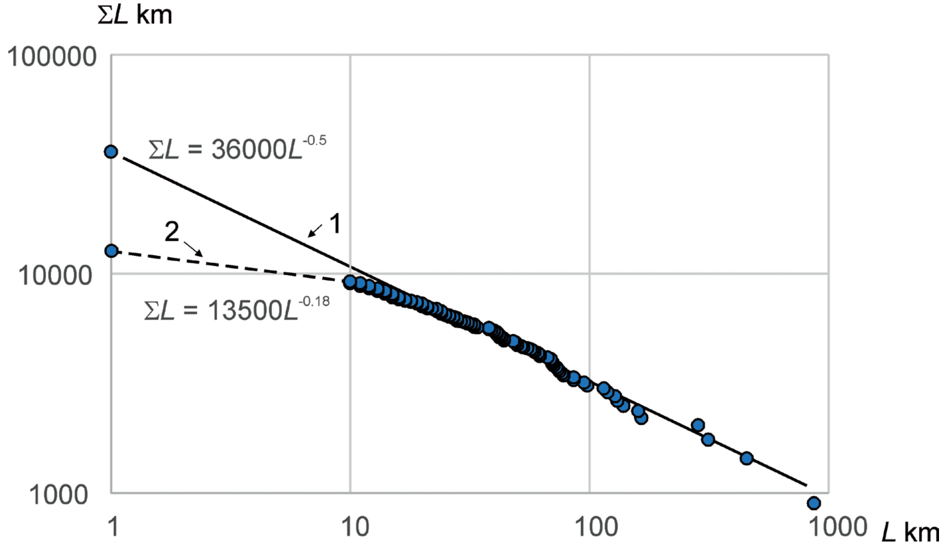

Fig. 2. The relationship between the stream length *L* and total length Σ*L* of the streams, equal and longer than *L*. Key: 1 – the relationship for the recent streams ≥10 km long and the Late Glacial streams <10 km long.; 2 – the relationship for the recent streams <10 km long

To estimate the number of dry valleys $N_{\Delta L}$ in a given range of length ΔL for a certain *j*-th catchment area, it is necessary to construct a regional function (2) in the differential form:

$$N_{\Delta L} = \frac{\Delta \sum L}{L_{0mean}} = M_j(1-D_j)L_{0mean}^{-1-D}\Delta L \quad (3)$$

In this formula M_j is regional total length of the network of streams more than 1 km long, D_j is regional fractal dimension, L_{0mean} is the length of a dry valley $(2L_0 + \Delta L)/2$. Since the fractal dimension can be calculated with sufficient accuracy only for a limited number of catchments, the linear relationship was obtained between the fractal dimension and the density *K* (km km^{-2}) of the entire network of streams:

$$(D-1) = 0.89K \quad (4)$$

The regional M_j value can be calculated with the region area F_j (km^2) and the network density K_j (km km^{-2}):

$$M_j = aK_jF_j \quad (5)$$

Here the coefficient a is equal to 1 and was used to keep dimension of *M* (km^D). The total volume *V* of the dry valley network for each region in the Khoper River basin is calculated by the formula

$$V = \sum_{L=1}^{L=10} N_{\Delta L} V_b \quad (6)$$

The regions with similar density of the stream net K_j and similar dry valley relief H_0 in the Khoper River basin were identified on the map «Erosion hazard in the territory of the USSR» compiled in the Institute of Geography of the Russian Academy of Science. The volume of the dry valleys with the lengths of 1-10 km was calculated for each region and for the entire basin with formulas (1-6). In the basin of the Khoper River, the total recent "negative" volume of the dry valleys is 24 km^3.

During the period of extremal surface runoff 16-18 ka ago all valleys, that are now dry, were deep intensively eroded gullies (Eremenko and Panin 2011). In average they were about 30% deeper compared to the modern erosional forms (Fig. 3). The total "negative" volume of the ancient gully erosion at the Khoper River basin, according Eq. 2-4 was then about 31 km^3.

The main rivers were also over-deepened during this extreme surface runoff episode along the total length of their channels.

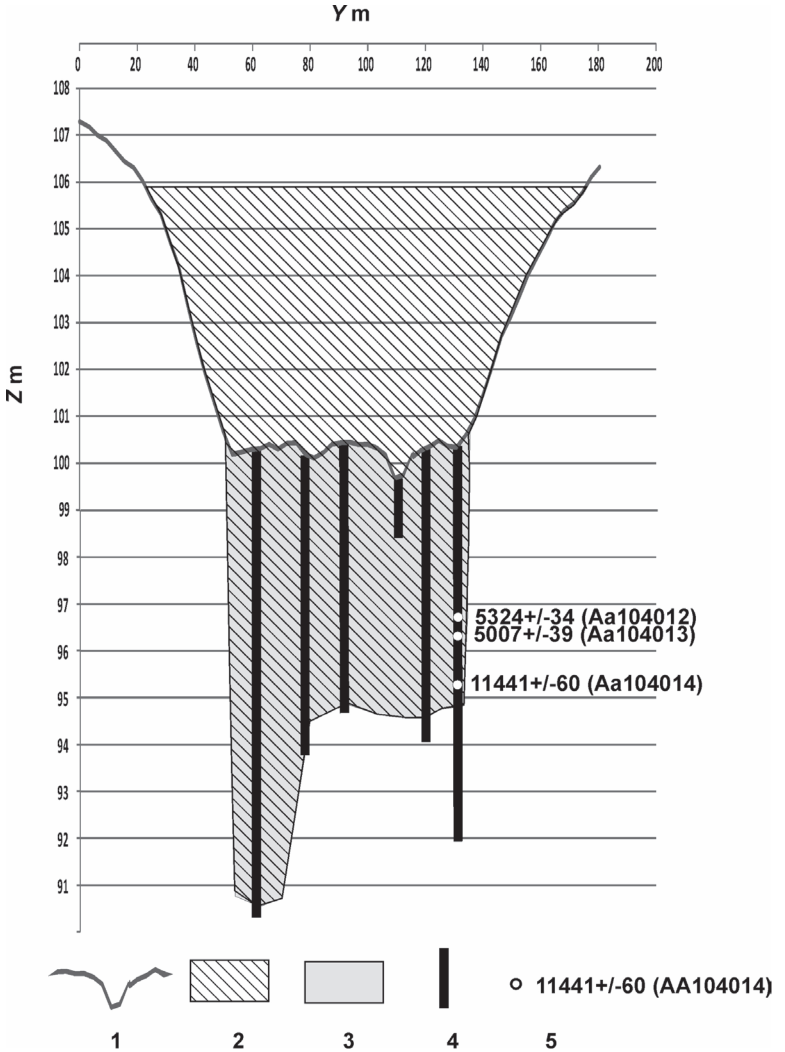

Fig. 3. The cross-section of Perepol'ye dry valley (the Khoper River basin, lat. 51.2° N, lon. 42.32° E), cored by the author and his colleagues in 1997. Key: 1 – the recent dry valley bed; 2 – the cut formed during the Late Glacial catastrophic surface runoff; 3 – the Late-Glacial/Holocene sediments; 4 – cores; 5 – ^{14}C dates (AMS)

Calculations with the equation, similar to 2-6 shows that about 7.5 km^3 were eroded at the Khoper River valley. This process was typical for all rivers on the East European plain (Sidorchuk et al. 2001).

The episode of extreme erosion was relatively short, about 2000-3000 years. The mean rate of gully and river-bed erosion was app. 250 t km^{-2} a^{-1} at the central part of the East European plain (Fig. 4). Such rate is extremely high for the lowland environment in the natural conditions.

The delivery ratio of the fluvial system on these lowland territory was presumably close to one during the event of catastrophic erosion. All sediments eroded on the slopes and within the river channels were delivered to the river mouths and to the seas. The distinct maximum of sedimentation rates was reported for the period 16-18 ka ago at the Black sea (Bahr et al. 2005). The large volume of Khvalyn sediments of the similar age (so called chocolate clays) was deposited in the Caspian Sea (Leonov et al. 2002).

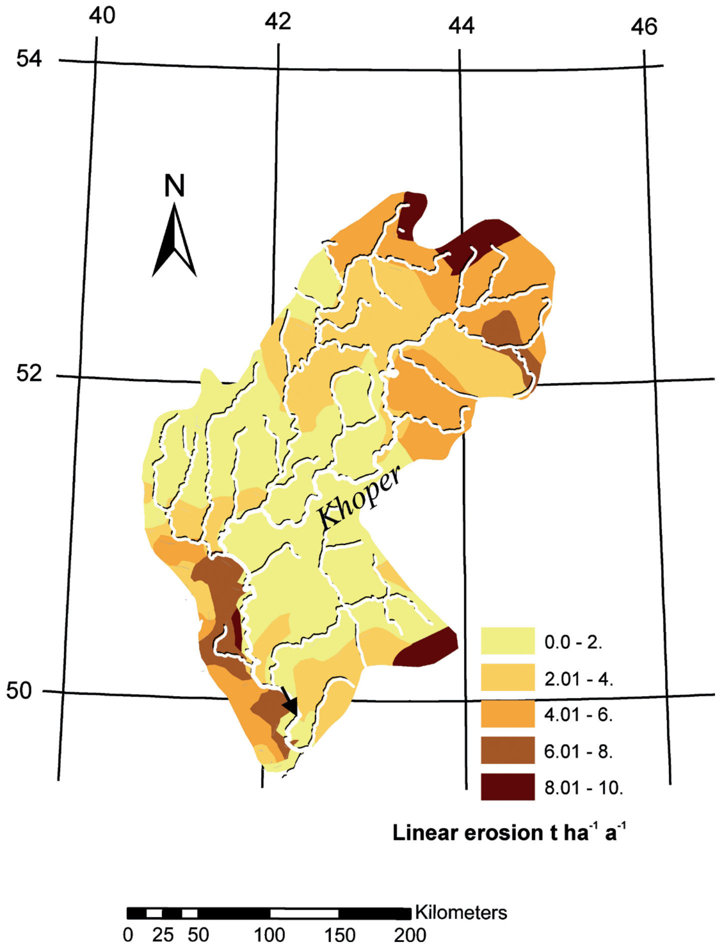

Fig. 4. Annual rate of linear erosion (t ha^{-1} a^{-1}) during the event of catastrophic surface runoff 16-18 ka ago, calculated from the "negative" volume of dry valleys at the Khoper River basin

The post-erosion deposition on the East European plain

After the episode of catastrophic erosion, the surface runoff generally decreased (with periods with higher and lower discharges) and reached the modern values at the beginning of the Holocene (Sidorchuk et al. 2008). This decrease of discharges in the wide channels led to a transport capacity decrease and to sediment deposition. The maximum rate of deposition in the Khoper River valley estimated for the cross-section shown in Fig. 1 in Sidorchuk (2003) occurred within the period from 8 to 14 ka BP. The deposition rate during the Holocene was lower (Fig. 5).

A potential for deposition is still very high in this environment. In such river valleys with a high potential for collecting the lateral sediment input "inherited" floodplains were formed (Sidorchuk 2003). The deposition in the gullies (now dry valleys on the slopes) was less effective: in average only about 25-30% of their "negative" volume was filled. The total volume of deposition in the fluvial system at the Khoper River basin was about 13 km^3 and this process lasted ~13-14 ka. The average annual erosion rate on the slopes (taking the modern delivery ratio for this basin) was 20-25 t km^{-2} during that period, being more intensive at the beginning of the process and with the significant decrease of this rate up to the

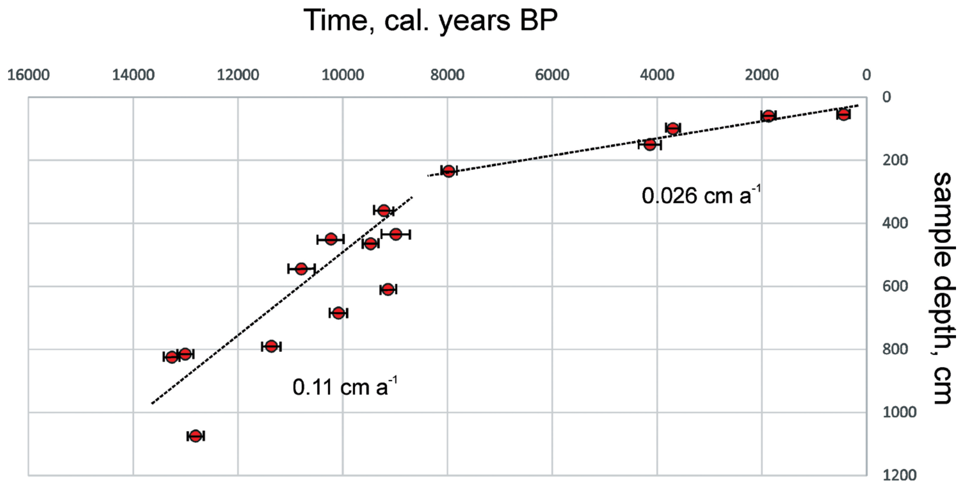

Fig. 5. Rate of deposition in the Late Glacial channels at the bottom of the Khoper River valley (cross-section at lat. 51.22° N, lon. 42.43° E), based on calibrated ^{14}C dating

time of intensive agriculture on these lands. The long lasted natural morphological evolution of the fluvial system on the East European plain after the catastrophic surface runoff event 16-18 ka ago slowly formed a graded channel network. The averaged hydrologic and morphometric characteristics of the rivers of different size and order were estimated by Rzhanitsin (1985) (Table 1, columns marked with "*"). The additional information about averaged channel width *W* (m) and depth *d* (m) for the bankfull discharge Q_{bf} ($m^3\ s^{-1}$) conditions (not inundated floodplain) was obtained from the measurements of the Russian Hydrological Survey at about 400 stations (R=0.85 for *W* and 0.6 for *d*):

$$W = 3.5Q_{bf}^{0.59} \qquad d = 0.84Q_{bf}^{0.24} \tag{7}$$

Sediment transport rate *T* (transport capacity of the flow in kg s^{-1}) for fine sediments was calculated with the formula of Zamarin (1951), which was calibrated for the lowland rivers of the East European plain

$$T = 0.22Q_{bf}\left(\frac{U}{\omega}\right)^{1.5}\sqrt{Sd} \tag{8}$$

Here *U* is flow velocity (m s^{-1}), *S* – flow surface slope (m m^{-1}), ω - particle fall velocity (m s^{-1}).

The sediment transport rate *T* for the flood period increases along the average fluvial system (Table 1), therefore the lowland rivers at the East European Plain were able to transport all suspended sediments without significant deposition in the conditions of low rate soil erosion on the slopes. The column of the Table 1 with T_{Lcr} shows the critical sediment supply to the channel from the slopes during the flood period *t*. When this value is exceeded, then deposition in the channel can occur. The pre-agriculture sediment yield at the forest-steppe and steppe zones of small rivers of the region was about 4.4 - 17.0 t $km^{-2}\ a^{-1}$ (see tables 2.11 and 2.15 in Dedkov and Mozzherin 1984). This is one-two orders of magnitude lower than the critical transport capacity, therefore rivers of all sizes and orders were capable to transport this amount of sediment.

The other situation is for the dry valleys, where post-erosion "negative" volume is still very large. These valley bottoms are dry the main part of the year and are flooded only during the snow thaw period and after intensive rain. The stream channel with the well-defined banks is rarely evident at dry valley bottoms, and only at the lower sections. The usual discharge in such valleys during rainfall exceeds the bankfull discharge and flood the wide valley bottoms, covered with the grass and

Table 1. The averaged hydrologic and morphometric characteristics of the permanent watercourses (mostly, rivers) on the East European Plain

N*	L* km	F km^2	Q* m^3 s^{-1}	t* days	S* m m^{-1}	W m	d m	U m s^{-1}	T kg s^{-1}	$TLcr$ t ha^{-1}	Dr	E t ha^{-1}
1	0.8	0.4	0.5	2	0.134	2.4	0.7	0.3	1.6	7.1	0.61	12.1
2	1.5	1.2	1.12	2	0.0492	3.8	0.9	0.3	2.9	4.2	0.48	9.0
3	2.8	3.6	2.51	2	0.02	6.1	1.0	0.4	5.5	2.6	0.39	7.1
4	5.1	10.7	5.6	2	0.0089	9.8	1.3	0.4	11.0	1.8	0.31	6.0
5	9.3	31.6	12.6	2.08	0.0042	15.9	1.5	0.5	23.0	1.3	0.25	5.3
6	16.9	92.5	28.2	4.7	0.00216	25.5	1.9	0.6	51	2.2	0.20	11.0
7	31	275.6	63	7.2	0.00114	41.0	2.3	0.7	111	2.5	0.16	15.4
8	57	825.0	141	10.1	0.00063	66.0	2.8	0.8	250	2.6	0.13	20.2
9	104	2435.2	316	17.5	0.00036	106.2	3.3	0.9	570	3.6	0.11	33.8
10	190	7205.0	710	21.5	0.00021	171.3	4.1	1.0	1330	3.4	0.08	40.5
11	338	20320.1	1590	29	0.000129	275.6	4.9	1.2	3160	3.9	0.07	56.7
12	620	60559.2	3560	40	0.000079	443.4	6.0	1.3	7490	4.3	0.06	77.3
13	1140	181260.7	7950	52	0.0000495	712.3	7.3	1.5	17900	4.4	0.04	99.9
14	2090	539682.3	17800	70	0.000031	1146.0	8.8	1.8	42906.4	4.8	0.04	134.7
15	3810	1590522.5	40000	90	0.00002	1847.8	10.7	2.0	104920.6	5.1	0.03	178.4

(N is watercourse order, L is river length, F – basin area, Q – mean maximum discharge, t – flood duration, S – channel slope, W – channel bankfull width, d – bankfull depth, U – mean flow velocity, T – suspended sediment transport rate, T_{Lcr} – critical sediment lateral input from slopes~Tt/F, Dr – sediment delivery ratio, E= T_{Lcr}/Dr – critical erosion on river basin slopes. Columns with ""are after Rzhanitsin (1985)*

shrubs. Therefore, most of the sediments, eroded on the slopes, are deposited on the dry valleys bottom surfaces.

The end of this long period of predominantly depositional processes in the fluvial system of the East European plain was characterised by some activation of linear erosion. Gullies were formed on the steep slopes of the river valleys and in the lower parts of the dry valley bottoms (Panin et al. 2009). This linear erosion was caused by some increase of precipitation and surface runoff about 5-6 ka ago and was not related to human activity.

The modern fluvial system of the East European plain

The main characteristic of the modern processes in the fluvial systems of the East European plain is the accelerated soil erosion on the slopes and rapid deposition of these eroded sediments in the river net headwaters. The calculated annual amount of fine (silt and clay) sediments (Litvin 2002), washed out in the recent human-influenced conditions (see, for example, Fig. 6) is 880 10^6 ton on about 1.43 10^6 km^2 of arable land.

The average erosion rate is about 6.2 t ha^{-1}, with the maximum of 25 t ha^{-1}. On over 22.7% of the arable land, the annual rate of erosion is less than 0.5 t ha^{-1}; on 24.1% it is in the range 0.5–2.0 t ha^{-}1; on 23.5% it is in the range 2.0–5.0 t ha^{-1}; on 12.6% it is in the range 5.0–10.0 t ha^{-1}; on 9.9% it is in the range 10.0–20.0 t ha^{-1}; and on 7.2% of the arable land the annual erosion rate is more than 20.0 t ha^{-1}. In total. the calculated volume of accelerated erosion on slopes in the river basins of the southern mega-slope of the East European Plain (2.2 10^6 km^2) during the period of intensive agriculture (the last 300-

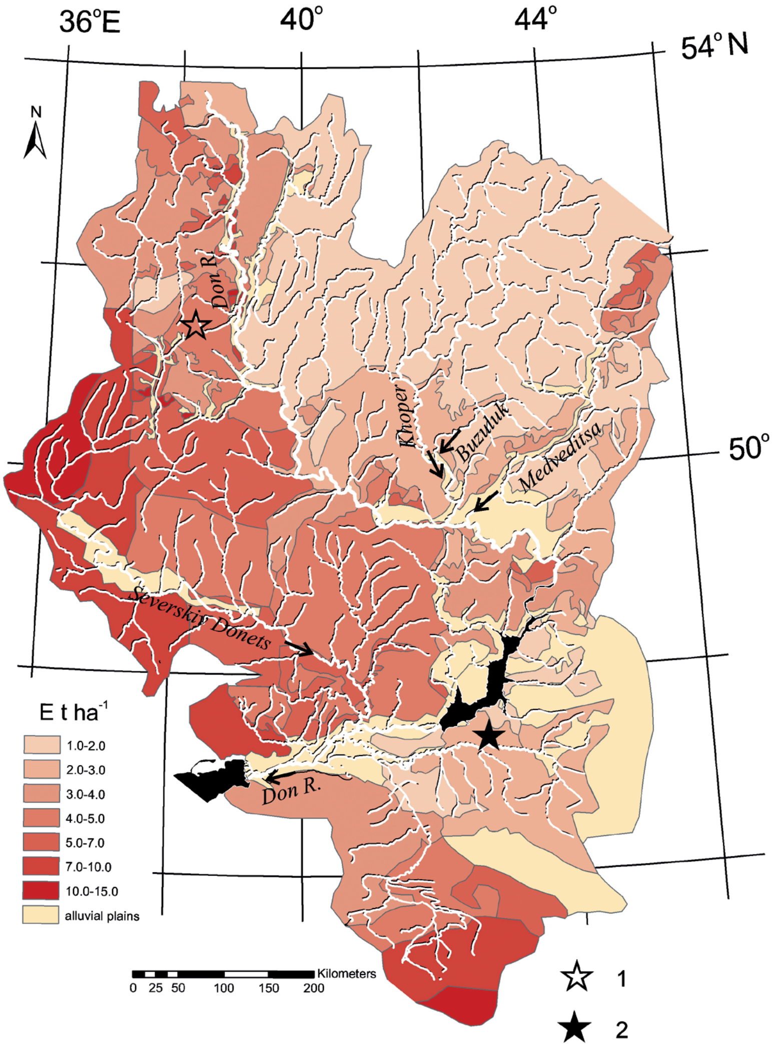

Fig. 6. The fragment of the Soil loss map of the East European Plain (Litvin , 2002) for the Don River basin. The stars show positions of gauging stations, used on Fig. 7

400 years) is about 76 10^9 ton (Sidorchuk and Golosov 2003).

The second important source of eroded material on the East European Plain is related to gully systems. There are about 1 10^6 gullies with a length over 70 m and a total volume of 3.5 10^9 m^3 (Litvin et al. 2003). These gullies were formed mainly during the period of intensive agriculture. The rate of gullies formation reached its maximum in the years 1860-1910 after the agricultural reform of 1861, when ~ 24% of now existing gullies were formed (Sidorchuk and Golosov 2003).

Sediments washed away due to soil erosion are delivered from the slopes to the water flows of different size. The comparison of calculated slope erosion *E* and measured sediment transport rate *T* for 343 river basins with hydrological stations at Volga, Dnieper and Don River basins allows the calculation of the sediment delivery ratio Dr (Golosov et al. 1991). Usually in the lowlands it decreases with basin area *F* km^2:

$$Dr = \frac{T}{E} \approx aF^{-b} \qquad (9)$$

The exponent *b* and the coefficient *a* vary in the broad range at different river basins. For example, for the Don River basin, where *T* values were measured at small catchments (Resources… 1973), *a*=0.23, *b*=0.32 (Fig. 7).

In the conditions of accelerated soil erosion the critical amount of sediment T_{Lcr}, which can be delivered from the slopes during floods without deposition (i.e. the amount equal to the specific transport rate) decreases along the flows with lengths of less than 10 km (Table 1). Such flows are potentially vulnerable to sedimentation if lateral sediment input from the basin is high enough. All dry valleys belong to this class. The last column in the Table 1 shows the critical erosion rate on the slopes E= T_{Lcr}/Dr. If the actual erosion on the slopes is more than critical value, the delivered to the watercourses amount of sediment is more than flow transport capacity. Therefore, according to Table 1, the permanent streams with the length 3-10 km can be depositional sinks in the condition of average annual soil erosion rate (6.2 t/ha), and at the areas with soil erosion rate of 25 t/ha even medium-size river with the length 50-60 km can be silted.

Measurements in different regions of the East European Plain (the Middle Oka, the Upper and Lower Don, the Lower Volga, the Ural River and Stavropol' Region) show that the thickness of sediments at the bottom of dry valleys with basin areas of 5-40 km^2 ranges from 1.0 to 2.8 m. The mean aggradation rates for the period of intensive agriculture vary within the range 3 to 38 mm a^{-1} (Golosov et al. 1991). About 60% of 76 10^9 ton of eroded material on the southern mega-slope of the East European Plain was deposited in the valleys less than 25 km long and about 90% of it in the valleys less than 100 km long (Table 2). The measurements in the deltas of the major rivers for the period before large reservoirs construction show that only 3-6% of eroded matter was transported to the sea, while its main part was sequestered in the fluvial systems (Sidorchuk 1995).

DISCUSSION AND CONCLUSION

The main geomorphic function of the global fluvial system is the land surface lowering by dissolution, erosion and sediment transport. It is one of the main sources of mineral matter, delivered to the oceans. This process is not continuous: sediment deposition in the channels accompanies erosion, therefore sediment transport occur in form of waves of different amplitudes and periods (Langbein and Leopold, 1964).

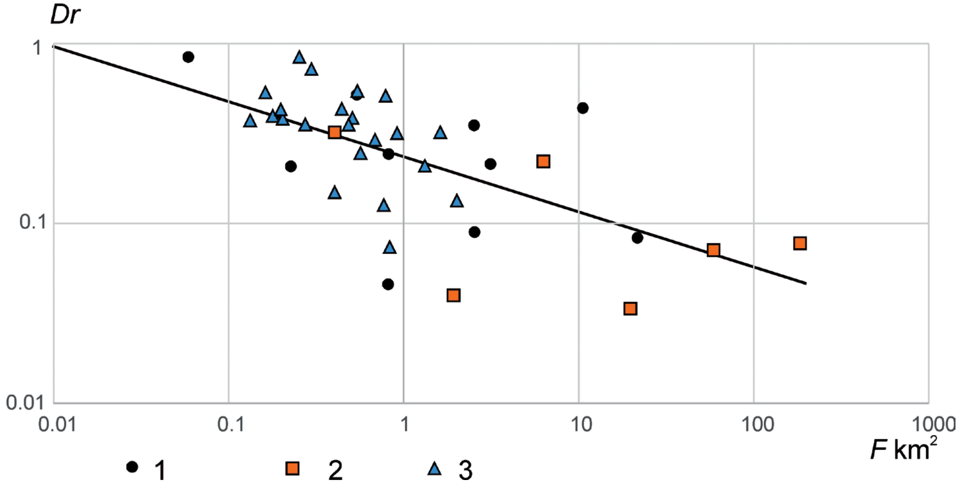

Fig. 7. Changes of the sediment delivery ratio *Dr* along the the rivers of the Don River Basin. Data from: 1 – gauging stations at Nizhne-Devitskaya water budget station (N 1 at Fig. 6); and 2 – gauging stations at Dubovskaya hydro-meteorological station (N 2 at Fig. 6); 3 – ponds infill in Buzuluk and Medvetitsa river basins

Table 2. Deposition of sediments, eroded from slopes in the river valleys less than 100 km long on the East European Plain

The river basin	F km^2	E t ha^{-1} a^{-1}	E_{agr} 10^9 t	Dr_{100}	D_{agr} 10^9 t
Dnepr upper Pripyat'	106000	2.10	5.2	0.07	4.9
Pripyat'	114300	2.10	5.6	0.04	5.4
Desna	88900	1.90	3.7	0.07	3.4
Dnepr lower Pripyat'	154700	3.60	9	0.05	8.6
Don upper Severskiy Donets	257000	1.30	5.3	0.20	4.2
Severskiy Donets	96250	2.20	4	0.05	3.8
Don lower Severskiy Donets	53025	1.30	0.6	0.05	0.6
Volga upper Oka	265200	1.20	8.4	0.05	8.0
Oka	245000	1.80	11	0.08	10.2
Sura	67500	2.40	3.1	0.30	2.2
Verluga	39400	0.90	0.9	0.08	0.8
Vishera	31200	0.40	0.2	0.30	0.1
Belaya	142000	0.90	1.3	0.30	0.9
Vyatka	129000	2.50	6.1	0.10	5.5
Kama without Vishera	204800	2.80	6.7	0.30	4.7
Volga lower Kama	224000	1.30	4.7	0.30	3.3
Total	2218275		75.8		66.5

(F – basin area; E – recent mean (for the whole river basin) accelerated erosion rate on the slopes; E_{agr} – amount of erosion during the period of intensive agriculture; Dr_{100} – the delivery ratio for the rivers 100 km long; D_{agr} 10^9 – the amount of deposition in the valleys less than 100 km long during the agricultural period)

The fluvial system is a sediment source at the reaches with positive balance between particle detachment and particle subsidence. The fluvial system is a sediment sink at the reaches with a negative transport rate change along the flow and/or high lateral sediment input from the basin slopes. Water flow regimen and vegetation cover are the main factors, which determine the periods and the amplitudes of erosion-deposition waves.

The waves of erosion and deposition are typical for the fluvial system on the East European plain. These waves have long periods, because Glacial-Interglacial-Glacial waves of climate change caused them. The Late Glacial event of high surface runoff is the global phenomenon first described by G. Dury (1965) and I. Volkov (1963). The duration of this erosion episode was about 2-3 ka, but the rates of the erosion on the slopes and in the river valleys usually were 200-400 t km^{-2} a^{-1} and often reached to 800-1000 t km^{-2} a^{-1} in the central East European Plain (see Fig. 4). That is close the modern accelerated erosion from the same territory. In West and Central Europe the headwaters of a great number of streams were over-deepened during the Late Glacial (Starkel 1995). The same evolution of the fluvial relief took place on the Great Plains of North America (Arbogast et al. 2008), Atlantic Coastal Plain (Leigh 2006) and the Gulf of Mexico region (Leigh and Feeney 1995). In Australia, the Riverine Plain was formed by much larger rivers than the recent Murrambidgee and Darling Rivers (Page et al. 2009). All fluvial systems on the lowlands were of erosional type

and were cleaned of a significant part of deposited sediments. These short events of catastrophic erosion have a periodicity of 100-120 ka (Vandenberghe 2003) and in spite of this the long-term delivery ratio in the lowland fluvial systems is close to one.
After this short episode of catastrophic erosion the surface runoff decreased and sediment deposition occur in the huge eroded "negative" volume of the fluvial system. The average erosion rate on the slopes of the central East European Plain was not high (about 20-25 t km^{-2} a year), but most of these sediments did not reached the river mouths. "Inherited" floodplains with the remnants of the large periglacial river channels are also widespread there (Sidorchuk 2003). The same is typical for all lowlands, which were affected by late-glacial catastrophic erosion. Lowlands were the territory of significant sediment sequestration, the fluvial systems along the main part of their length were of depositional type.

The morphological changes in the channels, caused by deposition, slowly led to the formation of a new equilibrium between erosion and sedimentation in the fluvial systems. Nevertheless, on the East European plain a dense network of dry valleys (the former late-glacial gullies) remain the sinks for sediments. The same was reported for the western European lowlands (Larsen et al. 2016). The duration of sediment deposition can last thousands of years.

This deposition in the fluvial systems on the East European Plain was refreshed by the accelerated soil erosion on the arable land, accompanied by the high rate of the lateral sediment input.

According to Dedkov and Mozzherin (1984), the mean specific sediment yield in the small lowland river basins in the forest-steppe of Europe and North America in pristine conditions was ~17±30 t km^{-2}. The mean specific sediment yield from the river basins of the same type in the forest-steppe areas used for agriculture is ~88±29 t km^{-2}. In the steppe zone, the difference is even greater: 4.4±3.1 and ~100±40 t km^{-2}, respectively. This is mainly the result of human activity and accelerated erosion on the bare slopes. The calculated volume of accelerated erosion on slopes in the river basins of the southern mega-slope of the East European Plain (2.2 10^6 km^2) during the period of intensive agriculture (the last 300-400 years) is about 76 10^9 ton. The modern deposition of these sediments is concentrated in the upper reaches of the lowland fluvial systems and on the wide floodplains, "inherited" from the Late Glacial erosion event.

The main difference between the modern accelerated and Late Glacial erosion is the extent of the erosion cut. The main area of the accelerated erosion are the slopes used for agriculture, because of their low protection by vegetation cover. The main area of deposition of eroded soil is the net of dry valleys and small rivers. As the delivery ratio decreases with the basin area (Eq. 9), the deposition rate rapidly decreases along the river length. The Late Glacial short event of catastrophic erosion was caused both by scarce vegetation and by extreme surface runoff. Therefore, the whole fluvial system was the area of intensive erosion, with the deep incision of gullies on the slopes, and channels in the river valleys. These sediments were delivered to the sea basins, and distinct maximum of sedimentation rates was reported for the period 16-18 ka ago for example at the Black sea (Bahr et al. 2005).

ACKNOWLEDGMENTS

This study was supported by the program "The Evolution and Transformation of Erosion–Channel Systems under Changing Environment and Human impact."

REFERENCES

Alayev E.B., Badenkov Yu. P., and Karavaeva N.A. (1990). The Russian Plain. In: B.L. Turner, W.C. Clark, R.W. Kates, J.F. Richards, J.T. Mathews and W.B. Meyer (Editors), The Earth as Transformed by Human Action. Cambridge University Press with Clark University, Cambridge, 543560 pp.

Arbogast A.F., Bookout J.R., Schrotenboer B.R., Lansdale A., Rust G.L. Bato V.A., (2008). Post-glacial fluvial response and landform development in the Upper Muskegon River valley in north-central Lower Michigan. U.S.A. Geomorphology 102, 615-623.

Bahr A., Lamy F., Arz H., Kuhlmann H., and Wefer G. (2005). Late glacial to Holocene climate and sedimentation history in the NW Black Sea, Marine Geology, 214, pp. 309-322.

Dedkov A.P. and Mozzherin V.I. (1984). Erosion and sediment yield on the Earth. Kazan' University Press, Kazan' (in Russian).

Dokuchaev V.V. (1878). The ways of the river valleys formation at the European Russia. Sankt-Petersburg: Tipografija V. Dermakova (Publ.), 221 p. (in Russian).

Domanitskiy A.P., Dubrovina R.G., and Isayeva A.I. (1971). Rivers and lakes of the Soviet Union. Leningrad: Gidrometeoizdat (Publ.), 104 p. (in Russian).

Dury G.H. (1965). Theoretical implications of underfit streams. US Geological Survey Professional Paper 452-B. USGS, Washington.

Eremenko E.A. and Panin A.V. (2011). An origin of the net of hollows in the central and southern regions of the East European Plain. Vestnik Mosk. un-ta, Seriya geogr., No. 3, pp. 59–66 (in Russian).

Golosov V.N., Ivanova N.N., Litvin L.F., Sidorchuk A. Yu., Chernov A.V. (1991). Change in sedimentation in small river catchments in the European USSR. In: Snischenko, B.F. (Ed.), Sovremennoye sostoyaniye malykh rek SSSR i puti ikh ispol'zovaniya, sokhraneniya i vosstanovleniya. Gidrometeoizdat, Leningrad, pp. 96-103 (in Russian).

Gregory K.J. and Walling D.E. (1976). Drainage basin form and process: a geomorphological approach. Edward Arnold, London, 458 p.

Ito A. (2007). Simulated impacts of climate and land-cover change on soil erosion and implications for the carbon cycle, 1901 to 2100. Geophys Res Lett 34:L09403.

Knighton D. (1984). Fluvial Forms and Processes. London: Edward Arnold, 218 pp.

Langbein W.B., Leopold L.B. (1964). River channel bars and dunes. Theory of kinematic waves: USGS Professional Paper: 422- L.

Larsen A., Heckmann T., Larsen J.R., Bork H.-R. (2016). Gully catchments as a sediment sink, not just a source: Results from a long-term (~12,500 year) sediment budget. Earth Surface Processes and Landforms 41, (4), pp. 486-498.

Leigh D.S. (2006). Terminal Pleistocene braided to meandering transition in rivers of the southeastern USA. Catena 66, 155-160.

Leigh D.S. and Feeney T.P. (1995). Paleochannels indicating wet climate and lack of response to lower sea level, southeast Georgia. Geology, V. 23. Pp. 687–690.

Leonov Yu.G., Lavrushin Yu.A., Antipov M.P., Spiridonova Ye.A., Kuzmin Ya.V., Jull E.J.T., Burr S., Jelinowska A., and Chalie F. (2002). New age data on sediments of the transgressive phase of the early Khvalyn transgression of the Caspian Sea. Doklady Earth Sciences, v. 386, pp. 748–751.

Litvin L.F. (2002). Geography of soil erosion in agricultural lands in Russia. Akademkniga (Publ), Moscow (in Russian)

Litvin L.F., Zorina Ye.F., Sidorchuk A.Yu, Chernov A.V., Golosov V.N. (2003). Erosion and sedimentation on the Russian Plain, part 1: Contemporary processes. Hydrological Processes 17 (16), pp. 3335-3346.

Makkaveev N. I. (1955). The River Channel and Erosion in its Basin. Akademizdat: Moscow, 346 p. (in Russian)

Meade R.H. (1996). River – sediment inputs to major deltas. In: Milliman J.D., Haq B.U. (Eds.), Sea-Level Rise and Coastal Subsidence. Kluwer Academic Publishing, Dordrecht, pp. 63 – 85.

Milliman J.D. and Farnsworth K.L. (2011). River Discharge to the Coastal Ocean: A Global Synthesis. Cambridge University Press, Cambridge.

Page K.J., Kemp J., and Nanson G.C.(2009). Late Quaternary evolution of Riverine Plain paleochannels, southeastern Australia. Australian Journal of Earth Sciences 56, 19-33.

Panin A. V., Fuzeina J. N., Belyaev V. R. (2009). Long-term development of Holocene and Pleistocene gullies in the Protva river basin, central Russia. Geomorphology, v. 108, pp. 71–91.

Resources of the Surface Waters in the USSR (1973). Don River Region. Gidrometeoizdat, Leningrad, V. 8 (in Russian).

Rzhanitsin N.A. (1985). Channel-Forming Processes in the Rivers. Gidrometeoizdat, Leningrad (in Russian).

Schumm S. A. (1977). The fluvial system. New York, John Wiley &Sons, 338 p.

Sidorchuk A. Yu. (1995). Erosion and accumulation on the Russian Plain and small river silting. In: Trudy Akademii vodokhozyaystvennykh nauk, vol. 1, Moscow, pp. 74-83 (in Russian).

Sidorchuk A. (2003). Floodplain sedimentation: Inherited memories. Global and Planetary Change, 39 (1-2), pp. 13-29.

Sidorchuk A. (2015). Sediment budget in the erosion-depositional systems. Geomorfologiya, 1, pp. 14-21 (in Russian).

Sidorchuk A., Borisova O., Panin A. (2001). Fluvial response to the Late Valdai/Holocene environmental change on the East European Plain. Glob. Planet. Change 28, pp. 303–318.

Sidorchuk A.Yu and Golosov V.N. (2003). Erosion and sedimentation on the Russian Plain, II: the history of erosion and sedimentation during the period of intensive agriculture. Hydrological Processes 17 (16), pp. 3347-3358.

Sidorchuk A. Yu., Panin A.V., Borisova O.K. (2008). Climate-induced changes in surface runoff on the North-Eurasian plains during the Late Glacial and Holocene. Water Resources 35 (4), pp. 386-396.

Starkel L. (1995). Palaeohydrology of the temperate zone. In: Gregory K.J., Starkel L., Baker V.R. (Eds.), Global Continental Palaeohydrology. Wiley, Chichester, pp. 233-258.

Wischmeier W. H. and Smith D. D. (1978). Predicting rainfall erosion losses. Agric. Handbook 537. Washington D.C.: U.S. Dept. Agric.

Vandenberghe J. (1995). Postglacial river activity and climate: state of the art and future perspectives. In: Frenzel B. (Ed.), European river activity and climatic change during the Lateglacial and early Holocene. G. Fischer Verlag, Stuttgart-Jena-NY. Paläoklimaforschung/ Palaeoclimate Research 14, pp. 1-9.

Vandenberghe J. (2003). Climate forcing of fluvial system development; an evolution of ideas. Quaternary Science Reviews, 22, pp. 2053–2060.

Van Oost K., Quine T. A., Govers G., De Gryze S., Six J., Harden J.W., Ritchie J. C., McCarty G.W., Heckrath G., Kosmas C., Giraldez J. V., da Silva J. R. M., and Merckx R.(2007). The impact of agricultural soil erosion on the global carbon cycle, Science, 318, 626–629.

Volkov I.A. (1963). Remnants of powerful flow in the valleys of southern part of the Western Siberia. Doklady AN SSSR 151 (3), 648-651 (in Russian).

Zamarin E.A. (1951). Open flow transport capacity. Stroyizdat, Moscow (in Russian).

Received on October 30th, 2017 Accepted on July 31st, 2018

AUTHORS

Aleksey Sidorchuk was born 1 March 1949. Educated in Moscow State University, Diploma (Hons) in Geography/Geomorphology, 1971, Candidate of Science, 1975, Doctor of Science, 1992. Performed field works, hydrological. geomorphological and palaeogeographical investigations in the rivers and river deltas of the western and eastern Siberia (Taz, Pur, Ob', Enisey, Yana, Lena), on the Niger River (Nigeria), the Alabuga River (Kirgiziya), the lower Terek River. Conducted analysis of gully erosion in Australia and Swaziland, erosion and thermo-erosion at the Yamal peninsula, mechanics of erosion processes and of the organic carbon transport in New Zealand. Investigated the morphological and palaeohydrological changes in the fluvial system due to climate change during the Late Glacial and the Holocene. Reconstructed the river flow and sediment yield at the Russian Plain during the period of abrupt climate changes. Developed and used the models of soil erosion, gully erosion, of transport and deposition in the fluvial system.

Anastasia K. Markova[1*], Andrey Yu. Puzachenko[1]
[1] Institute of Geography of the Russian Academy of Sciences, Moscow, Russia
*** Corresponding author:** amarkova@list.ru

MIDDLE PLEISTOCENE SMALL MAMMAL FAUNAS OF EUROPE: EVOLUTION, BIOSTRATIGRAPHY, CORRELATIONS

ABSTRACT. The paper is concerned with the small mammal fauna evolution in Europe in the Middle Pleistocene. The information on the faunas of the end of the Early Pleistocene has been also taken into consideration. The data available made possible identifying several stages in the small mammal evolution. Not all intervals within the Middle Pleistocene are provided with sufficient information for recognizing individual stages; that is particularly true for the cold periods of the Middle Pleistocene – the Donian and the Okian glaciations (=Elsterian, =Anglian). Based on the studies of small mammal localities, the biostratigraphic scheme has been developed, the principal phylogenetic lineages of Arvicolinae were traced, and maps of the Middle Pleistocene small mammal localities have been compiled

KEY WORDS: Middle Pleistocene, small mammals, Europe, biostratigraphy, evolution, correlations

CITATION: Anastasia K. Markova, Andrey Yu. Puzachenko (2018) Middle Pleistocene small mammal faunas of Europe: Evolution, Biostratigraphy, Correlations. Geography, Environment, Sustainability, Vol.11, No 3, p. 21-38
DOI-10.24057/2071-9388-2018-11-3-21-38

INTRODUCTION

Problems of evolution of the Middle Pleistocene small mammals and the synchronization of the principal stages of their evolution with geological and climatic events have been examined in many previous publications (Agadjanian 2009; Alexandrova 1976; Chaline 1972; Cuenca-Bescós et al. 2013; Heinrich 1990; Fejfar and Horaček 1990; Markova 1982, 2005, 2006, 2007, 2014; Markova and Kolfschoten 2012; Markova and Puzachenko 2016; Markova and Vislobokova 2016; Masini and Sala 2011; Maul 2001; Maul and Markova 2007; Maul et al. 2000, 2007; Nadachowski 1990; Rekovets 1994; Schreve 2004 a,b,c; Vislobokova and Tesakov 2013; van der Meulen 1973; van Kolfschoten 2014; von Koenigswald and van Kolfschoten 1996 and many others). In this paper we try to analyze generally the main stages in the evolution of the European small mammal faunas referring to the period from the Jaramillo paleomagnetic event (the end of the Early Pleistocene 1.07 – 0.99 Ma, ~MIS 26-30) till the end of the Middle Pleistocene – the end of Saalian (=Walstonian, =Dnieper) glaciation (MIS 6). The ages of the temporal intervals were given according to oxygen isotope curve (Lisiecki and Raymo 2005). A significant number of global climatic events, glaciations and interglacials, correspond to this period. We tried to recognize the response of the small mammal faunas to the different climatic events during the Middle Pleistocene, to synchronize the faunas of Eastern Europe with those of

Western Europe, to examine the principal evolutional changes in the different phylogenetic lineages of Arvicolinae during the Middle Pleistocene.

PRINCIPAL STAGES OF THE MIDDLE PLEISTOCENE SMALL MAMMAL FAUNAS

The end of the Early Pleistocene – the beginning of the Middle Pleistocene (MIS 31 – 19)

The analysis of small mammal faunal data from Eastern and Western Europe dated to the interval from the Jaramillo paleomagnetic event to the beginning of the early Middle Pleistocene (1.06-0.7 Ma) provided evidence for several phases in the small mammal evolution recognizable within this interval. It is established that the boundary between large mammal fauna stages corresponds to those of Tamanian and Tiraspolian mammal assemblages in Eastern Europe, Early/Late Galerian in Italy, and MNQ 20/MNQ 21 zones. A more detailed picture was revealed in the evolution of small mammal faunas during the regarded interval; the phases are distinguishable by changes in the species composition, first occurrences of new species, and evolutionary changes in a several phylogenetic lineages of Arvicolidae.

On the Russian Plain most of localities are found in great geological sequences studied not only paleontologically, but also by several methods including paleomagnetic stratigraphy. Those supplementary data help to determine the stratigraphic position of mammal faunas. Many localities in the region of the Black Sea coasts include, along with mammals, shells of brackish-water mollusks differing in their evolutionary level. The mollusk assemblages permit to correlate the mammal faunas directly with the Black Sea transgressions and paleogeographic events in the Eastern Mediterranean.

A relatively large part of localities in Western Europe are related to karst caves and fissures. In such localities faunal remains of different age are often found to be mixed, and paleomagnetic analysis data are also not quite reliable. There are, however, a number of multilayered localities (Kärlich, Shöningen, Sima del Elephante, Grand Dolina, Colle Curti, Castagnone, the localities related to the different Themes River terraces, and some others) where multidisciplinary studies (including paleomagnetic analysis and absolute dating) were performed.

Every phase in the evolution of small mammals is identifiable not only by appearance of new taxa, but also by the prevalence of certain morphotypes within a taxon. The main evolutionary transformations within the phylogenetic lineages resulted from anagenesis; several "paleontological" species were identified on the basis of the dominant tooth morphotypes. In the *Prolagurus - Lagurus* lineage, for example, we never found a single tooth morphotype in a certain time interval; there is always a considerable variability recorded. At the level of faunas correlatable with the Jaramillo event there are some steppe lemmings with morphotypes typical of *Prolagurus ternopolitanus (= P. praepannonicus)* against the background of prevailing tooth morphotypes characteristic of *P. pannonicus*. Faunas dated to the very end of the Matuyama reversed polarity epoch (the Karai-Dubina locality) include steppe lemmings with tooth morphotypes of *P. pannonicus, P. posterius, L. transiens*. More than 90% of the teeth feature morphotypes characteristic of *P. pannonicus*, while *L. transiens* is represented by a single specimen displaying the extreme variant of the morphological variability (Markova 1982). Therefore, it is easy to make a mistake in attributing a locality to another evolutionary stage (faunal assemblage) if the species list of the locality is considered formally in the absence of other datable materials. All these phenomena require a careful investigation of fossil materials. Certain difficulties in correlations between West European faunas and those in Eastern Europe arise from different levels of knowledge and different taphonomic features.

Small mammal faunas related to Jaramillo normal polarity event

Small mammal faunas confidently correlated with the Jaramillo normal polarity event contain remains of *Mimomys savini, M. pusillus, Clethrionomys sokolovi,* advanced *Allophaiomys, Borsodia fejervaryi, Prolagurus pannonicus, Lagurodon arankae, Eolagurus argyropuloi* (Masini and Sala 2011; van der Meulen 1973; Siori and Sala 2007; Markova 2007; Maul and Markova 2007). Characteristic for the Iberian faunas is the presence of archaic representatives of the endemic *Iberomys genus (I. huescarensis)*, voles of the *Ungaromys* genus and surprisingly finds of the water vole *Arvicola jacobensis* found together with *Allophaiomys lavocati* (Cuenca-Bescós 2013). It is noteworthy that no voles of *Microtus (Terricola), M. (Pallasiinus), Lasiopodomys (Stenocranius)* genera and subgenera have been recorded in faunas correlatable with the Jaramillo event. In Eastern Europe faunas of that evolutionary level had been earlier identified as **Kairian (=Ostrogozhskian)** small mammal faunas (Markova 1990, 2007; Shik 2014) (Fig. 1).

In Western Europe they have been correlated with West European Biharian faunas, with those of the Colle Curti stage (Colle Curti F.U.) in Italy and the "Allophaiomys lavocati" phase in Spain, etc. (Cuenca-Bescós et al. 2013; Masini and Sala 2011; Siori and Sala 2007) (Fig. 5).

The other opinion exists also that more advanced voles of *Allophaiomys - Microtus* linage (for example, *Microtus thenii*) also existed during Jaramillo event (Maul et al. 2007) (Fig. 2). For our opinion it is necessary to carry out the additional studies to resolve this problem.

Small mammal faunas related to post-Jaramillo interval. but located before Brunhes - Matuama paleomagnetic boundary

The next step in the small mammal evolution is represented by faunas with the first documented representatives of *Lasiopodomys (Stenocranius) hintoni* and *Microtus (Terricola)* sp., *Mimomys savini, M. pusillus, Allophaiomys pliocaenicus nutiensis, Prolagurus pannonicus* are also present in these faunas.

Those faunas were identified as the **Morozovkian** small mammal assemblage (Alexandrova 1976; Markova 1990) and fall within the Matuyama reversed polarity zone. It is possible that those East European faunas may be correlated with the faunas with *Microtus thenii* from Untermassfeld (Germany) (Maul 2001) (Fig. 1, 2, 5).

More advanced faunas are identified by the first occurrence of *Microtus* ex gr. *oeconomus (= M. protooeconomus, =M. ratticepoides)*. The bulk of the fauna is formed by *Prolagurus pannonicus* and *Eolagurus argyropuloi*; remains of *Mimomys savini* and *Allophaiomys pliocaenicus nutiensis* are present in small number. According to paleomagnetic data, these faunas are correlated to the end of the Matuyama epoch. The faunas at that stage of evolution are recognized as **Petropavlovkian** assemblage of small mammals in Eastern Europe (Alexandrova 1976; Markova 1998) (Fig. 1, 2, 5).

The faunas marked by the first appearance of *Microtus arvalinus* and *Prolagurus posterius* (Shamin locality, Don R. basin) occur in inversely magnetized deposits and are dated to the very end of the Matuyama epoch. The presence of the above named species makes the faunas closer to the **Early Tiraspolian** ones. In the localities pertaining to the beginning of the Brunhes epoch the rooted voles of *Mimomys* genus still persist. Steppe lemmings are represented mostly by *Prolagurus posterius*, though remains displaying the *Prolagurus pannonicus morphotype* were presented long enough (up to the end of the Don glacial epoch). The genus *Microtus* became more diversified at that time (Agadjanian 2009; Markova 1992, 2007).

New species appeared in Western and Eastern Europe more or less simultaneously. The comparison between West European and East European faunas is considerably hindered by almost a total absence in

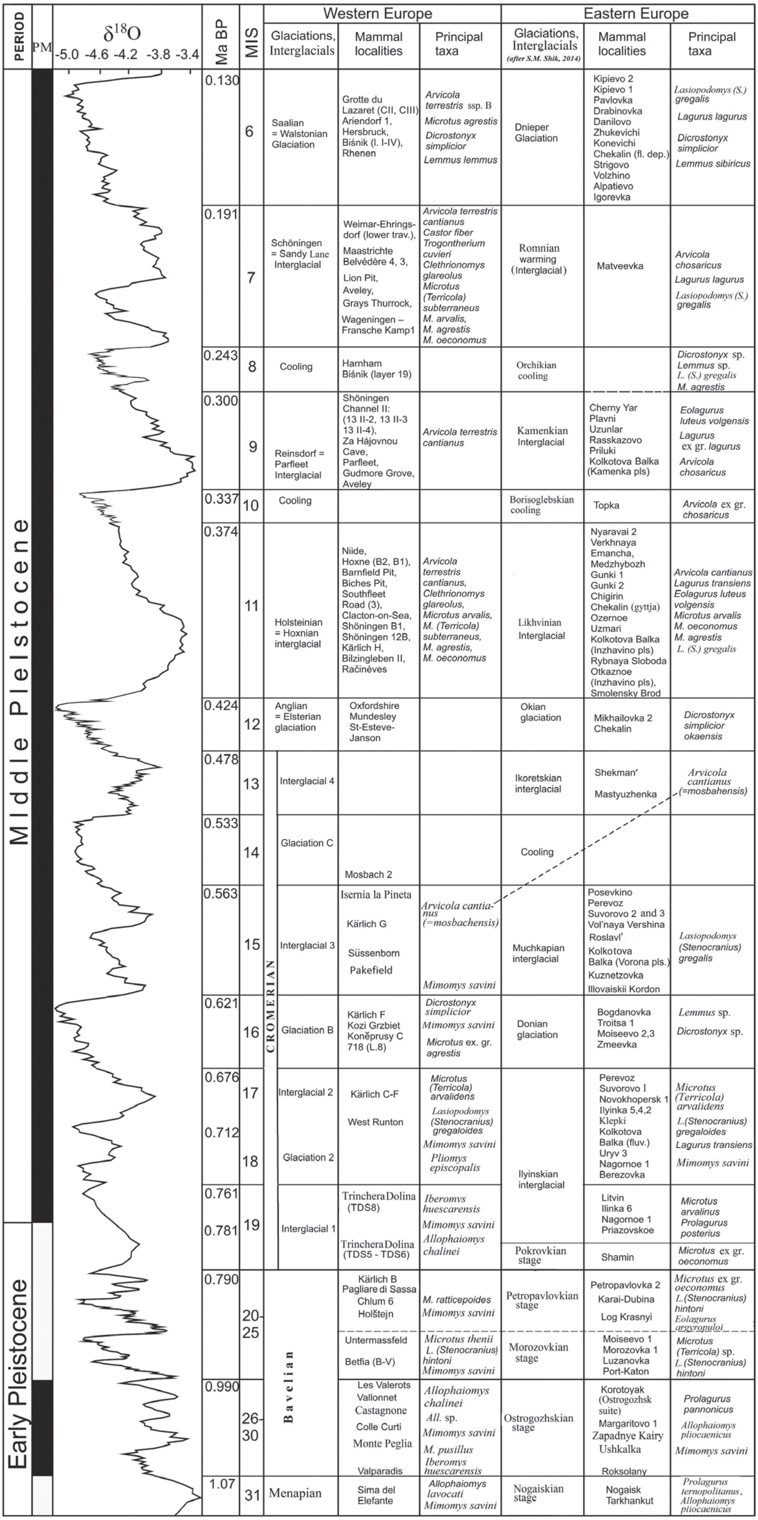

Fig.1. Biostratigraphical scheme of the Middle Pleistocene by small mammal data from Western and Eastern Europe

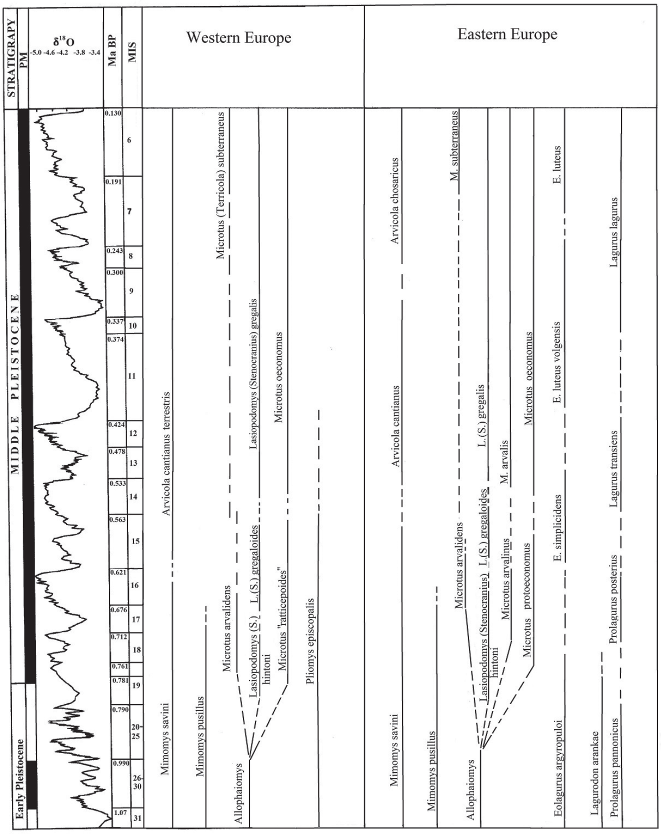

Fig. 2. Arvicolinae phylogenetic lines during the Middle Pleistocene by the materials from European localities

Western Europe of steppe lemmings belonging to the *Prolagurus* - *Lagurus* lineage. Those rodents show a highly dynamic evolution through the Pleistocene and are the best diagnostic taxa for the East European faunas. The variability in the morphology of the genus *Allophaiomys* teeth often used by European specialists as a basis for their biostratigraphical conclusions is undoubtedly extremely important. So the indexes of M/1 are used very widely as indicative of the main trends in evolution of this taxon (van der Meulen 1973; Agusti 1992; Maul and Markova 2007, Rekovets 1994) (Fig 3).

It should be noted, however, that correlations are often performed on small collections and on insufficiently representative remains recovered from different localities. In such cases, the comparison may lead to a false conclusion. On the whole, the analysis of small mammal remains dated to Early-Middle Pleistocene (and of Arvicolinae in particular) is a useful tool, as it enables the evolution process to be traced in various phylogenetic lineages, and the sediments from which they originate to be dated. This palaeontological dating is particularly important, as absolute dates are practically lacking for the interval under consideration; as to the paleomagnetic method in itself, unsupported by paleontological materials, it hardly can deliver a conclusive date.

First half of the Middle Pleistocene (MIS 18 – 12)

The main intervals of the first half of the Middle Pleistocene include: Ilyinian complex interglacial (MIS 18 and 17), that apparently corresponds to the glacial A of the Cromerian complex and interglacial Cromer II; the Donian glaciation (MIS16) = glaciation B of the Cromerian complex;

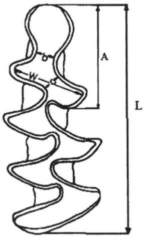

Localities	A/L				B/W				C/W			
	N	min	mean	max	N	min	mean	max	N	min	mean	max
Nagornoe 1	5	40,82	44,31	49,02	5	11,67	21,16	31,25	5	15,79	20,83	25,00
Shamin	1		44,16		1		22,58		1		16,66	
Karai-Dubina	7	41,82	43,65	46,00	7	11,76	17,38	37,50	7	11,11	18,92	30,00
Untermassfeld	31	44,02	48,68	52,38	53	2,44	6,65	17,95	53	5,00	21,13	32,43
Morozovka 1	7	46,90	48,6	51,6								
Port-Katon	7	40,00	44,59	47,00	7	13,33	19,56	26,67	7	21,43	25,97	28,57
Castagnone	6	42,10	44,31	44,89	8	5,13	14,67	25,76	10	15,94	27,66	30,00
Monte Peglia (terra rossa)	101	42,00	46,00	51,00	148	<5	13,90	33,00	147	6,00	22,40	37,00
Monte Peglia (breccia)	81	41,00	45,70	49,00	48	13,00	22,80	32,00	40	6,00	19,60	28,00
Vallonnet	8	43,8	45,6	47,7								
Les Valerots (A. nutiensis)			47,21				6,88					
Les Valerots (A. burgundiae)			45,80				14,78					
Ushkalka	7	40,00	45,33	46,00	7	12,50	19,88	22,50	7	11,76	18,62	25,00
Zapadnye Kairy	4	43,40	45,07	46,00	4	16,67	21,68	28,89	4	16,67	21,02	26,32
Korotoyak (ostrogozhsk suite)	6	42,11	44,73	47,56	7	16,13	20,34	26,88	7	12,90	20,83	25,92
Colle Curti	2	41,22	41,57	41,92	2	26,88	28,23	29,41	2	18,18	19,79	22,58
Roksolany	6	37,50	40,48	42,86	6	18,95	23,54	31,25	6	13,68	19,43	25,00
Sima del Elefante	301	43,55	48,74	54,54								

Fig. 3. *Allophaiomys* M_1 quotient by the materials from European localities

the Muchkapian interglacial complex =Cromer III (MIS 15). The Muchkapian interglacial stage (by the data from Eastern Europe) includes Glazov and Konakhov warm phases and the cool interval (Podrudnyansky) separating them (MIS 15). The Navlinian cooling (MIS 14) and the later Ikoretskian warming (MIS13) follow it. The Navlinian cooling probably corresponds to the cooling (glaciation) C of the Cromerian complex, the Ikoretskian interglacial corresponds to Cromer IV (MIS 13), and the Okian glaciation (=Anglian glaciation = Elsterian glaciation) corresponds to MIS 12 (Shik 2014). Durations of these intervals are given according to Lisiecki and Raymo (2005) (Fig 1, 2, 5). In this paper, when dealing with the materials from Eastern Europe, the authors follow the last stratigraphic scheme, proposed by Shik (2014). The West European stratigraphic subdivisions are given according to Gibbard et al. (2004).

The analysis performed on the European small mammal faunas dated to the first part of the Middle Pleistocene gives ground for distinguishing several stages in their evolutionary development during ~0.76-0.42 Ma BP.

Ilyinian complicated interglacial = glacial A of the Cromerian complex and Cromer II interglacial

The faunas of these intervals correspond to MIS 18 and MIS 17 (~0.780 Ma - 0.676 Ma). They are characterized by the presence of rhizodont voles *Mimomys pusillus, M. savini, Pliomys episcopalis*, steppe lemmings *Prolagurus pannonicus, P. posterius* (dominating), *Lagurus transiens*, voles *Lasiopodomys (Stenocranius) gregaloides, Microtus (Terricola) arvalidens, M. arvalinus, M.* ex gr. *oeconomus (=M. protooeconomus, = M. ratticepoides)*, and *Microtus hyperboreus*. Insectivores are represented by *Sorex runtonensis* and *S. (Drepanosorex) savini*. Voles of *Allophaiomys* genus are absent from these faunas (Agadjanian 2009; Maul and Parfitt, 2010; Markova 2007 et al) (Fig. 1, 2, 5).

Donian glaciation

The next evolutionary stage of small mammal faunas is correlatable with the Donian glaciation, well expressed in Eastern Europe (MIS 16, ~0.676 - ~0.621 Ma). There are known several localities of this age. These faunas differ from the earlier ones by the presence of cold-adapted species: *Dicrostonyx* ex gr. *simplicior* and *Lemmus* sp. Rhizodont voles of *Mimomys (M. savini)* and *Pliomys* genera are parts of these faunas. The steppe lemmings are represented by *Prolagurus posterius* and *Lagurus transiens*; the narrow-skulled voles – by *Lasiopodomys (Stenocranius) gregaloides. M. (Terricola) arvalidens, M. arvalinus, M. oeconomus (= M. ratticepoides)*, and *M. hyperboreus* also are present in these faunas (Agadjanian 2009, Markova 1982, 1992). According to the material from West European localities, the first documented appearance of *Microtus agrestis* is dated to that time (Nadachowski 1985) (Fig. 1, 2, 5).

Muchkapian interglacial (=Cromer III)

The Eastern European faunas, correlated with the Muchkapian interglacial (MIS 15, Cromer III, ~0.621 = ~0.563 Ma), are characterized by the presence of rhizodont voles *Mimomys savini*, steppe lemmings *Prolagurus posterius* and *Lagurus transiens*, voles *M. (Terricola) arvalidens, M. arvalinus*, and *M. oeconomus*. The narrow skulled voles are represented by *L. (Stenocranius) gregalis*, though the morphotypes of the teeth, typical for *L. (S.) gregaloides*, still are present in small numbers. The first appearance of *L. (S.) gregalis* distinguishes these faunas from the previous ones. In Western Europe at the beginning of this interglacial. The fauna with *Mimomys savini* was described (Pakefield site) (Stuart and Lister, 2001). In the second part of this interglacial. the first *Arvicola* was distinguished (van Kolfschoten and Turner, 1996) (Fig. 1, 2, 5). Thus, there is a significant difference in the first *Arvicola* appearance (FAD) in Eastern and Western Europe.

Ikoretskian Interglacial (=Cromer IV)

In the localities attributed to the Ikoretskian interglacial in Eastern Europe (Cromer IV in Western Europe, MIS 13, 0.533-0.478 Ma), the first appearance of the archaic water voles *Arvicola cantianus* is recorded. *Rhizodont* voles of *Mimomys* genera are not detected in these faunas (Iosifova et al. 2006). In West-European faunas of that age *Sorex runtonensis*, *Drepanosorex savini, Arvicola cantianus, Microtus arvalinus, M. agrestis*, and *M. oeconomus* have been found (Pitts and Roberts 1997 and others) (Fig. 4).

Okian (=Elsterian, = Anglian) glaciation

In the faunas, correlatable with the Okian (= Elsterian, = Anglian) glaciation (MIS 12; ~0.478 - ~0.424 Ma), *Lemmus* sp., *Dicrostonyx simplicior okaensis, Lagurus transiens*, and *L. (Stenocranius) gregalis* have been described in Eastern Europe (Agadjanian 2009). This assemblage of small mammals undoubtedly reflects the glacial conditions of that time. *Spermophilus* sp., *Allocricetus bursae, Lemmus lemmus, Arvicola cantianus,* and *L. (Stenocranius) gregalis* have been described for this period in Western Europe (van Kolfschoten and Turner 1996). In various parts of Europe that glacial stage is represented by glacial till, fluvioglacial sediments and by loesses. The small mammal data reflect the drastic cooling and aridization during this glaciation (Fig. 1, 2, 5).

The second half of the Middle Pleistocene (MIS 11 - MIS 6)

Likhvinian (= Holsteinian, = Hoxnian) interglacial (MIS 11)

The beginning of the second half of

Stratigraphy	MIS	Western European localities	SDQ values				Eastern European localities	SDQ values			
			N	min	mean	max		N	min	mean	max
Saalian = Walstonian= Dnieper Glaciation	6	Grotte du Lazaret, CII	47		107,9						
		CIII	8		108,6		Igorevka	15	110	125	135
Schöningen= Sandy Lane =Romny Interglacial	7	Weimar-Ehringsdorf (lower trav.)	30	102	112	126	Matveevka	1		102	
		Maastrichte Belvédère 4,	4	86	102	113					
		Maastrichte Belvédère 3	66	94 100,65	102	114 107,1					
		Biśnik Cave, L.19									
Cooling	8										
Reinsdorf= Parfleet= = Kamenka Interglacial	9	Shöningen-Channel II:					Cherny Yar	12	98	108	125
		13 II-2	61	100	119	150	Uzunlar	1		110	
		13 II-3	117	94	118	160					
		13 II-4	135	99	115	137	Plavni	13	105	112	122
		Aveley	2		120						
		Parfleet	4		130	147					
		Gudmore Grove	48	105	133,3						
Cooling	10										
Holsteinian= Hoxnian= Likhvin Interglacial	11	Niide	58	124	146	169	Medzhybozh				
		Hoxne	8	110	140	162	L.10-11	25	91	107	125
		Swanscombe,	4		140		L. 14-15	17	90	116	155
		Bilzingleben II,	52	121	132	145	Gunki 1,	23	120	125	169
		Barnham	14	120	142	170	Gunki 2,	12	120,5	132	170
							Chigirin,	48	101,7	129	167
							Verkhnaya Emancha,	33	100	125	170
							Osernoe,	36	122	130	145
							Rybnaya Sloboda,	14	112	125	160
							Uzmari,	52	112	130	140
							Smolensky Brod	16		124	
Elsterian= Anglian= Oka Glaciation	12										

Fig. 4. Water vole *Arvicola* enamel thickness quotient SDQ by the materials from the Middle Pleistocene European localities

Middle Pleistocene (or the beginning of the Middle Neopleistocene in Russian stratigraphical schemes) is recognized by a noticeable warming of interglacial order – the Likhvinian (Holsteinian, Hoxnian) interglacial. This interglacial is most close to the Holocene optimum in its climatic characteristics. The deposits attributed to the Likhvinian (Holsteinian, Hoxnian) interglacial overlie those of the preceding glaciation (Elsterian in Western Europe, Anglian in Great Britain, Oka glaciation in Eastern Europe). The deposits exposed in the Hoxne stratotype in Great Britain (Layer C) have been dated by uranium series and ESR at 404+33/-42 ka BP, which fits well enough into the time limits of MIS 11 (Grün and Schwartz 2000). More than ten localities of this age were found in Eastern Europe (Markova 2006). They are distributed from the Upper Volga basin to the northern Black Sea region. Studies of the loess-paleosol series on the Russian Plain permitted to identify a horizon of fossil soil – the Inzhavino paleosol – attributable to the Likhvinian Interglacial (Velichko et al. 1992; Shik 2014).

Several very important localities were found in Western Europe. Among them, there is the famous Barnfield Pit locality in Great Britain (Swanscombe, Kent) in the south of the Thames drainage basin. The bone-bearing layers lie on those dated to the Anglian glacial epoch. The fauna was described by D. Schreve under the name

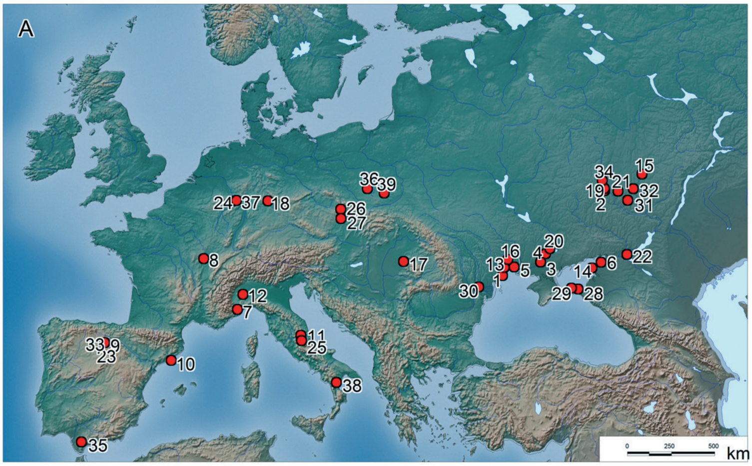

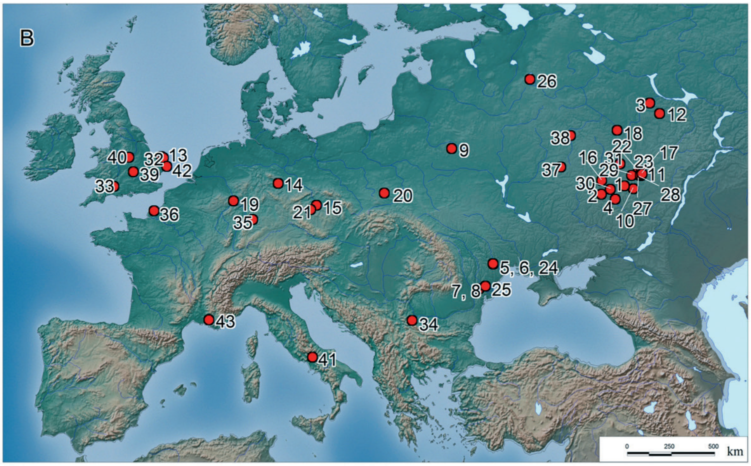

Fig. 5. A – European small mammal localities related to the end of the Early Pleistocene – to the beginning of the Middle Pleistocene (MIS 31 – MIS 19): 1 - Roksolany, 2 - Korotoyak (Ostrogozhsk suite), 3 - Zapadnye Kairy, 4 - Ushkalka, 5 - Limany, 6 - Margaritovo, 7 - Vallonnet, 8 - Les Valerots, 9 - Sima del Elefante, 10 - Vallparadis, 11 - Colle Curti, 12 - Castagnone, 13 - Morozovka 1, 14 - Port-Katon, 15 - Moiseevo 1, 16 - Chirkovo, 17 - Betfia B-V,18 - Untermassfeld, 19 - Petropavlovka 2, 20 - Karai-Dubina, 21 - Log Krasny, 22 - Shamin, 23 - Trinchera Dolina (TD5-TD6), 24 - Kärlich B, 25 - Pagliare di Sassa, 26 - Chlum 6, 27 - Holštejn, 28 - Priazovskoe, 29 - Litvin, 30 - Nagornoe 1, 31 - Ilyinka 6, 32 – Novokhopersk (l.7), 33 - Trinchera Dolina (TD8), 34 - Uryv 3, 35 - El Chaparral. 36 - Zalesiaki IA, 37 - Kärlich C, 38 - Sant'Arcangelo, 39 - Kozi Grzbiet. B – European small mammal localities related to first half of the Middle Pleistocene (MIS 18 - MIS 13): 1-Ilyinka, 2 -Veret'e, 3 - Zaplatino, 4 - Klepki, 5 - Kolkotova Balka (alluv.), 6 - Levada, 7 - Nagornoe I (strip. 4), 8 - Nagornoe II (strip. 2,3,5), 9 - Korchevo, 10 - Novokhopersk 1, 2, 11 - Korostylevo 1, 12 - Berezovka, 13 - West Runton, 14 - Voigtstedt, 15 - Přezletice, 16 - Bogdanovka, 17 - Moiseevo 2,3, 18 - Troitsa 1, 19 - Kärlich F, 20 - Kozi Grzbiet, 21 - Koněprusy -C-718 (L. 8), 22 - Posevkino, 23 - Perevoz, 24 - Kolkotova Balka (Vorona paleosol), 25 – Suvorovo 2, 3, 26 - Roslavl', 27 - Vol'naya Vershina, 28 - Kuznetsovka, 29 - Zherdevka, 30 - Mastyuzhenka, 31 - Shekhman', 32 - Ostend, 33 – Westbury (Unit 15/2 þ 4), 34 - Kozarnika (L.10в), 35 - Mosbach 2, 36 -Boxgrove, 37 - Mikhailovka 2, 38 - Chekalin (Oka glacial deposits), 39 - Oxfordshire, 40 - Mundesley, 41 - Isernia la Pineta, 42 - Pakefield, 43 - St-Esteve-Janson (layers F, G, H).

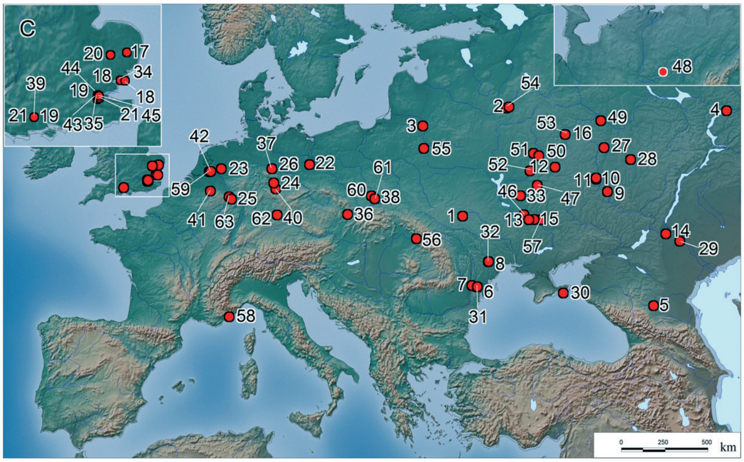

Fig. 5. C – European small mammal localities related to second half of the Middle Pleistocene (MIS 11 – MIS 6): 1 – Medzhibozh, 2 – Smolensky Brod, 3 – Nyaravai-2, 4 – Rybnaya Sloboda, 5 – Okaznoe, 6 – Ozernoe, 7 – Uzmari, 8 – Kolkotova Balka (Inzhavin. paleosol), 9 – Vladimirovka 2, 10 – Strelitsa, 11 – Verkhnaya Emancha, 12 – Mikhailovka 3, 13 – Pivikha, 14 – Raigorod, 15 – Gun'ki 1, 2, 16 – Chekalin (gittja), 17 – Hoxne (layers B2 and B1), 18 – Clacton-on-Sea, 19 – Southfleet Road (L. 3), 20 – Biches Pit, 21 – Barnfield Pit, 22 – Račinéves, 23 – Niide, 24 – Bilsingleben II, 25– Kärlich H, 26 – Shöningen (13 1, 12 B), 27 – Topka, 28 – Rasskazovo, 29 – Cherny Yar, 30 – Uzunlar, 31 – Plavni, 32 – Kolkotova Balka (Kamenk.paleosol), 33 – Priluki, 34 – Gudmor Grouve, 35 – Parfleet, 36 – Za Hájovnou Cave, 37 – Shöningen (L. 13 II-1, II-2, II-3, II-4), 38 – Biśnik (L. 19), 39 –Harnham, 40 – Weimar-Ehringsdorf (lower travert.), 41 – Maastrichte-Belvédère (L. 3,4), 42 – Waginingen Fransche Kamp 1, 43 – Grays Thurrock, 44 – Aveley, 45– Lion Pit, 46– Matveevka, 47 – Igorevka, 48 – Kipievo 1, 2, 49 – Alpatievo, 50 – Pavlovka, 51 – Volzhino, 52 – Strigovo, 53 – Chekalin (fluviogl. deposits), 54 – Konevichi, 55 – Zhukevichi, 56 – Danilovo, 57 – Drabinovka, 58 – Grotte du Lazaret, 59 – Rhenen, 60 – Deszczowa (layers I-IV), 61 – Biśnic (L. 15-14), 62 – Hersbruk, 63 – Ariendorf 1

of Swanscombe Mammalian Zone, MAZ (Schreve 2004a). Of particular interest are remains of primitive *Arvicola terrestris cantianus* with SDQ index equal to ~140 (n=4) (Fig. 1, 2, 4, 5). The Kärlich H locality (Germany) also attributed to this interglacial (van Kolfschoten and Turner 1996).

When studying the faunas dated to that period, much attention is given to evolutionary changes in the phyletic line of *Arvicola* water voles. It should be noted that the earliest stage in this genus evolution is known under different names in different European countries: *Arvicola mosbachensis*, or *A. cantianus* or *A. terrestris cantianus*. When describing particular faunas in the paper, we used the name of the taxon given by the author. An index designating the enamel surface ratio in the *Arvicola* teeth has been widely used in determination of the water vole evolutionary stage and the relative age of enclosing deposits (Markova 1975, 1981; Heinrich 1978) (Fig. 4).

The small mammal faunas of this interglacial are characterized by archaic water voles *Arvicola cantianus (A. mosbachensis, = Arvicola cantianus-terrestris), Lagurus transiens, L. (Stenocranius) gregalis, M. arvalis, M. oeconomus.* The rhizodon voles of *Mimomys* and *Pliomys* genus are absent from these faunas. The SDQ index of *Arvicola* enamel indicates the "mimomys" structure of the teeth (Fig. 4). The intensive evolutionary changes were revealed for the steppe lemming *Prolagurus – Lagurus* phylogenetic linage. *Lagurus transiens* (progressive type) was typical for the localities of Likhvinian in Eastern and Central Europe (= Holsteinian, = Hoxnian) interglacial (Fig. 2).

Borisoglebskian cooling (MIS 10)

The only locality with small mammals, Topka locality (the Don R. drainage basin), was discovered in the deposits overlying those of the Likhvinian Interglacial and in all probability belonging to the cold interval correlatable with the Borisoglebsk loess horizon (MIS 10) (Krasnenkov and Kazantseva, 1993). The locality yielded remains of *Arvicola chosaricus*, but no voles of the *"Terricola= Pitymys"* subgenus typical for Pre-Okian faunas have been found at the Topka (Fig. 1). No small mammal localities of that age are known in Western Europe (Fig. 1, 2, 5).

Kamenkian =Reinsdorf= Parfleet Interglacial (MIS 9)

The well pronounced warming – the Kamenka interglacial (MIS 9, 337–300 ka BP) is represented in Eastern European loess-paleosol sequence by Kamenka paleosol. This paleosol is widely spread over the Russian Plain (Velichko et al. 1992). Several localities of small mammals were described directly in this paleosol (Markova 1982) (Fig. 1, 5). The most characteristic to this interval are *Lagurus* ex gr. *transiens – lagurus (=L. chosaricus), Arvicola chosaricus, L. (Stenocranius) gregalis, Microtus arvalis, Microtus oeconomus.* The above-listed materials possibly are correlatable with the fauna from the Cherny Yar stratotypical section in the Volga drainage basin (Astrakhan Region). The Cherny Yar fauna including *Arvicola chosaricus, Lagurus lagurus pleistocaenicus, Eolagurus volgensis* described by Alexandrova (1976) was recovered from the same layers as the large mammal fauna described by Gromov (1948) and known since then as Khozarian mammal assemblage. The latter includes *Mammuthus trogontherii chosaricus, Camelus knoblochi, Megaloceros euryceros germaniae (= M. giganteus ruffii), Bison priscus longicornis, Equus caballus chosaricus*. The water vole *Arvicola chosaricus* is evolutionary more advanced species as compared with *A. cantianus* and is an indicator species of the Khozarian faunas (Fig. 2, 4). In steppe lemmings of the *Lagurus* genus the 'lagurus' morphotype is dominant in the faunas of the Khozarian type; more archaic 'transiens' morphotypes have been recorded in the steppe lemming remains, but their proportion is rater small (Markova 1982). The new OSL data indicate however more younger age of Khozarian fauna from the Cherny Yar stratotype locality (Zastrozhnov et al. 2017). So, till now the position of the Khozarian faunas is discussed.

The locality of Schöningen 13-II, Layers 13 II-1, II-2, II-3, II-4 includes *Arvicola terrestris cantianus, Microtus (Terricola) subterraneus, M. arvalis, M. agrestis, M. oeconomus, L. (Stenocranius) gregalis, Apodemus sylvaticus* and others. Geological data and the Arvicolinae morphological characteristics gave grounds for dating the fauna to an interglacial younger than Holsteinian – to the **Reinsdorf** one correlatable with MIS 9 (van Kolfschoten 2014) (Fig. 1, 2, 4, 5).

The Purfleet locality (Great Britain) is usually assigned to the second interglacial that followed the Anglian glacial stage and is correlated with MIS 9 (Schreve 2004b). The mammal fauna includes 21 taxa. Among the identified taxa are *Sorex araneus, S. minutus, Arvicola terrestris cantianus, Microtus agrestis, M. arvalis, Apodemus sylvaticus* and others. The water vole teeth are distinct for more advanced morphology than have *Arvicola* from the Barnfield Pit locality with SDQ=130, but more archaic than those described in water vole remains from the localities correlatable with MIS 7 (Fig. 1, 2, 4, 5). Schreve (2001b) described this fauna as belonging to the Purfleet Mammal Assemblage-Zone – MAZ Purfleet. Unfortunately the lagurides are practically absent from Western European faunas.

Orchikian cooling (MIS 8)

The Kamenka (=Purfleet, =Reinsdorf) interglacial was followed by a new cooling (MIS 8, 300-243 ka BP), which was named after the name of loess horizon distributed on the Russian Plain as the Orchikian one (Velichko et al. 1992). The faunas of this age are absent from Eastern Europe. A few localities of this age were found in Western Europe. The Harnham locality was discovered in the south of Great Britain, at the Avon and the Ebble interfluve. It was dated by OSL to approximately 250 ka BP and attributed to the end of MIS 8 (Bates et al. 2014). The locality yielded some mammal bones: *Apodemus* sp., *Clethrionomys* sp. *Microtus oeconomus*, Microtus sp. (Fig.1, 2, 5). A unique multilayered cave site with artifacts of the Middle Palaeolithic was discovered in Poland in the south of Częstochowa Upland (Biśnic cave, layer 19) (Fig. 1, 2, 4, 5). The sequence includes several cultural layers spanning time interval from MIS 9 (?) to MIS 2 (Cyrec et al. 2010). Layer 19 correlated by Cyrec and his coauthors with MIS 8-8/7 and with the Odra glaciation yielded remains of mammal fauna, including cold-tolerant, steppe, aquatic, and forest species (Socha 2014). The fauna is dominated by cold-adapted (lemmings, narrow-skulled vole) and eurybiont species. As follows from the enamel index of water vole teeth (SDQ = 100.65-107.12) (Fig.4), the fauna may be dated to the second half of the Middle Pleistocene.

Romnian, = Schöningen, = Sandy Lane interglacial

The fauna found in the Matveevka locality on the Sula R. (the Dnieper R. drainage basin, Cherkassy Region, Ukraine, 49º31´ N, 32º41´ E) may be assigned to the end of the Romnian warming (MIS 7). The sequence includes a layer of sand and gravel with bone remains of small mammals. Upwards it is replaced with loess layer overlain in turn with the Dnieper till; still higher a loess-like loam occurs including a paleosol horizon (Krokhmal and Rekovets 2010; Rekovets, 1994). The fauna composition is as follows: *Lagurus lagurus, Eolagurus* sp., *Arvicola chosaricus, Microtus arvalidens, M. arvalis, M. oeconomus, L. (Stenocranius) gregalis,* et al. (Fig. 1, 2, 4, 5). The Lion Pit locality in the lower reaches of the Thames R. (West Thurrock, Great Britain) yielded mammal fauna including *Apodemus sylvaticus, Vulpes* cf. *vulpes, Ursus arctos, Mammuthus trogontherii, Palaeoloxodon antiquus, Equus ferus, Stephanorhinus kirchbergensis,* et al. The fauna was attributed by Schreve (2004c) to the Sandy Lane Mammal Assemblage Zone (MIS 7) (Fig. 1, 2, 5). The Aveley locality, Great Britain, was exposed in a sand quarry; the fauna includes *Arvicola terrestris cantianus, Microtus agrestis* or *Microtus arvalis, Apodemus sylvaticus*, and others. The enamel index of water voles SDQ=120 (Parfitt 1998; Schreve 2004c) (Fig. 4).

In Central Europe several faunas were correlated with MIS 7. The small mammal fauna of the Wageningen - Fransche Kamp 1 locality (the Netherlands) includes *Arvicola cantianus, Microtus arvalis/agrestis, Apodemus sylvaticus, A. maastrichensis* and others and undoubtedly corresponds to a warm interval. Van Kolfschoten (2014) correlates the locality with the interglacial preceding the Saale glaciation and with MIS 7 to the **Shöningen Interglacial** (Fig. 1, 2, 5). A fauna closely resembling the above listed was described in the Maastrichte-Belvédère, layers 3-4. In the opinion of van Kolfschoten, it is synchronous to the previous locality and in common with it corresponds to MIS 7 (Fig.1, 2) (van Kolfschoten 2014). A rich locality of Weimar-Ehringsdorf (Lower Travertine) in Thuringia, Central Germany, contains *Clethrionomys glareolus, Arvicola cantianus, Microtus oeconomus, Microtus subterarraneus, Lasiopodomys gregalis* and others [Maul 2000]. Judging by the water vole enamel index (SDQ) equal to 113.5 (Heinrich, 1990), it corresponds to MIS 7 (7e/7c). The U-series dates confirm the validity of the deposits attribution to MIS 7: >350,000–200,000 yr BP (Blackwell and Schwarcz 1986). Van Kolfschoten agrees with the locality dating to the last Middle Pleistocene interglacial. MIS, 7 (van Kolfschoten 2014).

Dnieper, = Saalian, = Walstonian glaciation (MIS 6)

More than ten Eastern European localities are correlated with the Dnieper glaciation (MIS 6). They distributed from 65º N to 49º N on the Russian Plain (Fig. 7) (Agadjanian 2009; Krokhmal and Rekovets 2010; Markova 1992; Motuzko 1985 et al.). The fauna includes cold-tolerant species *(Dicrostonyx* cf. *simplicior, Lemmus sibiricus, L. (Stenocranius) gregalis)*, several steppe species (*Spermophilus* sp., *Ellobius* sp., *Eolagurus* cf. *luteus, Lagurus lagurus* and others), and also sub-aquatic and meadow-plain animals (*Arvicola* cf. *chosaricus, Microtus oeconomus, Microtus arvalis*). The forest species are practically absent from the localities of this age; only *Microtus agrestis* and *Clethrionomys glareolus* occur occasionally in these faunas (Fig. 1, 2, 4, 5).

Several important localities were found in Western Europe (the Ariendorf 1 and the Hersbruck cave locality, Germany; the Biśnic cave locality, layers 15-14 and the Deszczowa in Poland; the Rhenen locality in the Netherlands; the Grotte du Lazaret in France) (van Kolfschoten 1990; von Koenigswald and Heinrich, 1999; Nadachowski et al. 2009; Krajcarz 2012; Chaline 1972; Socha 2014 and others). Among the small mammals recovered are *Dicrostonyx* cf. *henseli/gulielmi, D. simplicior, Lemmus lemmus, Arvicola cantianus (=terrestris ssp.A), Clethrionomys glareolus, Microtus agrestis, Microtus arvalis, M. oeconomus, L. (S.) gregalis*, and others. In the south of France (Grotte du Lazaret) bones of *Marmota marmota, Eliomys quercinus, Microtus (=Terricola) duodecimcostatus, Pliomys lenki (=coronensis), Apodemus sylvaticus* were also found (Chaline 1972). The dates obtained (by U-Th series and ESR techniques) for the cultural layer of the Grotte du Lazaret permit the site to be attributed to MIS 6 and to the last Middle Pleistocene glacial stage (Fig. 1, 2, 4, 5).

CONCLUSION

The principal trends in the small mammal evolutionary changes during the very end of the Early Pleistocene and the Middle Pleistocene have been revealed, and the East European and West European faunas were compared. An integrated analysis of theriological. geological. and geochronological data available from the Middle Pleistocene localities in Europe has shown marked changes in the small mammal fauna through the period under consideration and provided information on the climate and environments at different time intervals. The changes in Arvicolinae phyletic lines made possible a correlation between the West European and East European mammal localities. They are traceable by changes in the species composition, first occurrences of new species, and morphological changes in several phylogenetic lineages.

There are some difficulties in correlation between West European faunas and those in Eastern Europe which arise from different levels of knowledge and different taphonomic features of the localities. On the Russian Plain most of the localities are found in great geological sequences (mostly in the fluvial sequences overlain by the well studied loess-paleosol series). These sequences were investigated not only paleontologically, but also by several geological methods including paleomagnetic analysis. Those supplementary data help to determine the stratigraphic position of mammal faunas. Most of the localities in the region of the Black Sea coasts include, along with mammals, shells of brackish-water mollusks varying in their evolutionary level. The mollusk assemblages permit the mammal faunas to be directly correlated with the Black Sea transgressions and palaeogeographic events in the Eastern Mediterranean (Mikhailesku and Markova 1992). As is known, a significant part of localities in Western Europe are related to karst caves and fissures. In such localities faunal remains of different age are often found to be mixed, and data of palaeomagnetic analysis are also not quite reliable. There are, however, a number of multilayered localities (Kärlich, Shöningen, Sima del Elephante, Grand Dolina, Colle Curti, Castagnone), the localities from the fluvial sequences from the Thames R. terraces and some others) where multidisciplinary studies (including palaeomagnetic analysis and absolute dating) were performed. The correlation between the East European localities and those mentioned above are very realistic.

The relatively long time interval of the Middle Pleistocene is noted for several climatic events of global scale (glaciation – interglacial) that occurred during it. The biostratigraphic scheme of the Middle Pleistocene has been developed and maps of small mammal localities compiled (Fig. 1, 2, 5).

Thus, faunas of small mammals related to the long Middle Pleistocene interval allow assessment of their taxonomy and evolutionary development. These data can also help us to divide the geological deposits by age and permit reconstruction of the palaeogeographic picture of the past. The results obtained may serve as an important component for compiling biostratigraphic schemes of the Middle Pleistocene and of the Pleistocene in general.

ACKNOWLEDGMENTS

This study was supported by the RFBS grant No 13-05-00056 and by the project of Institute of Geography RAS "Mammal faunas of Northern Eurasia in the Late Pleistocene – Holocene: taxonomy, diversity and evolution". We are very grateful for our reviewers for their constructive comments.

REFERENCES

Agadjanian A.K. (2009). Small mammals of the Pliocene – Pleistocene of the Russian Plain. Moscow: Nauka Press (in Russian).

Agusti J. (1992).The Allophaiomys complex in Southern Europe, Geobios, 25 (1), pp. 133-144

Alexandrova L.P. (1976). Anthropogene rodents of the European part of USSR. Moscow: Nauka Press (in Russian).

Bates M.R., Wenban-Smith F.F., Bello S.M., Bridgland D.R., Buck L.T., Collins M.J., Keen, J., Leary D.H., Parfitt S.A., Penkman K., Rhodes E., Ryssaer C. and Whittaker J.E. (2014). Late persistence of the Acheulian in southern Britain in an MIS 8 interstadial: evidence from Harnham, Wiltshire. Quaternary Science Reviews, 101, pp. 159-176.

Blackwell B. and Schwarcz H.P. (1986). U-Series analyses of the Lower Travertine at Ehringsdorf, DDR. Quaternary Research, 25 (2), pp. 215-222.

Chaline J. (1972). Les Rongeurs du Pleistocéne moyen et supérieur de la France. Paris: Cahiers de Paléontologie, CNRF.

Cuenca-Bescós G., Rofes J., López-García J.-M., Blain H.-A., Rabal-Garcés R., Sauqué V., Arsuaga J.L., Bermúdez de Castro J. M. and Carbonell, E. (2013). The small mammals of Sima del Elefante (Atapuerca, Spain) and the first entrance of Homo in Western Europe. Quaternary International. 295, pp. 28–35.

Cyrek K., Socha P., Stefaniak K., Madeyska T., Miroslaw-Grabowska J., Sudoł M. and Czyźewski Ł. (2010). Palaeolithic of Biśnic Cave (Southern Poland) within the environmental Background. Quaternary International. 220, pp. 5–30.

Gibbard P.L., Cohen K.M., Boreham S. and Moscariello A. (2004). Global chronostratigraphical correlation table for the last 2.7 million years. Subcommission on Quaternary Stratigraphy, International Commission on Stratigraphy: Cambridge.

Gromov V.I. (1948). Palaeontological and archaeological foundation of the stratigraphy of the Quaternary continental deposits in the territory of the USSR. Moscow: the USSR Academy of Sciences (in Russian).

Grün R. and Schwartz H.P. (2000). Revised open system U-series/ESR age calculations for teeth from Stratum C at the Hoxnian interglacial type locality, England. Quaternary Science Reviews, 19, pp.1151-1154.

Heinrich W.-D. (1978). Zur biometrischen Erfassung eines Evolutionstrends bei Arvicola (Rodentia, Mammalia) aus dem Pleistozän Thüringens. Berlin: Säugetierkdl. Inform., 2, pp. 3-21.

Heinrich W.-D. (1990). Some aspects of evolution and biostratigraphy of Arvicola (Mammalia, Rodentia) in the central European Pleistocene. Prague: Int. Symp. Evol. Phyl. Biostr. Arvicolids., pp. 165-180.

Fejfar O. and Horaček I. (1990). Review of fossil arvicolids (Mammalia, Rodentia) of the Pliocene and Quaternary in Czechoslovakia. Int. Symp. Evol. Phyl. Biostr. Arvicolids. Prague: Geological Survey, pp. 125–132.

Iosifova Yu.I., Agadjanian A.K., Pisareva V.V., and Semenov V.V. (2006). The Upper Don basin is the stratotype of the Middle Pleistocene of Russian Plain. Palynological Reconstructions: Stratigraphy, Geoecology. S.-Petersburg: Nedra Press, pp. 41–121 (in Russian) .

Krasnenkov R.V. and Kazantceva, N.E. (1993). The discovery of the early Dnieper alluvium in the Upper Don terraces, Bull. of regional commission of Central and Southern Russian Platform, 2, pp.153-161 (in Russian).

Krajcarz M.T. (2012). Small fossil wolverine Gulo from Middle Pleistocene of Poland. Acta zoologica cracoviensia, 55(1), pp. 79-87.

Krokhmal A.I. and Rekovets L.I. (2010). Pleistocene small mammal localities of Ukraine and adjacent territories. Kiev: LAT and K Press (In Russian)

Lisiecki L.E. and Raymo M.E. (2005). A Pliocene-Pleistocene stack of 57 globally distributed benthic δ18O records. Paleoceanography, 20 (1), PA1003. doi:10.1029/2004PA001071.

Markova A.K. (1975). Pleistocene rodents of Dnieper basin and its significance for the palaeogeography and stratigraphy. Aftoref. disser. na soisk. uch. stepeni kand. geogr. nauk. Moscow: Institute of Geogr. Ac. Nauk USSR Press (in Russian).

Markova A.K. (1981). Morphological changes of water voles teeth during the Pleistocene, In: A.A.Velichko and S.M. Shik, eds., The questions in Pleistocene palaeogeography of glacial and periglacial regions. Moscow: Nauka Press, pp. 91-110 (in Russian).

Markova A.K. (1982). Pleistocene rodents of the Russian Plain. Moscow: Nauka Press (in Russian).

Markova A.K. (1990). The sequence of Early Pleistocene small-mammal faunas from the South Russian Plain. Quartärpaläontologie, 8, pp. 131-151.

Markova A.K. (1992). Pleistocene microtheriofauna of Eastern Europe. In: A.A. Velichko and S.M. Shik, eds., Stratigraphy and Paleogeography of Quaternary of Eastern Europe, Moscow: Inst. of Geography RAS, pp. 50-94 (in Russian).

Markova A.K. (1998). Pleistocene rodents of the Central and Southern Russian Plain. In: J.J. Saunders, B.W. Styles and G. F. Baryshnikov, eds., Quaternary Paleozoology in the Northern Hemisphere. Illinois State Museum Scientific papers, XXVI, pp. 119-143.

Markova A.K. (2005). Eastern European rodent (Rodentia, Mammalia) faunas from the Early-Middle Pleistocene transition. Quaternary International. 131, pp. 71-77.

Markova A.K. (2006). Likhvin Interglacial small mammal faunas of Eastern Europe. Quaternary International. 149 (1), pp. 67-79.

Markova A.K. (2007). Pleistocene mammal faunas of Eastern Europe. Quaternary International. 160, pp. 100-111.

Markova A.K. (2014). European small mammal faunas during the end of the Early Pleistocene – the beginning of the Middle Pleistocene. Izvestia RAS, Seria geograph., 5, pp. 83-98 (In Russian)

Markova A. and van Kolfschoten T. (2012). Middle Pleistocene small mammal faunas of Eastern and Western Europe: chronology, correlation. Geography, environment, sustainability, 5(4), pp. 17-23. Available at: https://doi.org/10.24057/2071-9388-2012-5-4-17-23.

Markova A.K. and Puzachenko A.Yu. (2016). The European small mammal faunas related to the first half of the Middle Pleistocene. Quaternary International. 420, pp. 378-390.

Markova A.K. and Vislobokova I.A. (2016). Mammal faunas in Europe at the end of the Early – beginning of the Middle Pleistocene. Quaternary International. 420, pp. 363- 377.

Masini F. and Sala B. (2011). Considerations on an integrated biochronological scale of Italian Quaternary continental mammals. Italian Journal of Quaternary Sciences, 24 (2), pp. 193-198.

Maul L.C. (2000). Die Fossilfundstelle Weimar-Ehringsdorf. Eine Überisicht. Geowiss. Mitt. Thüringen, 10, pp. 167-174.

Maul L.C. (2001). Die Kleinsäugerreste (Insectivora, Lagomorpha, Rodentia) aus dem Unterpleistozän von Untermassfeld. In: R.-D. Kahlke, ed., Das Pleistozän von Untermassfeld bei Meiningen (Thüringen). Monographien des Römisch-Germanischen Zentralmuseums Mainz, 40 (3), pp. 783–887.

Maul L.C., Heinrich W.-D., Parfitt S.A. and Paunescu, A.-C. (2007). Comments on the correlation between magnetostratigraphy and evolution of Microtus (Arvicolidae, Rodentia, Mammalia) during the Early and early Middle Pleistocene. Courier Forschungsinstitut Senckenberg, 259, pp. 243-263.

Maul L. and Markova A.K. (2007). Similarity and regional differences in Quaternary arvicolid evolution in Central and Eastern Europe. Quaternary International. 160 (1), pp. 81-99.

Maul L. and Parfitt S.A. (2010). Micromammals from the 1995 Mammoth Excavation at West Runton, Norfolk, UK: Morphometric data, biostratigraphy and taxonomic reappraisal. Quaternary International. 228, pp. 91-115.

Maul L.C., Rekovets L., Heinrich W.-D., Keller T. and Storch G. (2000). Arvicola mosbachensis (Schmidtgen 1911) of Mosbach 2: a basic sample for the early evolution of the genus and a reference for further biostratigraphical studies. Senckenbergiana lethaea, 80 (1), pp. 129-147.

Mikhailesku C.D. and Markova A.K. (1992). The paleogeographical stages of fauna development on the south of Moldova in Anthropogene. Kishinev: Shtiintsa Press. (In Russian).

Motuzko A.N. (1985). Anthropogene rodents of Belorussia and adjacent territories. Minsk: Nauka i Tekhnika Press, pp.173-186 (In Russian).

Nadachowski A. (1985). Biharian voles (Arvicolidae, Rodentia, Mammalia) from Kozi Grzbiet (Central Poland). Acta zool. Cracov., 29(2), pp. 13-28.

Nadachowski, A. (1990). Review of fossil Rodentia from Poland (Mammalia). Senckenbergiana Biologica, 70(4/6), pp. 229-250.

Nadachowski A., Žarski M., Urbanowski M., Wojtal P., Miekina B., Lipecki G., Ochman K., Krawczyk M., Jakubowski G. and Tomek T. (2009). Late Pleistocene Environment of the Czêstochowa Upland (Poland) reconstructed on the basis of faunistic evidence from archaeological cave sites. Kraków: Institute of Systematic and Evolution of Animals, Polish Academy of Sciences.

Parfitt S. (1998). The interglacial mammalian fauna from Barnham. In: N. Ashton, S.G. Lewis and S. Parfitt, eds., Excavations at the Lower Palaeolithic Site at East Farm, Barnham: 1989-94. London: British Museum Occasional Paper, 125, pp. 111-147.

Pitts M. and Roberts M. (1997). Fairweather Eden: Life in Britain half a million years ago as revealed by the excavations at Boxgrove. London: http://en.wikipedia.org/wiki/Random_House ISBN 9780712676861.

Rekovets L.I. (1994). Anthropogene small mammals from the southern part of Eastern Europe. Kiev: Naukova Dumka Press (In Russian).

Schreve D.C. (2004a). The mammalian fauna of Barnield Pit, Swanscombe, Kent. The Quaternary mammals of Southern and Eastern England. Field Guide. EuroMam UK, pp. 29 -48.

Schreve D.C. (2004b). Late Middle Pleistocene (MIS 9) river Thames terrace deposits at Purfleet, Essex. The Quaternary mammals of Southern & Eastern England. Field Guide. EuroMam UK, pp. 49 -67.

Schreve D.C. (2004c). The mammalian fauna of the penultimate (MIS 7) interglacial in the lower Themes valley. The Quaternary mammals of Southern and Eastern England. Field Guide. EuroMam UK, pp. 69 – 79.

Shik S.M. (2014). Neopleistocene of central European Russia (the new ideas on stratigraphy and palaeogeography). Stratigraphy. Geol. Correlation, 22 (2), pp. 108-120 (In Russian).

Siori M.S. and Sala B. (2007). The mammal fauna from the late Early Biharian site of Castagnone (Northern Monferrato, Piedmant, NW Italy). Geobios, 40, pp. 207-217.

Socha P. (2014). Rodent palaeofaunas from Biśik Cave (Krakow-Częstochowa Upland, Poland): palaeoecological. palaeoclimatic and biostrtigraphic reconstruction. Quaternary International. 326-327, pp. 64-81.

Stuart A.J. and Lister A.M. (2001). The mammalian faunas of Pakefield/Kessingland and Corton, Suffolk, UK: evidence for a new temperate episode in the British early Middle Pleistocene. Quaternary Science Reviews, 20, pp. 1677–1692.

Van Kolfschoten T. (2014). The Palaeolithic locality Schöningen (Germany): A review of the mammalian record. Quaternary International. 326-327, pp. 469-480.

Van Kolfschoten T. (1990). Review of the Pleistocene arvicolid faunas from the Netherlands. Prague: Int. Symp. Evol. Phyl. Biostr. Arvicolids, pp. 255-274.

Van Kolfschoten T. and Turner E. (1996). Early Middle Pleistocene Faunas from Kärlich and Miesenheim I and their biostratigraphic implication. In: Turner C., ed., The early Middle Pleistocene in Europe. Balkema, Rotterdam, pp. 227–253.

Van der Meulen A.J. (1973). Middle Pleistocene smaller mammals from the Monte Peglia (Oriento, Italy) with special reference to the phylogeny of Microtus (Arvicolidae, Rodentia). Quaternaria, 17, pp. 1-144.

Velichko A.A., Markova A.K., Morozova T.D., Nechaev V.P., Svetlitckaya T.V., Tcatckin A.I. and Chichagova O.A. (1992). The geochronology of loess-soil formation S-W of the Russian Plain by new data. Geochronology of the Quaternary. Moscow: Nauka Press, pp. 28-33 (In Russian).

Vislobokova I. and Tesakov A. (2013). Early and Middle Pleistocene of Northern Eurasia. In: Elias S.A., ed., The Encyclopedia of Quaternary Science, vol. 4. Amsterdam: Elsevier, pp. 605-614.

Von Koenigswald W. and Heinrich, W.-D. (1999). Mittelpleistozäne Säugetierfaunen aus Mitteleuropa – der Versuch einer biostratigraphischen Zuordnung. Darmstädter Beiträge zur Naturgeschichte, 9, pp. 53-112.

Von Koenigswald W. and van Kolfschoten, T. (1996). The Mimomys – Arvicola boundary and the enamel thickness quotient (SDQ) of Arvicola as stratigraphic markers in the Middle Pleistocene. In. Turner C., ed., The early Middle Pleistocene in Europe. Balkema, Rotterdam, pp. 211-226.

Zastrozhnov A., Danukalova G. and Murray A. (2017). New data on the age of the Neopleistocene deposits of the lower Volga sites according to the OSL method results. Fundamental problems of Quaternary: the results of investigation and the main directions in the future. Moscow: GEOS, pp. 139-140.

Received on June 21st, 2018 Accepted on July 31st, 2018

AUTHORS

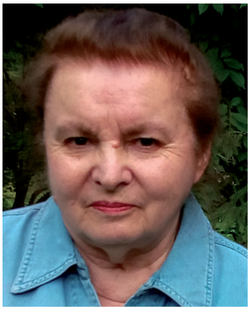

Anastasia K. Markova is specialist of Quaternary palaeontology and historical biogeography and works in the Laboratory of Biogeography of the Institute of Geography RAS. She is the Doctor of Geographical Sciences. Her main fields of interests focused on the evolutional peculiarities of Pleistocene small mammals, their taxonomy, geographical distribution in the past and palaeoecology. She leaded the intra-institutional scientific collective, which study the species composition, biodiversity and distribution of Late Pleistocene and Holocene mammals of Northern Eurasia. She is the member of Russian Quaternary Commission and the member of editorial board of the journal "Stratigraphy. Geological correlation". A.K. Markova published more than 250 scientific papers including 4 monographs, chapters in 8 collective monographs and chapters in 4 palaeogeographical atlases.

Andrey Yu. Puzachenko is a specialist in vertebrate zoology and historical biogeography. He works in the Laboratory of Biogeography of the Institute of Geography RAS. He is the Doctor of biological Sciences. His main fields of interests focus on morphological diversity of recent and extinct mammal species and the evolution of the Pleistocene mammalian faunas in the Holarctic during the Middle and the Late Pleistocene. A. Yu. Puzachenko published 191 scientific articles in Russian and international journals, and chapters in 13 collective monographs.

Ekaterina Filep[1*], Christine Bichsel[1]
[1] Department of Geosciences, University of Fribourg, Fribourg, Switzerland
*** Corresponding author:** ekaterina.filep@unifr.ch

TOWARDS A RESEARCH AGENDA ON STEPPE IMAGINARIES IN RUSSIA AND THE SOVIET UNION

ABSTRACT. This article proposes that there is a need for a sustained engagement with and deconstruction of steppe imaginaries in Russian and Soviet literature in the twentieth century. It argues that "steppe" is not solely a term describing a particular environment, but also a pivotal idea which has shaped and shapes identities, cultural assumptions, political reasoning and even geopolitical thought. Based on the review of existing scholarship, the paper demonstrates the centrality of the steppe as a key imaginary for Russian history until the nineteenth century. However, it also reveals that the research on the relevance of such imaginaries for Russian and Soviet political history in the twentieth century is largely absent. Yet, it was during this period that the steppe environments underwent largescale transformations through processes of land reclamation, irrigation development and industrial agriculture.

KEY WORDS: Russia, steppe, imaginary, Soviet Union, literature, landscape

CITATION: Ekaterina Filep and Christine Bichsel (2018) Towards a research agenda on steppe imaginaries in Russia and the Soviet Union. Geography, Environment, Sustainability, Vol.11, No 3, p. 39-48
DOI-10.24057/2071-9388-2018-11-3-39-48

INTRODUCTION

For Russian geographer and eminent steppe expert Alexander Chibilev, there are two kinds of steppe: one kind is the physical environment, the other is a literary figure (Chibilev 1990: 2, 1997: 1). A. Chibilev (2009) further stresses the significance of this latter kind of steppe in his book Steppe Masterpieces, which contains a rich collection of nineteenth and twentieth century writings, including poetry, prose, letters and memoirs by authors from Russia to Hungary devoted to the steppe. The historical importance of steppe as a symbolic figure is demonstrated by its prominent place in works of Russian literary writers such as Anton Chekhov, Nikolai Gogol and Ivan Turgenev. Furthermore, steppe imaginaries significantly characterize geographical descriptions in Soviet scientific and popular literature (Bichsel 2012; 2017). Beyond past times, the steppe as a geopolitical narrative also resurfaces in current political debates. For example, in her analysis of recent political events, Russian journalist and writer Sonja Margolina raises the question whether the political strategy of present-day Russia will attempt to centre its mythological origins and cognitive map rather on the steppe regions of the Volga and Central Asia as opposed to the more European Kievan Rus (Margolina 2014). Overall, the research within and outside Russia reflects the high significance of the steppe for understanding Russian cultural and political space.

During the last several decades, scholars have given considerable attention to exploring the material and symbolic aspects of the steppe for Russian history and identity until the nineteenth century. Their works, which point to the centrality of steppe as a key imaginary, are mainly drawing on artistic writings, but also other types of sources. This article provides a comprehensive review of these scholarly works and arranges them into thematic sections. Based on this review, the paper argues that there remains a need for further research on steppe as a symbolic figure beyond 1900, as it was precisely during this period that steppe's environment underwent significant physical transformation. Thus, the paper directs scholarly attention towards an identified gap in steppe research and explains the continued relevance of steppe and steppe imaginaries in the twentieth century.

The article opens with the discussion of publications which focus on the symbolic significance of the steppe to Russian statehood and nation building. Then, it reviews the research that demonstrates the link between literary and artistic representations of nature and the formation of Russians' perceptions of self and nation. In its last section, the paper discusses scholarly works, which focus on the representations of nature in Soviet artistic, scientific and popular literature. The article concludes with the suggestions on the possible directions and potentials for future research.

MATERIALS AND METHODS

The empirical data for this paper consists mainly of scholarly research devoted to the analysis of the physical and symbolic significance of the steppe to Russian social and political thought. In addition, we consider artistic and scientific literature in Russian language written during the 19th and 20th century. The artistic literature represents novels and stories (Rus. "roman", "povest'", "rasskaz") in Russian language which address the theme of the steppe. We conceive of this literature as a product of culture being situated in particular social and political contexts. The scientific literature includes texts written by scientists and naturalists in Russian language which offer geographical descriptions of the steppe. Geographical description is understood as the attempt to characterise a geographical region or a particular environment based on its physical. historical. economic, political and cultural features. These works were produced for a scientific, but sometimes also for a more general public. The selected scientific texts and further secondary literature was obtained through library research in the Russian State Library in Moscow as well as in the library of the Institute of Geography, Russian Academy of Sciences. We adopt historical discourse analysis as the methodology for this paper. Historical discourse analysis attempts to uncover the historical changes of statements in the course of time which produce, but are also produced by new forms of being, thinking and acting. It seeks to explain how discourses change in a historical process, and also themselves change social. political. economic and philosophical constellations in history (Landwehr 2008: 21).

RESULTS AND DISCUSSION

The Eurasian steppe and Russian statehood

Recent international research proposes that statehood in Russia is intimately tied to the environment of the steppe. Iver B. Neumann and Einar Wigen contend that the emergence of the Russian polity towards the end of the fifteenth century was modelled on what they term a "steppe tradition" which has ordered politics in the Eurasian steppe for almost three thousand years (Neumann and Wigen 2013). This element, in their view, distinguishes Russia and Turkey from other European states. Russia and Turkey, they argue, expose a rationality of rule that is a hybrid of European and steppe elements (see also A. Chibilev, S. Bogdanov, M. Sdykov 2011). They suggest that this historically emerging pattern is still significant today and offers an explanatory frame to historians and other scholars of Russian imperialism and culture, of Russia's perception of self, its borders and the relationship with its neighbours.

In his detailed historical analysis, Willard Sunderland shows how the Eurasian steppe was gradually but persistently transformed over time as it was included in the Russian state between the sixteenth and the nineteenth century. By the beginning of the twentieth century, he argues, "… the steppe had been so profoundly transformed by Russian imperialism that it was difficult for contemporaries to determine whether it constituted a borderland, a colony, or Russia itself" (Sunderland 2004: 223). While the colonization of the steppe was discursively constructed by statesmen as providing order and security as well as progress and enlightenment, the observed reality of the steppe often contradicted these schemes. Sunderland stresses how the physical and the imagined steppe were mutually constitutive for this process. He demonstrates how these two realities "were deeply intertwined and mutually influential. with statesmen, scholars, literature, natives, 'resettlers', and sundry other colonizers all playing their irreplaceable parts in the steppe's material and symbolic creation" (ibid. 224). The steppe as imaginary, in this view, must be understood in its interplay with observed states of the physical environment.

Similarly, in his historical analysis Michael Khodarkovsky points to the diachronically changing definitions of the steppe with the expansion of the Russian settlement toward the south between the fifteenth and the eighteenth century (Khodarkovsky 2002). He shows the complex relationship between Russia and the steppe for this historical period during which the steppe was a frontier that, through intricate transformations, became a part of the Russian Empire. Such a transformation was not a uniformly unfolding process, but was characterised by alternating periods of peaceful interaction and violent clashes between Russians and nomadic peoples who inhabited the steppe. Through the expansion of Russian settlement southward, he argues, the former "wild field" of the steppe became tamed materially and discursively and thus became an integral physical and conceptual part of the Russian Empire. During this process, he argues, Russian understanding of the steppe repeatedly changed. His research suggests that the steppe cannot be understood as a historically stable category, but must be questioned for its contingent meaning over time.

Further research has been carried out on the ethnic groups or regions of the steppes by such scholars, as Barrett, (1999), O'Rourke, (2000), Khodarkovsky (1992) or agriculture on the steppes (Moon 2008; 2013).

However, while the above-discussed authors trace the symbolic significance of the steppe for Russian history as far back as the ninth century, their reflections mostly end with the late nineteenth century and only marginally touch or do not address the twentieth century. Yet, as recent research has shown, the steppe continues to be a key theme of Russian and then Soviet political development beyond the nineteenth century.

Landscape and Russian national identity

Recent literature in the field of literary and art criticism as well as in the emerging field of environmental history has argued that the perception of the Russian landscape and its environment is important to understanding the emergence and development of Russian national identity. In his analysis of Imperial Russia, Mark Bassin stresses the importance of geographical imaginaries for processes of nation-building and establishing national identity (Bassin 1999, 2000; Bassin et al. 2010). In his book *Imperial Visions: National imagination and geographical expansion in the Russian Far East 1840—1865*, Bassin examines Russia's imaginative geographies through the analysis of perception of the new territory of the Amur region which came under Russian rule through imperial expansion. He argues that not only specific landscapes, but also entire geographical regions are subject to cultural constructions in specific political context. He thus proposes to analyse not only social institutions and processes, but also these cultural constructions for their perceived and signified ideological content (Bassin 1999).

Christopher Ely takes this reflection further by insightfully demonstrating the close link between literary and artistic representations of nature with the formation of Russians' perceptions of self and nation (Ely 2002). He reveals the historically contingent cultural construction of Russia's landscape which dramatically changed during the nineteenth century. According to Ely, during the early 1800s, Russians commonly accepted the Western European view that their landscape was unattractive and monotonous. An important reason for this was that it did not offer diversity in morphological forms over small distances — a central feature of contemporary aesthetic theory. However, over the next several decades, writers, travellers, painters and photographers sought to offer new interpretations as well as appreciations of their own nature and space in opposition to the dominance of Western European aesthetic models. This must be understood in the light of the political developments, more specifically the growing importance of the concept of the nation. Ely argues that it was during this period that vast, open spaces such as the steppe were no longer thought to be monotonous and non-descript, but rather began to signify immensity and to imply a special Russian sense of freedom (Ely 2002).

In a similar vein, Jane Costlow examines how images of the Russian forest served as icons in the process of articulation of national and spiritual identity in nineteenth century Russian culture (Costlow 2013). Based on her explorations of Russian literary writers such as Turgenev, Tolstoi and Korolenko, along with the scientific foresters and visual artists, she argues that the meaning attributed to natural species or habitats cannot be understood outside a cultural context. Such a cultural context, she contends, consists of "… a dense tissue of stories, images, and metaphors, a thick braid of meanings that emerge over time as authors and artists explore the emotional resonance and cultural significance of place" (ibid. 5). Costlow highlights the role of forest as the "megatext" of Russia's landscape which is foundational for understanding Russian culture (ibid. 6). At the same time, by reference to Russian thinkers, she confirms the importance of both forest and steppe as "elemental nomadic expansiveness" in the wandering Russian Soul which becomes apparent in the '… poetry of elemental spaciousness of Pushkin, Lermontov, and Kol'tsov" (ibid.).

The importance of landscape in Russian history and the construction of Russian national identity is by no means the sole concern of European and US scholars. It has also been extensively discussed by Russian scholars in the field of History, Geography, Philosophy and Literary Studies. Russia's preeminent historian of the late nineteenth century, Vasilii Kliuchevskii, asserted the centrality of environmental spaces, namely the forest, the steppe and the river to bestow meaning to Russian thought and consciousness, or, in his words, "… in the construction of the life and ideas of the Russian individual" (Kliuchevskii, 1906: 82). In a similar vein, philosopher Nikolai Berdyaev equates the expanse of the Russian land with the Russian soul, both characterised, in his words, by the same "boundlessness, formlessness, aspiration to infinity, width" (Berdyaev 1990: 8). Russian scholar Irina Belyaeva identifies the dominance of spatial over temporal imaginations which characterise Russian consciousness (Rus. natsional'noe samosoznanie) (Belyaeva 2008: 59). In her view, this accounts for the centrality that images of boundless, vast spaces have for Russian writers and poets. She argues that both forest and steppe have become "the geocultural symbols of Russia" (ibid. 60). But while the forest is perceived as dense and protective, the steppe is associated with the idea of "transitivity" (perehodnost') and perceived as a space of wandering (bluzhdanie), linked to the ideas of "movement, journey, search" (ibid.).

Regarding the steppe, Alexander Chibilev identifies a narrative which shapes much of Russian classical literature (Chibilev 1990: 3). In his understanding, the steppe is the primary element (prirodnaya stichiya), to which history and destiny of the Russian state are closely tied. This element, he argues much in C. Ely's vein, is rendered aesthetic and affective through its attributes of vastness, expanse which signify freedom and liberty (razdol'e). Such an aesthetic interpretation of the steppe characterises, in his analysis, much of Russian classical literature written by authors such as Aksakov, Shevchenko, Gogol', Chehov, Gorkiy, Sholokhov. Emblematic for such a narrative is, in Chibilev's understanding, the poem by Russian Romantic poet and writer Mikhail Lermontov which he quotes:

The steppe stretches as a lilac veil,
It is so fresh, and so dear to the soul,
As if created solely for freedom.

With his analysis, Chibilev points to the affective qualities of spatial imaginaries. Commenting on Lermontov's poetry, Chibilev asks: "Aren't these the feelings that nurtured our national character?" (Chibilev 1990: 3). In his understanding, such descriptions are not merely abstract formulations, but rather images which please the senses for their aesthetic and poetic content, but also serve to construct a sense of collective belonging mediated through metaphors.

In turn, Russian literary scholar Michail Stroganov's work explores the discursive politics of naming landscapes to produce "imagined communities" (Stroganov 2009). He argues that for Russian national discourse it was of central importance to distinguish the Eurasian steppe linguistically from other, geographically similar landscapes such as the Northern American prairie. That is why the term "prairie" was integrated into Russian language during the nineteenth century to describe this Northern American landscape. For instance, the title of James F. Cooper's novel "The Prairie" was changed from "American steppe" (first edition from 1829) to "Prairie" in its Russian translation in a later edition. During the same period, the yet unnamed landscapes of southern Kazakhstan and Uzbekistan started to be referred to in Russian as "steppe" despite their different environmental characteristics in comparison with steppes in the European part of Russia. He argues that this different treatment in Russian language of American and Central Asian landscapes can be explained by the perception of the American steppes as a foreign, distant landscape for Russians, associated with a different culture, different nationality and, consequently, requiring another verbal description. In turn, Central Asian steppes, although initially also perceived as a foreign space, were not distant, but adjacent to Russia's territory. Thus, the term "steppe" masked cultural and national differences, and served as a prerequisite for mastery in the sense of conquest and Russification without a further need for discursive change (ibid.). Stroganov argues that such discursive framing is related to the association of the Russian state with ideas of expansive, open spaces. He opposes this to the image of Russia as a swamp, representing a dirty and confined space, which he argues is 'anti-state'. Both images, in his view, have been exploited for political propaganda and were illustratively and allegorically used to underline the contrasting visions of the state (ibid). Stroganov thus points out not only the cultural construction, but also the deeply political nature of spatial imaginaries in Russia.

All the above-mentioned scholarly research on landscape in Russian artistic literature, painting and poetry suggests the centrality of spatial imaginaries in Russian philosophical and political thought. While anecdotal research exists, the cultural construction of the steppe in Russian thought in the twentieth century remains insufficiently explored. This observation contradicts the above-outlined centrality attributed by several scholars to this particular imaginary.

The representations of nature in Soviet scientific, artistic and popular literature

The twentieth century saw the appearance of many vibrant portrayals of a new transformed steppe. The economy centred changes induced by the Soviet state during this period brought into play a fundamentally altered interpretation of this natural environment. Poems by tselinniki, enthusiastically depicting the first achievements in the early years of Virgin Lands Campaign are a vivid example of this. The steppe in many of these representations appears as an abundant and productive space achieved by means of human transformation in a modernist framework of thought.

At full gallop ran gophers and foxes
Away from the fields, that they for ages inhabited...
All around, in place of the feather-grass,
the conqueror - wheat
stands there stirring its whiskers.[1]

Some authors have noted the prevalence of the mastery of nature theme in Soviet discourse about the natural world in literature and poetry produced during the twentieth century. So, in her article "From dry hell to blossoming garden: metaphors and poetry in Soviet irrigation literature on the Hungry Steppe, 1950–1980" Christine Bichsel explores the discursive framing of irrigation development as expressed in scientific texts and public media between the 1950s and 1970s. She discusses how in the texts on irrigation development on the Hungry Steppe water technologies, infrastructure and landscapes were described by use of not only factual prose, but also metaphorical expressions. Bichsel argues, that these texts, discussing the transformation from a steppe landscape into a landscape of industrial agriculture, served to propagate, interpret and justify largescale environmental transformations (Bichsel 2017).

Furthermore, William B. Husband in his article "'Correcting Nature's Mistakes': Transforming the Environment and Soviet Children's Literature, 1928–1941" analyses the ways in which Soviet mass propaganda systematically promoted applied science and technology to adults and children as a solution to Russia's "backwardness", and in doing so, favoured the representations of planned and improved environment over the environment in its natural state.
Additionally, Frank Westerman (2003) in his explorations of Soviet literature discusses the Soviet strategies of co-opting artistic writing to influence people's interpretation regarding an important process of transforming the steppe: the building of large-scale waterworks. He brings to light the complex and at times conflicting relationships between the field of applied sciences and engineering, and the domain of literary writing. While the engineers' tasks were the technical planning and realization of large-scale infrastructural projects, in turn literary writers such as Maxim Gorki or Konstantin Paustowski sought to shape popular interpretation by praising the achievements of the former, and by pushing them to always plan and build even more boldly for the glory of socialism. He also explores the fate of those Soviet writers such as Andrei Platonov whose accounts of the Soviet transformation of nature did not match the ideological requirements, and who were subsequently refused publication of their works, subjected to institutional exclusion from the Writer's Union and sometimes also legally prosecuted. Westerman's work thus shows the politics of exclusion and inclusion pertaining to representations of the environment, as well as the complicit, mutually reinforcing and at the same time contradictory relationship between scientific and literary accounts in this field.

Furthermore, in her analysis of the extractive industries of Russia's north Alla Bolotova (2004) discusses, on the one hand, the Soviet dominant discourse on nature, which defined the environment as useless, unless exploited for human needs and, on the other, she explores the experience of the actual people – geologists, whose perceptions of the environment remarkably differed from the hegemonic Soviet discourse. For geologists, as Bolatova writes, "nature was not simply the 'house of treasures' that official rhetoric cherished but also an archipelago of freedom" (Bolotova 2004: 104). Her research further proposes that the Soviet leadership sought to rework people's interpretation of their lived experience by means of providing the words and images through which phenomena could be understood.

[1] Own translation of Anatoliy Bragin's poem "About tselina". For more examples of tselina inspired poetry see: http://soil.biblrub.ru/smotri-i-slushaj/stihi/ [Accessed 12 March 2018].

Overall, existing research points to the central role attributed politically to artistic literature for shaping public perceptions during the first half of the twentieth century. Moreover, it stresses the close exchange between a more science and policy-oriented literature with artistic writing in the form of novels and poetry. While scholars have explored these relationships for extractive industries or waterworks, research on the steppe and its transformations during this period is lacking so far. Existing research on the steppe suggests, however, that similar processes shape its imaginaries. This paper, thus, suggests that there is a need to address this gap in research on steppe imaginaries in artistic and scientific literature during the twentieth century.

Furthermore, there is a lack of scholarly research exploring the literary work produced during the twentieth century by the authors whose accounts of the Soviet transformation of nature did not match the ideological requirements and presented adversarial representations of steppe. Interesting in this regard, would be the writings of such authors as Ivan Bunin, Andrei Platonov, Evgenii Nosov and others.

On the historical transformation of scientific views and ideas about the steppe

Lastly, although with a lesser focus on the political and social significance of steppe imaginaries, research has been done to analyse the transformation of scientific understandings of and ideas about the steppe in historical perspective (Chibilev and Grosheva 2004; Grosheva 2002). For instance, in their article "Conceptual Evolution of Steppe Landscape in Russian Geography" Chibilev and Grosheva refer to Russian scientist M.N. Bogdanov, who in his work "Birds and animals of blackearth stripe of Povolzhie and the valleys of middle and lower Volga" wrote: *"Large or small areas of dry plains are referred to by a Russian person as steppe, open field or wild field. Unlike a wild field, plaughed up land and land under crop are called bread field"* (Chibilev and Grosheva 2004: 53). Their analysis further shows that this view did not receive further development as most of the leading scientists of the twentieth century such as A.N. Beketov, A.N. Krasnov, G.I. Tanfiliev, L.S. Berg or F.N. Milkov predominantly agreed that the territories within the steppe areas do not stop being steppes in a geographical sense, even if they have been ploughed up and exploited in economic ways for centuries (ibid. 54). So, for instance, at the very beginning of the twentieth century, Russian botanist G. Vysotskiy writes: *"Not every surface covered in grass can be called steppe (fields, meadows, swamps), on the other hand, ploughed up steppe, occupied by cultivated crops, none the less remains steppe"* (ibid.). Their research points to a long and contradictory process of the ongoing formation of the geo-ecological ideas and imaginaries about the steppe landscape which started in Imperial Russian and continued later in Soviet science. Chibilev and Grosheva's work could be considered a useful starting point for the analysis of a broader picture of how steppe imaginaries came to inform the works of scientists, and how, in turn, the works of scientists produce and re-produce the steppe imaginaries.

CONCLUSIONS

Drawing on analysis of existing research in History, Geography, Political Science and other fields this article demonstrates the importance of the steppe in Russian history. It shows that for the Russian cultural space, the term steppe cannot be reduced to solely describing a physical environment against the background of which political developments unfold. Rather, in the symbolic domain the steppe becomes a key imaginary for the emergence and consolidation of Russian statehood and identity. While existing research has provided rich insight into how perceptions and interpretations of environmental spaces became incorporated into the project of nation-building until the end of the nineteenth century, scholarship so far only marginally covers and lacks sustained engagement with the twentieth century. At the same time, it is precisely during this period that the steppe environments underwent their greatest transformation through processes of land reclamation, irrigation development and industrial agriculture. However, scientific insights on how these changes were accompanied by changing imaginaries of the steppe in literature are largely absent. This observation contradicts the outlined above centrality attributed by several scholars to this imaginary. Therefore, although all the works discussed in this article have made notable contributions to the expanding scope of research on steppe imaginaries, there remains a gap in this topic when it comes to the twentieth century, which this paper calls to fill.

REFERENCES

Barrett T. M. (1999). At the edge of empire: the Terek Cossacks and the North Caucasus frontier, 1700-1860. Boulder: Westview Press.

Bassin M. (1993). Turner, Solov'ev, and the 'frontier hypothesis': the nationalist signification of open spaces. The Journal of Modern History, 65(3), pp. 473-511.

Bassin M. (2000). Reading the Natural and the Social. In: Sargen G., ed., Nature as space: (re) understanding nature and natural environments. Ankara: METU Faculty of Architecture Press, pp. 1–11.

Bassin M. (2006). Imperial visions: nationalist imagination and geographical expansion in the Russian Far East, 1840-1865. New York: Cambridge University Press.

Bassin M., Ely C., and Stockdale M. K. (2010). Space, place, and power in modern Russia: essays in the new spatial history. DeKalb: Northern Illinois University Press.

Belyaeva I. (2009). Steppe in the structure of space of Turgenev's and Goncharov's proze. In: Kokovina N. and Stroganov M., eds., Wide steppe: the spatial images of Russian culture. Kursk: KGU., pp. 27-29 (in Russian).

Berdyaev N. (1990). The origin of Russian communism. Moscow: Nauka (in Russian).

Bichsel C. (2012). 'The drought does not cause fear'. Irrigation history in Central Asia through James C. Scott's lenses. Revue d'études comparatives Est-Ouest (RECEO), 44(1-2), pp. 73-108.

Bichsel C. (2017). From dry hell to blossoming garden. Metaphors and poetry in Soviet irrigation literature on the hungry steppe. Water History, 9(3), pp. 337-359.

Bolotova A. (2004). Colonization of nature in the Soviet Union: state ideology, public discourse, and the experience of geologists. Historical Social Research, 29(3) (109), pp. 104-123.

Chibilev A. (1990). The face of the steppe: ecological-geographical sketches about the steppe zone of the USSR. Leningrad: Gidrometeoizdat (in Russian).

Chibilev A. (1997). Reserved steppes. Orenburg: Institute of Steppe, Russian Academy of Sciences (in Russian).

Chibilev A. and Grosheva O. (2004). The evolution of views on the steppe landscape in national geography. Vestnik of Voronezh State University, Geography, Geoecology №.1 pp. 51–57 (in Russian).

Chibilev A., ed. (2009). Steppe masterpieces. Orenburg: Orenburgskoe knizhnoe izd-vo. (in Russian).

Chibilev A., Bogdanov S. and Sdykov M. (2011). The phenomenon of the historical-geographical continuity of nomadic empires in Eurasian steppes. Geography, Environment, Sustainability 4(2), pp. 72-84.

Costlow T. J. (2013). Heart-pine Russia: Walking and writing the nineteenth-century forest. Ithaca: Cornell University Press.

Ely C. (2002). This meager nature. Landscape and national identity in Imperial Russia. DeKalb: Northern Illinois University Press.

Grosheva O. (2002). The development of geo-ecological ideas about the steppe landscapes of Northern Eurasia in XVIII-XX centuries. Orenburg: Institute of Steppe, Russian Academy of Sciences (in Russian).

Husband W. (2006). 'Correcting nature's mistakes': transforming the environment and Soviet children's literature, 1928–1941. Environmental History 11(2), pp. 300-318.

Khodarkovsky M. (2002). Russia's steppe frontier: the making of a colonial empire, 1500-1800. Bloomington: Indiana University Press.

Kliuchevskii V. (1906). A course of Russian history. Reprinted ed. 2016. St Petersburg: Alfaret (in Russian).

Landwehr A. (2008). Historische Diskursanalyse. Frankfurt: Campus Verlag.

Margolina S. (2014). Alle Wege führen nach Kiew. Neue Zürcher Zeitung 139, p. 51.

Moon D. (2008). The Russian steppes: an environmental history, 1700-1914. CRCEES Working Papers. Available at: https://www.gla.ac.uk/media/media_209913_en.pdf [Accessed 20 July 2018].

Moon D. (2013). The Plough that broke the steppes. Agriculture and the environment on Russia's grasslands, 1700-1914. Aldershot: Ashgate.

Neumann I. and Wigen E. (2013). The importance of the Eurasian steppe to the study of international relations. Journal of International Relations and Development, 16(3), pp. 311-330.

O'Rourke S. (2000). Warriors and peasants: the Don Cossacks in late Imperial Russia. New York: Palgrave Macmillan.

Stroganov M. (2009). Landscape and identity of the 'imagined communities. In: Kokovina N. and Stroganov M., eds., Wide steppe: spatial images of Russian culture. Kursk: KGU, pp. 7-29 (in Russian).

Sunderland W. (2004). Taming the wild field: colonization and empire on the Russian steppe. Ithaca: Cornell University Press.

Tolczyk D. (1999). See no evil: literary cover-ups and discoveries of the Soviet camp experience. New Haven and London: Yale University Press.

Westerman F. (2003). Ingenieure der Seele. Schriftsteller unter Stalin - eine Erkundungsreise. Berlin: Christoph Links Verlag.

Received on April 18th, 2018 Accepted on July 31st, 2018

AUTHORS

Dr. Ekaterina Filep (Geography Unit, Department of Geosciences, University of Fribourg) holds a PhD in Geography from the University of Bern, an MA in Gender Studies from Central European University and a Diploma in Linguistics from the Russian-Tajik (Slavic) University. Filep has received multiple research grants and international scholarships and awards from the Swiss National Science Foundation (SNSF) (2009-2013), the Swiss Government (ESKAS) (2008-2009), Soros Foundation (2006-2007), ECLA (2007-2008) and IREX (2003-2004). Filep's research interests include poststructuralist approaches to the construction of space, politics, state, gender, citizenship and national identities in the former republics of the Soviet Union. She has dealt with such topics as arranged marriages and women's political participation in Tajikistan, female migration, gender and development. Currently, she is working on a project funded by the SNSF, entitled 'Deconstructing steppe imaginaries in Russian and Soviet artistic and scientific literature from 1890 to 1960'.

Prof. Dr. Christine Bichsel (Geography Unit, Department of Geosciences, University of Fribourg) is a Professor of Human Geography at the University of Fribourg. She specializes in Political and Historical Geography with a regional focus on the former Soviet Union and in particular Central Asia. Her research and teaching interests centre on spatial histories of the environment, changing social relations over land and water (in particular irrigation systems), histories of modernization schemes and the nexus of conflict, violence and subjectivity. Her analytical focus on power both as a repressive and productive force links these fields of inquiry. Theoretically, her research is inspired by poststructuralist thinkers, in particular by the work of French philosopher Michel Foucault. She has a strong interest in reflexive methodologies including ethnography and discourse analysis. Christine Bichsel has a long track record in research, teaching and consultancy in and on post-Soviet Central Asia. Christine Bichsel's current research focuses on the history of territory in Central Asia and steppe imaginaries in Russian and Soviet literature.

Le Hung Trinh[1*], Vladimir R. Zablotskii[2], Thi Giang Le[3], Thi Thu Hien Dinh[4], Thi Trinh Le[5], Thi Tham Trinh[5], Thi Thu Nga Nguyen[1]
[1] Le Quy Don Technical University, Hanoi, Vietnam
[2] Moscow State University of Geodesy and Cartography, Moscow, Russia
[3] Vietnam National University of Agriculture, Hanoi, Vietnam
[4] Electric Power University, Hanoi, Vietnam
[5] Hanoi University of Natural Resources and Environment, Hanoi, Vietnam
*** Corresponding author:** trinhlehung125@gmail.com

ESTIMATION OF SUSPENDED SEDIMENT CONCENTRATION USING VNREDSAT – 1A MULTISPECTRAL DATA, A CASE STUDY IN RED RIVER, HANOI, VIETNAM

ABSTRACT. The traditional methods for measuring water quality variables are time-consuming and do not give a synoptic view of a water body or, more significantly, a synoptic view of different water bodies across the landscape. However, remote sensing technology with advantages such as wide area coverage and short revisit interval have been effectively used for environmental pollution applications, such as for monitoring water quality parameters. Many studies around the world show that optical satellite imagery can be used effectively in evaluating suspended sediment concentration. This article presents results of monitoring suspended sediment concentration in Red River, Hanoi, Vietnam through ground truth measurements and VNREDSat-1A multispectral data. The results obtained in the study can be used to serve the management, monitoring and evaluation of surface water quality.

KEY WORDS: remote sensing, multispectral image, suspended sediment, surface water quality, VNREDSat-1A

CITATION: Le Hung Trinh1, Vladimir R. Zablotskii, Thi Giang Le, Thi Thu Hien Dinh, Thi Trinh Le, Thi Tham Trinh, Thi Thu Nga Nguyen (2018) Estimation of suspended sediment concentration using VNREDSat – 1A multispectral data, a case study in Red River, Hanoi, Vietnam. Geography, Environment, Sustainability, Vol.11, No 3, p. 49-60
DOI-10.24057/2071-9388-2018-11-3-49-60

INTRODUCTION

The quality of surface water is a major concern around the world. The major factors affecting surface water quality are suspended sediments (Chalov et al. 2017), chlorophyll, nutrients and pesticides (Ritchie et al. 1990). Remote sensing technique can be an efficient tool for mapping terrigeneous substances in surface water, and hence provide information to help managers in monitoring and controlling water quality. Although the digital numbers and radiance of satellite imagery (Ritchie et al. 1987) have been used to indicate surface water quality parameters, reflectance is more widely used, because the model based on the reflectance value can be applied to other satellite images. Most algorithms used for calculating water quality parameters were based on the reflectance model, which is a function of the inherent optical properties of water, and these in turn can be related to the concentration of the water quality parameters (Lim et al. 2009; Wang and Tian 2013). Many domestic and foreign studies show that the reflectance of surface water, which determined from optical remote sensed data is strongly correlated with the concentration of water quality parameters (Frohn and Autrey 2007; Gilerson et al. 2010; Ritche et al. 1974), icluding suspended sediment (Mobley 1994; Ritchie and Cooper 1988; He et al. 2008; Nguyen et al. 2016; Markert et al. 2018). Therefore, optical satellite imagery has been used effectively for the assessment and monitoring of suspended sediment concentration.

The relationship between Landsat data and suspended sediment concentration has been proven by many researchers (Chalov et al. 2017; Olet 2010; Ritchie et al. 1990; Wang et al. 2009; Zhou et al. 2006; Trinh and Tarasov 2016; Wakerman et al. 2017; Yepez et al. 2018). In the study (Doxaran et al. 2006), the authors used the ratio of the near-infrared and green bands of Landsat ETM+ multispectral images to determine concentration of suspended sediment and turbidity in the Gironde estuary (southest France). In the study (Trinh and Tarasov 2016), the authors used Landsat 7 ETM+ data and 10 ground truth sampling stations for calculating suspended sediment concentration in Tri An reservoir, Vietnam. Li et al. describe an empirical algorithm using MODIS data to identify areas with suspended sediments in turbid waters and shallow waters with bottom reflections (Li et al. 2003). MODIS data also used in study (Guzman and Santaella 2009) to calculate concentration of suspended sediment in Mayaguez Bay (Puerto Rico). Chen et al. have used EO-ALI satellite imagery and found negative regression model between water turbidity in the Pearl River Estuary and reflectance at 570 nm (Chen et al. 2009).

Today, many satellites with high enought spatial resolution have been used in water quality monitoring studies. For instance, Nguyen et al. found that the ratio of band 5 and band 4 using Sentinel-2A multispectral image yielded a good estimation of chlorophyll-a and suspended sediment in West Lake, Hanoi, Vietnam (Nguyen et al. 2016). Doxaran et al. (2002), Gernez et al. (2015) investigated the relationship between suspended sediment concentration and spectral paramerters of SPOT 4 and SPOT 5 sensors data. Sentinel 2 MSI data was used in study (Liu et al. 2017) to retrieve suspended particulate matter concentrations in Poyang lake (China).

Because each river has a unique spectral characteristics, models for calculating suspended sediment concentration must be created for each of them. This study focused on established and analyzed the VNREDSat-1A multispectral imagery to retrieve suspended sediment concentration on the Red river in Hanoi city, Vietnam.

THE STUDY AREA

The selected study area is the Red river in Hanoi city, Vietnam (Fig. 1). Hanoi is the capital of Vietnam and the country's second biggest city. Its population in the year 2017 was estimated at 7.68 million people. With the rapid growth of industrialization in urban area, the surface water in Hanoi is getting more polluted. The weakness in industrial wastewater management is the main cause of water pollution. Industrial wastewater is directly discharged into lakes and rivers, causing serious pollution of surface water in Hanoi (Ministry of Natural Resources and Environment of Vietnam 2012). The observation data show that, suspended sediment concentration in surface water of Red river is high, with mean values greater than 90 mg/l in dry season.

MATERIALS AND METHODS

Remote sensing data

In this study, VNREDSat-1A multispectral image acquired in December 21, 2017 was collected (Fig. 2). VNREDSat-1A (Vietnam Natural Resources, Environment and

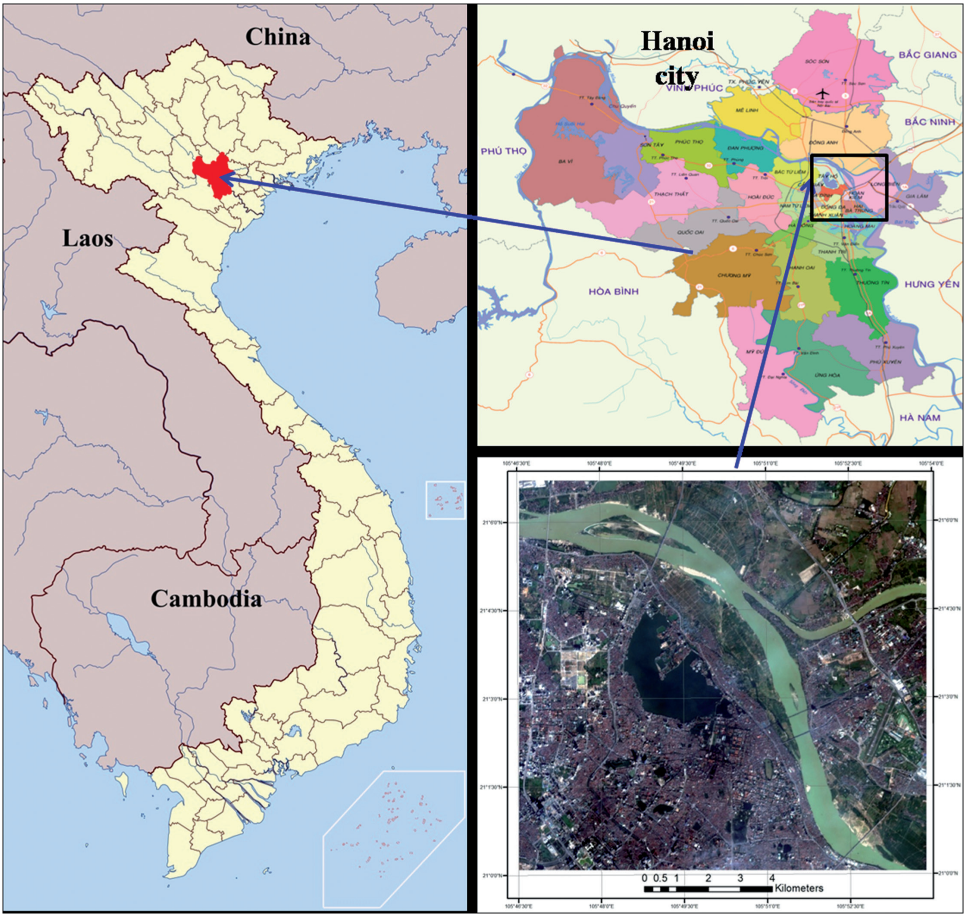

Fig. 1. The study area in Red river, Hanoi, Vietnam

Disaster Monitoring Satellite) is the first optical Earth observing satellite of Vietnam was successfully launched on May 5, 2013 at Guiana space centre by a Vega rocket. Its primary mission is to monitor and study the effects of climate change, predic and take measures to prevent natural disasters and optimise the management of Vietnam's natural resources. VNREDSat-1A has collected images using five spectral bands in different wavelengths of visible and near-infrared to observe a 17.5 kilometer wides swath of the Earth in 2.5 (panchromatic band) and 10 (multispectral bands) meter spatial resolution (Table 1). While the design life of VNREDSat-1A was only 5 years, this satellite is likely to produce imagery for a few more years (Vietnam Academy of Science and Technology 2018).

The necessary image pro-processing included radiometric correction, atmospheric correction, and geometric correction. The reflectance values were obtained from VNREDSat-1A image for all 15 water samples based on the GPS locations.

Ground truth data

The 15 representative water samples were collected during research cruises in the dry season in December 21, 2017 (Fig. 3), roughly coinciding with the time of VNREDSat-1A image acquisition. In the dry season, concentration of suspended sediment in surface water of Red river is often much lower than in the rainy season (Ministry of Natural Resources and Environment of Vietnam, 2012). These samples evenly distributed in the study

Table 1. Characteristic of VNREDSat-1A multispectral image

STT	Band name	Bandwidth (μm)	Resolution (m)
1	Band 1 (blue)	0.45 – 0.52	10
2	Band 2 (green)	0.53 – 0.60	10
3	Band 3 (red)	0.62 – 0.69	10
4	Band 4 (near infrared)	0.76 – 0.89	10
5	Band 5 (panchromatic)	0.45 – 0.75	2.5 (at nadir)

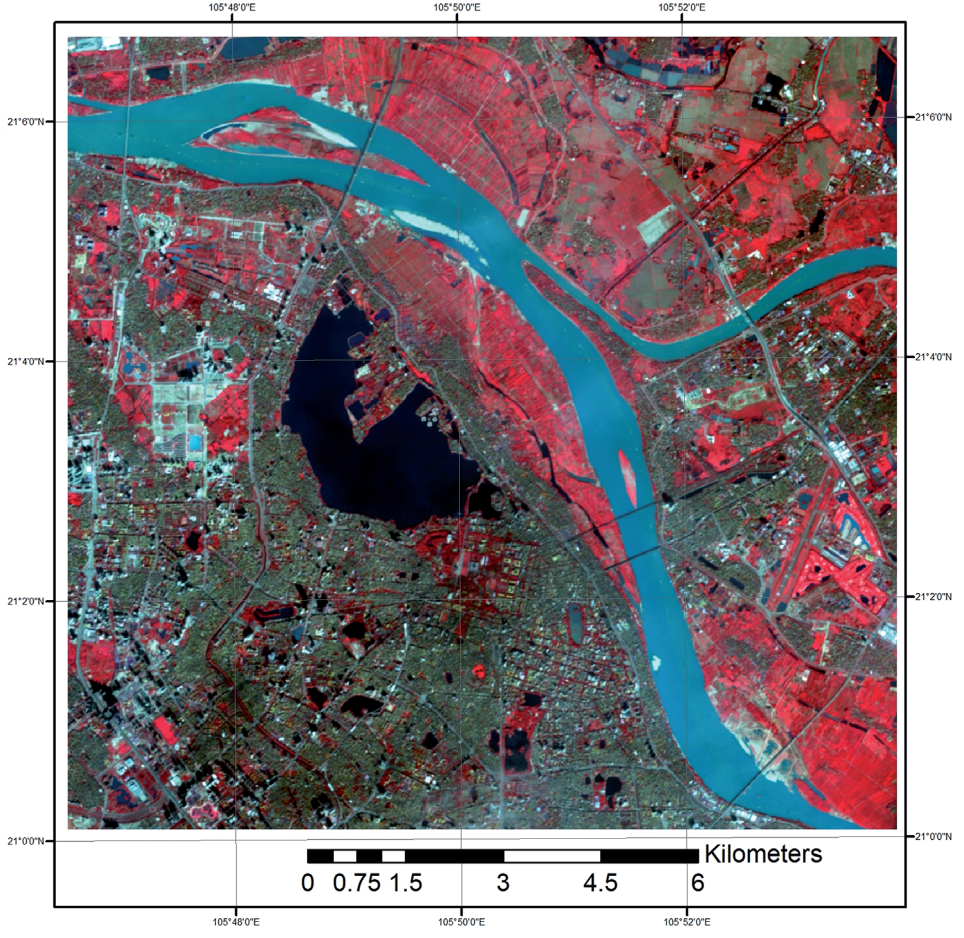

Fig. 2. VNREDSat-1A multispectral image in Hanoi city, December 21, 2017, RGB:432

area (Fig. 2). In order to ensure accuracy, the sampling position should be as close as possible to the part which satellite observes directly (Wang and Ma 2001; Nguyen et al. 2016). Thus, these 15 surface water samples were collected for each site just beneath the surface.

The water samples are stored in dark plastic bottles and analyzed in the lab. The sampling and chemical analyses were on the standard methodology. The concentration of suspended sediment was determined using water filtration method (Ministry of Natural Resources and Environment of Vietnam 2015). The 11 water samples were randomly selected from 15 total samples for modeling and the remaining 4 samples for verification. In addition, in this study we also used 2 water samples which collected by the end of December, 2017 to evaluate accuracy of regression model. The authors also collected 27 other water samples in dry season (April 28, 2018) to evaluate the spatial distribution of suspended sediment concentrations in Red river. These water samples are not used for regression due to not collected in time of satellite image acquisition. Table 2 shows the coordinates of all water sampling points and concentration of suspended sediment (mg/l).

METHODOLOGY

In the first step, the digital number of VNREDSat-1A multispectal bands is converted to spectral radiance using the sensor calibration parameters by the following equation:

$$L_\lambda = Gain \cdot DN + Bias \qquad (1)$$

Where:
L_λ – spectral radiance at the sensor's aperture in watts/m^2.ster.µm;
Gain – rescaling gain factor for each band;
Bias – rescaling bias factor for each band;
DN – the quantized calibrated pixel value in digital number.

Gain and Bias factors are found for each band from metadata file of the VNREDSat-1A data (Table 3).

In the second step, the theoretical radiance of a "dark object" is computed with the theoretical reflectance of 1% as proposed

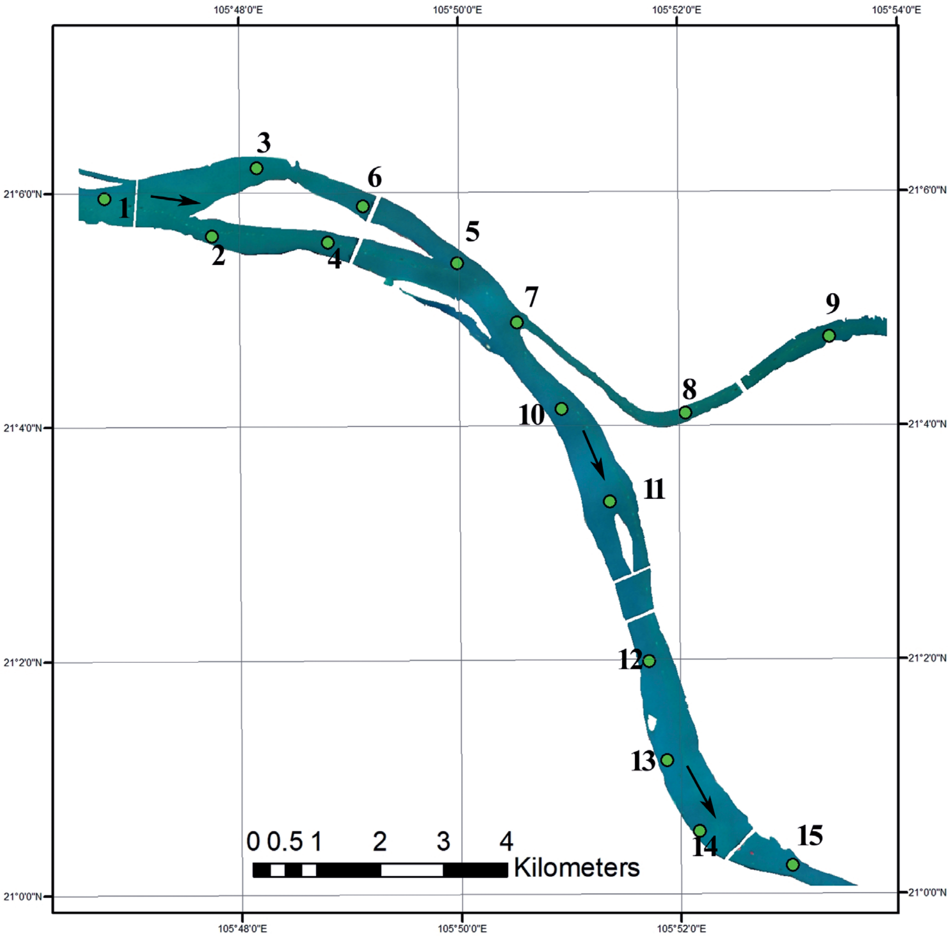

Fig. 3. Location of the water quality monitoring points

Table 2. Ground truth data of suspended sediment concentration

Sampling locations	Coordinates (m)		Concentration of suspended sediment (mg/l)
	X	Y	
1	580960	2333334	70
2	582656	2332738	88
3	583366	2333815	91
4	584488	2332646	97
5	586527	2332326	95
6	585038	2333219	98
7	587466	2331386	102
8	590124	2329966	100
9	588175	2329859	97
10	592392	2331180	99
11	588932	2328569	98
12	589560	2326058	112
13	589842	2324488	115
14	590354	2323379	99
15	591819	2322842	108
P1	590466	2323234	75
P2	590629	2323012	91

Table 3. VNREDsat-1A spectral radiance range

No.	Band name	Gain (watts/(m2.ster. µm/DN)	Bias (watts/(m2.ster.µm)
1	Band 1 (blue)	1.6382548072236700	0.0000
2	Band 2 (green)	1.6213056650501201	0.0000
3	Band 3 (red)	1.8478962570830899	0.0000
4	Band 4 (near infrared)	2.5112173640667201	0.0000

by Chavez (1988, 1996) and Moran et al. (1992):

$$L_{\lambda 1\%} = \frac{0.01 \cdot \cos(\theta_s) \cdot d^2}{\pi \cdot ESUN_\lambda} \quad (2)$$

Where:
$ESUN_\lambda$ – the mean exoatmospheric solar spectral irradiance (watt/m2.ster.µm);
θ_s – the solar zenith angle in degrees;
d – Earth - Sun distance in astronomical units.

Step 3 computes a value for the haze that may be present in the image:

$$L_{\lambda haze} = L_\lambda - L_{\lambda 1\%} \quad (3)$$

The last step converts spectral radiance to surface reflectance values. Surface reflectance can be calculated using following equation:

$$\rho = \frac{\pi \cdot d^2 \cdot (L_\lambda - L_{\lambda 1\%})}{ESUN_\lambda \cdot \cos(\theta_s)} \quad (4)$$

After atmospheric correction, geometric correction was applied to the VNREDSat-1A image by using ground control points collected in fieldwork. Image processing was done at the Department of National Remote Sensing (Vietnam). In turbid sediment-dominated water, the reflectance of visible and near infrared bands are highly correlated to ground truth measurements data (Doxaran et al. 2007; Trinh 2016). In this study, we used the reflectance values of VNREDSat-1A visible and near infrared bands, and ground truth data to build the regression model for calculating concentration of suspended sediment. The topographic map of Hanoi (scale of 1:25 000) was used to extract boundary of Red river, and then created the water mask using ERDAS Imagine 2014 program.

RESULTS AND DISSCUSSION

Based on the multispectral band of VNREDSat-1A image on December 21, 2017, the retrieval models were applied to predict the spatial distributions of suspended sediment over the Red river in Hanoi, Vietnam. Good relationships for suspended sediment and reflectance values were found in multiple linear regressions using all four multispectral bands. Regression analysis is performed using Data Analysis tool in Microsoft Excel 2013.

In order to find the best model, model for estimating suspended sediment concentration have been selected following equation:

$$TSS\left(\frac{mg}{l}\right) = 1953.588\lambda_1 + 1311.897\lambda_2 \ldots \\ -1150.910\lambda_3 + 585.871\lambda_4 - 251.769 \quad (5)$$

Where: λ_1, λ_2, λ_3, λ_4 are surface reflectance values of blue, green, red and near-infrared bands of VNREDSat-1A multispectral image. In this model, multiple R is 0.905, R-square is 0.909 and RMSE (Root Mean Square Error) is 3.664 (mg/l).

To convert the digital numbers of VNREDSat-1A image into suspended sediment concentration we use the calculating module of ERDAS Imagine 2014. To show how the empirical relation (equation 5) behaves when applied to the surface water, we extract the suspended sediment concentration distribution map (Fig. 4) for regions in Red river of Hanoi city, Vietnam. The modeling results for suspended sediment concentration are shown in Fig. 4.

In this study, 4 water samples (sampling locations No. 2, 6, 9 and 15) and two other water samples (P1 and P2) was used to evaluate the accuracy of the regression model. Comparison between concentration of suspended sediment at the measurement points and the results calculated from the VNREDSat-1A satellite image is presented in Table 4. It can be seen, the difference between concentration of suspended sediment calculated from remote sensing imagery and ground truth data range from 1.12 – 8.40%.

Table 4. Comparison of suspended sediment concentration estimated using VNREDsat-1A image and ground truth data

No. sampling locations	Suspended sediment concentration (mg/l)		Difference (mg/l)
	Ground truth data	From remote sensing imagery	
2	88	89.0	1.0
6	98	94.1	-3.9
9	97	102.7	5.7
15	108	105.3	-2.7
P1	75	81.3	6.3
P2	91	88.2	-2.8

The distribution map of suspended sediment concentration in Red river (Hanoi city, Vietnam) is shown in Figure 4. In this example, the estimation of suspended sediment concentration ranges from 67.9 to 142.6 (mg/l). In Fig. 4, ten zones of suspended sediment concentration are identified using the "natural breaks" classification method in ArcGIS 10 program with the following values: 68 – 85, 85 – 93, 93 – 96, 96 – 99, 99 – 102, 102 – 104, 104 – 108, 108 – 112, 112 – 120 and 120 – 143 (mg/l). The brown pixels represent areas with high concentration of suspended sediment. Meanwhile, areas with low concentrations of suspended sediment are represented by blue colored pixels.

The results show that, the surface water in Red river (Hanoi, Vietnam) has high concentration of suspended sediment, especially in the south of the study area. This can be explained by the effects of agricultural production (the central part of the study area and the east coast of the south part of the study area). Besides, surface water quality in the southern part of study area is also highly affected by domestic and industrial waste water from the inner of Hanoi city. Meanwhile, the suspended sediment concentration in the north part of the study area (suburban area) is low due to less influence of domestic and industrial waste water.

In this case, all surface water of Red river has concentration of suspended sediment greater than 50 (mg/l), so is higher than permitted standards when compared with Vietnam National technical regulations on surface water quality. The obtained results in this study indicate that the surface water of Red river is only suitable for irrigation purposes or similar water quality purposes with low quality water requirements. The

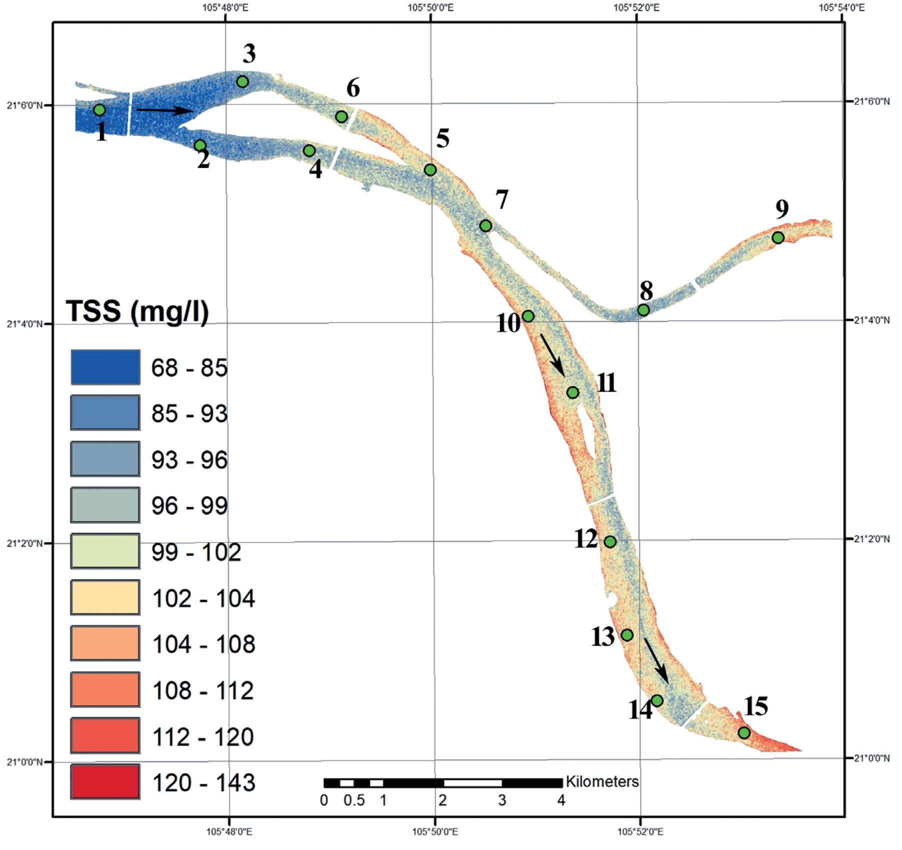

Fig. 4. Spatial distribution of model retrieval result with VNREDSat-1A image of December 21, 2017 for suspended sediment

results obtained in this study were also consistent with the suspended sediment concentrations distribution in 27 water samples of Red River, which collected in dry season (April 28, 2018). In these water samples, the minimum and maximum suspended sediment concentration was 65 mg/l and 170 mg/l, respectively.

CONCLUSION

Nowadays, water pollution has become a global issue, directly caused by human populations grow, industrial and agricultural activities. This study showed that there existed a statistical significant correlation between reflectance values of VNREDSat-1A data and concentration of suspended sediment in surface water of Red river, Hanoi (Vietnam). The square of the correlation coefficient (R2) in this example was 0.909. In this study, we used 4 water samples to verify regression model. Overall, there is a very good correlation between the concentration of suspended sediment calculated from remote sensing imagery and ground truth data.

The obtained model for calculating suspended sediment concentration in this study (equation 5) can be used for surface water monitoring in the future not only for the Red river, but also for other similar rivers. In the case of multi-temporal datasets, the necessary radiometric normalization is applied to empirically reducing the differences between images in time series or mosaics related to differences in the image acquisition time or date. This result can also be applied to the same remote sensing data, such as SPOT 5 image.

Remote sensing was further confirmed to be very useful on establishing a time-cost effective method for the routine monitoring of surface water body. The obtained results in this study are an important source of information for managers in the assessment, monitoring and sustainable use of surface water resources.

REFERENCES

Chalov S., Golosov V., Tsyplenkov A., Zakerinejad R., Marker M., Samokhin M. (2017). A toolbox for sediment budget research in small catchments, Geography, Environment, Sustainability, 10(4), 43- 68, https://doi.org/10.24057/2071-9388-2017-10-4-43-68.

Chalov S., Bazilova V., Tarasov M. (2017). Modeling suspended sediment distribution in the Selenga River Delta using LandSat data, Proc. IAHS, 375, 19-22, doi:10.5194/piahs-375-19-2017.

Chavez P.S. (1996). Image based atmospheric corrections-revisited and improved, Photogrammetric Engineering and Remote Sensing, 62(9), 1025-1036.

Chavez P.S. (1988). An improved dark-object subtraction technique for atmospheric scattering correction of multispectral data, Remote Sensing of Environment, 24, 459 – 479.

Chen S., Fang L., Zhang L., Huang W. (2009). Remote sensing of turbidity in seawater intrusion reaches of Pearl River Estuary – A case study in Modaomen water way, China, Estuarine, Coastal and Shelf Science, 82(1), 119–127, https://doi.org/10.1016/j. ecss.2009.01.00.

Doxaran D., Froidefond J.M., Lavender S., Castaing P. (2002). Spectral signature of highly turbid waters application with SPOT data to quantify suspended particulate matter concentrations, Remote Sensing of Enviroment, 81, 149 – 161.

Doxaran D., Castaing P., Lavender S.J. (2006). Monitoring the maximum turbidity zone and detecting fine-scale turbidity features in the Gironde estuary using high spatial resolution satellite sensor (SPOT HRV, Landsat ETM+) data, International Journal of Remote Sensing, Vol. 27, No. 11, 2303 – 2321.

Frohn R.C., Autrey B.C. (2007). Ohio River water quality assessment using Landsat 7 data, SWIMS Conference, Chicago, IL, January 30 – February 01.

Gernez P., Lafon V., Lerouxel A., Curti C., Lubac B., Cerisier S., Barille L. (2015). Toward Sentinel 2 high resolution remote sensing of suspended particulate matter in very turbid waters: SPOT 4 (take 5) experiment in the Loire and Gironde estuaries, Remote Sensing, 7(8), 9507 – 9528, doi:10.3390/rs70809507.

Gilerson A.A., Zhou J., Gurlin D., Moses W.J., Uoannou I., Ahmed S.A. (2010). Algorithms for remote estimation of chlorophyll-a in coastal and inland waters using red and near-infrared bands, Optics Express, 18, 24109 – 24125.

Guzman V.R., Santaella F.G. (2009). Using MODIS 250m Imagery to Estimate Total suspended sediment in a Tropical open bay, International Journal of Systems Applications, Engineering & Development, Vol. 3, Issue 1, 36 – 44.

He W., Chen S., Liu X., Chen J. (2008). Water quality monitoring in slightly – polluted body through remote sensing – a case study in Guanting Reservoir Beijing, China, Frontiers of Environmental Science & Engineering, Vol. 1, 11 pp.

Li R.R., Kaufman Y.J., Gao B.C., Davis C.O. (2003). Remote sensing of suspended sediment and shallow coastal waters, IEEE Transactions on Geosciences and Remote Sensing, Vol. 41, No. 3, 559 – 566.

Lim H.S., MatJafri M.Z., Abdullah K., Wong C.J. (2009). Total suspended solids (TSS) mapping using ALOS imagery over Penang island, Malaysia, 2009 Sixth International Conference on Computer Graphics, Imaging and Visualization, DOI: 10.1109/CGIV.2009.39.

Liu H., Li Q., Shi T., Hu S., Wu G., Zhou Q. (2017). Application of Sentinel 2 MSI images to retrieve suspended particulate matter concentrations in Poyang Lake, Remote Sensing, 9(7), 761, doi:10.3390/rs9070761.

Markert K., Schmidt C., Griffin R., Flores A., Poortinga A., Saah D., Muench R., Clinton N., Chishtie F., Kityuttachai K., Someth P., AndersonE., Aekakkararungroj A., Ganz D. (2018). Historical and operational monitoring of surface sediments in the lower Mekong basin using Landsat and Google Earth Engine cloud computing, Remote Sensing, 10, 909, doi:10.3390/rs10060909.

Ministry of Natural Resources and Environment of Vietnam (2012). National environment report, chapter 3: surface water.

Ministry of Natural Resources and Environment of Vietnam (2015). National technical regulation on surface water quality, QCVN 08:2015/BTNMT.

Mobley C.D. (1994). Light and water: radiative tranfer in natural waters, Academic Press: San Diego, CA.

Moran M.S., Ray D.J., Slater P.N., Teillet P.M. (1992). Evaluation of simplified procedures for retrieval of land surface reflectance factors from satellite sensor output, Remote Sensing of Environment, Vol.41, 169 – 184.

Nguyen T.T.H., Bui D.C., Nguyen T.P.T., Bui T.N. (2016). First experience in modelling spatial distribution of chlorophyll-a concentration and TSI in the West Lake water using Sentineal-2A image, Journal of Science: Earth and Environmental Sciences, Vietnam National University, Vol. 32, Issue 2S, 121 – 130.

Olet E. (2010). Water quality monitoring of Roxo reservior using LANDSAT images and In – situ measurements, International Institute for Geo-information Science and Earth Observation Enschede, the Netherlands, 69 pp.

Ritchie J.C., McHenry J.R., Schiebe F.R., Wilson R.B. (1974). The relationship of reflected solar radiantion and the concentration of sediment in the surface water of resevois, Remote Sensing of Earth Resources, Vol.3, The University of Tennessee Space Institure, Tullahoma, TN, 57 – 72.

Ritchie J.C., Cooper C.M., Jiang Y. (1987). Using Landsat multispectral scanner data to estimate suspended sediments in Moon lake, Mississippi, Remote Sensing of Environment, 23, 65 – 81.

Ritchie J.C., Cooper C.M. (1988). Comparision of measured suspended semdiment concentration with suspended sediment concentrations estimated from Landsat MSS data, International Journal of Remote Sensing, 9(3), 379 – 387.

Ritchie J.C., Cooper C.M., Schiebe F.R. (1990). The relationship of MSS and TM digital data with suspended sediments, chlorophyll, and temperature in Moon lake, Mississippi, Remote Sensing of Environment, 33, 137 – 148.

Trinh L.H., Tarasov M.K. (2016). Evaluation of suspended sediment concentrations in surface water of the Tri An water reservoir using remote sensing, Moscow University Bulletin. Series 5. Geography, Vol.2, 38 - 44.

Vietnam Academy of Science and Technology (2018). The success of the first remote sensing satellite project in Vietnam, http://vast.ac.vn.

Wackerman C., Hayden A., Jonik J. (2017). Deriving spatial and temporal context for point measurements of suspended sediment concentration using remote sensing imagery in the Mekong Delta, Continental Shelf Research, Vol.147, 231 – 245.

Wang J., Tian Q. (2013). Estimation of total suspended solids concentration by hyperspectral remote sensing in Liaodong bay, Indian Journal of Geo-Marine Science, Vol. 44(8), 1137 – 1144.

Wang J.J., Lu X.X., Liew S.C., Zhou Y. (2009). Retrieval of suspended sediment concentrations in large turbid rivers using Landsat ETM+: an example from the Yangtze River, China, Earth Surface Processes and Landforms, 34, 1082 – 1092.

Wang X.J., Ma T. (2001). Application of remote sensing techniques in monitoring and assessing the water quality of Taihu Lake, Bulletin of Environmental Contamination and Toxicology, 67(2), 863 – 870.

Yepez S., Laraque A., De Sa J., Carrera J., Castenllanos B., Gallay M., Lopez J. (2018). Retrieval of suspended sediment concentrations using Landsat 8 OLI satellite images in the Orinoco River (Venezuela), Comptes Rendus Geoscience, Vol.350, Issues 1-2, 20 – 30.

Zhou W., Wang S., Zhou Y., Troy A. (2006). Mapping the concentrations of total suspended matter in Lake Taihu, China using Landsat 5 TM data, International Journal of Remote Sensing, 27(6), 1177 – 1191.

Received on April 13th, 2018 Accepted on July 31st, 2018

FIRST/CORRESPONDING AUTHOR

Le Hung Trinh, PhD in Remote Sensing and Geographic Information System (GIS), Associate Professor. He is now the vice head of Department of Geodesy and Cartography, Le Quy Don Technical University, Hanoi, Vietnam. He got Ph.D. degree in 2012 from Moscow State University of Geodesy and Cartography. His research interests are application of Remote Sensing and Geographic Information System for monitoring natural resources and environment. He is corresponding author for this paper.

Ekaterina P. Rets[1], Roald G. Dzhamalov[1], Maria B. Kireeva[2], Natalia L. Frolova[2], Ivan N. Durmanov[1], Anna A. Telegina[1], Ekaterina A. Telegina[1], Vadim Yu. Grigoriev[1]
[1] Water Problems Institute, Russian Academy of Sciences, Moscow, Russia
[2] Faculty of Geography, Lomonosov Moscow State University, Moscow, Russia.
*** Corresponding author:** retska@mail.ru

RECENT TRENDS OF RIVER RUNOFF IN THE NORTH CAUCASUS

ABSTRACT. Based on observational data from 70 hydrological stations in the North Caucasus an evaluation of present values of mean annual runoff, minimum monthly winter and summer runoff was carried out. Series of maps was drawn. Significant changes in mean annual. minimum monthly and maximum runoff during last decades have been revealed in the North Caucasus. A rise in both amount of water availability and potential natural hazard is characteristic of the most of the North Caucasus that is considered to be caused by recent climate change. Mean annual runoff during 1978-2010 increased compared to 1945-1977 by 5-30 % in the foothills and by 30-70% in the plain area. An increase in winter minimum monthly runoff is as well most intensive in the plain part of study area (>100%). Within the foothills it amounts to 50-100%. In mountainous area long-term oscillation of winter minimum monthly discharge strongly depends on local factors, such as geological structure. The rate of the increase in summer minimum monthly discharge regularly grows from central foothill part of Northern Caucasus (30-50%) to the Western plain territory (70-100%). In Kuban river basin 30% of analyzed gauging stations show positive trend in maximum instantaneous discharge, while 9% negative. On the contrary, in the Eastern part – Terek river basin – negative trend in maximum instantaneous discharge is prevalent: 38% of gauging stations. Positive trend in Terek river basin is characteristic of 9.5% of analyzed gauging stations.

KEY WORDS: Water resources, mean annual runoff, minimum monthly runoff, maximum discharge, climate change, hydrological hazards, North Caucasus

CITATION: Ekaterina P. Rets, Roald G. Dzhamalov, Maria B. Kireeva, Natalia L. Frolova, Ivan N. Durmanov, Anna A. Telegina, Ekaterina A. Telegina, Vadim Yu. Grigoriev (2018) Recent trends of river runoff in the north caucasus. Geography, Environment, Sustainability, Vol.11, No 3, p. 61-70
DOI-10.24057/2071-9388-2018-11-3-61-70

INTRODUCTION

Due to specific climatic conditions, contrasts in relief, high density of population the North Caucasus is one of the most complicated in terms of hydrological conditions parts of Russia. Herewith problems connected with both scarcity and abundance of water resources is characteristic of this region. Mean annual damage caused by river flooding in the North Caucasus amounts to 700 mln USD (Grishenko et al. 2003). That is almost equal to the corresponding value for Volga and Amur river basins (Grishenko et al. 2003), whereas the total area of the North Caucasus region (258 000 km^2) is 5 times less then the Volga river basin (1 360 000 km^2) and 7 times less than the Amur river basin (1 855 000 km^2). The North Caucasus is also leading in terms of dangerous floods occurrence (from 1 to 20 a year) (Semenov and Korshunov 2008). Floods are observed in the North Caucasus during the spring-summer period and are usually aroused by imposition of heavy rainfall on intensive melting wave. The same factors bring about other various hazardous natural processes in this region, such as debris flows, snow avalanches and glacier lakes outburst floods.

The foothill and lowland part of the North Caucasus is one of the most important agricultural regions in Russia with high level of irrigation. Severe water shortages are occasionally observed here during low-flow periods.

In the beginning of the 21th century frequency and intensity of dangerous hydrological processes in North Caucasus was substantially higher then during the previous years that is usually associated with recent climate change (Frolova et al. 2017, Semenov and Korshunov 2008; Bazeluk and Lurie 2014; Rets et al. 2016; Rets and Kireeva 2010; Malneva and Kononova 2012; Seynova 2008).

Some components of hydrological regime in certain parts of North Caucasus were recently analyzed by different authors. Lurie (2002) gives a thorough description of physic-geographical conditions of river runoff forming in the North Caucasus, calculates water balance in North Caucasus according to Lvovich method. Rets and Kireeva (2010) provides information on main features of water regime in Terek river basin and dependencies of mean annual and minimum monthly runoff and maximum water levels on characteristics of river basin. Regional dependencies of mean annual runoff on mean elevation and mean annual runoff mapping for Kuban river basin for the period 1967–2008 is given in (Melnikova 2010). The conditions of formation of the maximum runoff in the rivers of the North-West Caucasus were analyzed by Melnikova (2011), maximum river discharges are provided for some gauging stations in the study region as well.

However, the last thorough and generalized study of water resources in North Caucasus as whole dates back to the 70s (Resources… 1973). Consequently, it is of current interest to reassess river water resources in North Caucasus for the modern period and reveal present-day trends in main runoff characteristics.

STUDY AREA AND METHODS

The North Caucasus region with the total area of more then 350 000 km^2 is situated on the southern border of European territory of Russia. It can be divided into three parts: plain territory on the north, foothills and mountainous part in the south. The alpine zone extends above the orographic snowline which height is approximately 2000 m in North Caucasus. Elevation of the basin ranges from –28 to 5642 m. The climate here is moderate continental. The precipitation decreases both southeastwards and with a decrease in elevation. Annual precipitation sum varies from 400-600 mm in Eastern plain part and 600-800 mm in Western plain part to 800-1300 and more in mountainous part with the maximum of 3242 mm (Achishkho plateau). Annual distribution of precipitation differs greatly through the region this combined with altidudinal zonality of climate results in great differences in river flow regime in North Caucasus. The overall main source of river water in North Caucasus basin is snow and ice melting, though snow melting flood can be distinguished not for all rivers of the region. The main river basins in North Caucasus are the Kuban river basin (57 900 km^2), Terek river basin (43 200 km^2), Kuma river basin (33 500 km^2), Sulak river basin (15 200 km^2) and Samur river basin (7 330 km^2).

Mean annual. minimum monthly winter and summer unit discharges were estimated for 70 hydrological stations for the period 1945-2010 (Fig. 1). The analysis of maximum annual discharge trends was based on instantaneous data for the period from 1920s to 2015 from 23 and 21 hydrological stations in the Kuban and Terek basins respectively. Methods of mathematical statistics were used to reveal statistically significant directed changes in main characteristics of annual. minimum river runoff and maximum annual discharges. Fisher and Student test were used to reveal the statistical heterogeneity in mean annual and minimum monthly discharges time series.

The trends in maximum discharges were tested using Spearman's rank order correlation coefficient with 5% significance level.

Series of maps have been drawn covering the reassessment of annual and minimum river runoff characteristics for the modern period and their change compared to the previous period. The threshold year (1978) was detected by analysis of difference-integrating curves of river runoff characteristics.

RECENT CLIMATE CHANGE IN NORTH CAUCASUS

Tendencies in main climatic characteristics are appear to be not homogeneous throughout the study region (Toropov et al. 2018). However, some main features can be outlined. According to the majority of studies (Alekseev et al. 2014; Toropov et al. 2018; Rets and Kireeva 2010) a statistically significant positive trend in air temperature is observed in the summer period in the region amounting to 0.7 – 1°C/10 years. According to (Rets and Kireeva 2010) this tendency is more clear cut in plain territory and foothills. In winter period the observed tendencies in air temperature are very inhomogeneous: Alekseev et al (2014) report statistically insignificant positive trend. Toropov et al. (2018) claim a statistically significant rise in air temperature of winter period is observed in the Eastern Caucasus, close to the Caspian Sea and in the Krasnaya Polyana vicinity. In the study (Rets and Kireeva 2010) a decrease in air temperature of winter period was revealed in the mountainous part of the North Caucasus.

Tendencies in precipitation sums in the North Caucasus have been multidirectional and complicated in the last 30-40 years. Observed tendencies in precipitation characteristics differ to a great extent seasonally (Toropov et al. 2018). According to different studies either positive trend in annual precipitation sum (5%/10 years (Alekseev et al. 2014), or no statically significant trend is observed for the most of the territory (Toropov et al. 2018). Alekseev et al. (2014) report rise in precipitation mostly in spring and autumn. Most distinct positive trend in annual precipitation is characteristic of the Eastern part of North Caucasus close to the Caspian Sea (Alekseev et al. 2014). In the same region a statistically significant rise in precipitation intensity up to 0.5 mm/day per 10 years is observed (Toropov et al. 2018). An increase in annual precipitation sum was revealed for the most of mountainous station and a number foothill of the central part of Northern Caucasus (Rets and Kireeva 2010). Decrease in precipitation sum and precipitation intensity in winter period is detected on the Black Sea shore and in steppe regions of Krasnodarky kraj (Toropov et al. 2018).

The intensive degradation of glaciation is observed in the North Caucasus (Zemp et al. 2015; Shahgedanova et al. 2014). The area of glaciers in the North Caucasus dropped by 12.6% during 1970–2000 (Voitkovskiy et

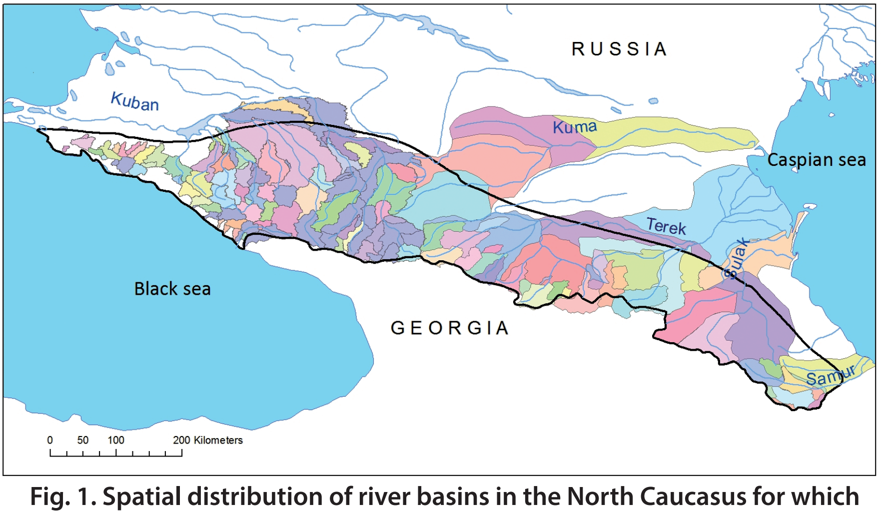

Fig. 1. Spatial distribution of river basins in the North Caucasus for which characteristics of mean annual and minimum monthly unit discharge were calculated

al. 2004), and by 4.7% between 2000 and 2010/2012 (Shahgedanova et al. 2014), amounting to approximately 17% in total during 1970–2012. A substantial intensification of deglaciation during the last decade in the region is reflected in mass-balance measurements on representative of the central part of the North Caucasus, Djankuat glacier. Mean rates of ice mass loss increased from -0.13 m w.e./yr (meters of water equivalent per year) in 1966-2003 (Shahgedanova et al. 2007) to -1.03 m w.e./yr in 2010-2015 (www.wgms.ch).

ANNUAL WATER RESOURCES

Mean annual river runoff rate decreases with the decrease in elevation from Southwest to Northeast and from West to East with the increase in aridity (Fig. 2). The maximum value of mean annual unit discharge (60-70 litres/(s*sq.km)) is observed on the southern slopes of the Western part of the Caucasian mountain range where local climatic conditions result in a high precipitation rate. In the most alpine zone of the North Caucasus annual unit discharge varies from 20-30 to 50-60 litres/(s*sq.km). In the foothills mean annual runoff unit discharge sharply declines to 5-15 litres/(s*sq.km). The vast plain territories not add much to the total runoff of rivers: the values of unit discharge decrease gradually in the Northeast direction down to zero and even less. Here the most evident changes in annual runoff occurred during last 3 decades: it has increased by 30-70%. Whereas in the mountainous part only a slight positive tendency can be observed. In the orographicaly highest areas and in the Eastern part of the North Caucasus the long-term mean value on annual runoff remains stable.

MINIMUM RUNOFF PERIOD

Contrasts in climatic conditions in the region results in great differences in river nourishment structure and, consequently, annual river runoff regime (Rets et al. 2017a). Rivers with a substantial share of glacial and high-elevation snowfield melt in nourishment structure are characterized by a high-water period lasting from late spring up to September and stable winter low-flow period (Rets et al. 2017b). With a decrease of mean elevation of river watershed the share of snowmelt in river runoff diminishes, simultaneously, the beginning of high-water and winter low-flow periods shifts to earlier dates, rain floods start playing a more substantial role in maximum discharges, winter low flow period is more often interrupted by snowmelt winter floods. Annual water regime of rivers with watersheds situated mostly in the plain territory depends on annual distribution of precipitation. In the central and Eastern North Caucasian plain territory precipitation occurs mostly in summer that results in summer flood period and both winter and summer low-flow periods. Winter precipitation maximum is characteristic of the Western part of North Caucasus. Hence, no

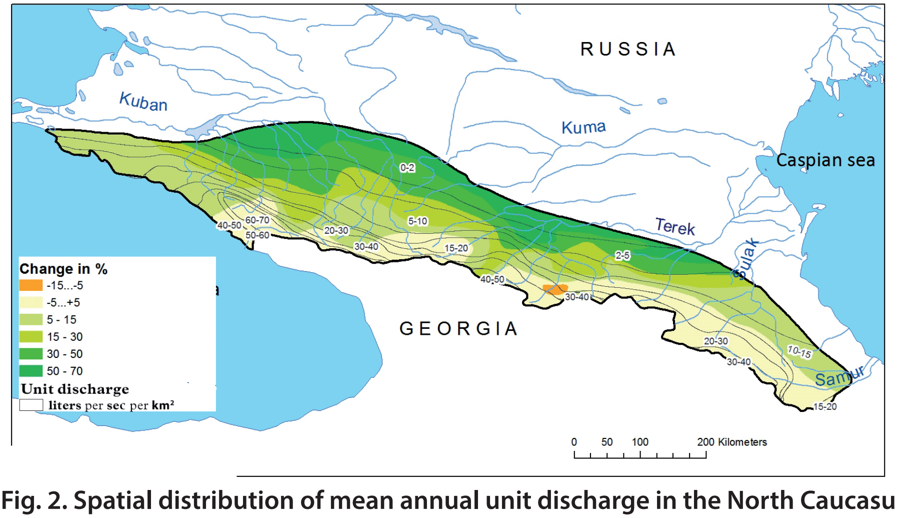

Fig. 2. Spatial distribution of mean annual unit discharge in the North Caucasus (averaged for 1978-2010), and its change compared to the previous period (1945-1977)

winter low-flow period is observed here.

Summing up, a winter low-flow period is observed on the most of territory of North Caucasus (except for the utmost Western part) (Fig. 3). Summer low-flow period is characteristic only of Northern and Eastern part (Fig. 4). Winter and summer minimum monthly unit discharges are practically equal in central Northern are (from 0-1 to 1-2 litres/(s*sq.km). Summer low flow period is higher then winter in central foothills (2-7 compared to 2-5 litres/(s*sq.km). Distribution of winter minimum monthly unit discharge in mountainous part is not so even, that is connected with geological structure. Also a maximum in Western mountainous part (20-30 litres/(s*sq.km) is raised by closeness to the territory with prevailing winter precipitation. Summer minimum monthly unit discharge is also correspondingly maximum in the neighboring area.

A dramatic rise in minimum monthly discharges (both for winter and summer) is characteristic for the study area. The peculiarities of modern climate bring about the increase in amount, duration and extent of thaws and general reduction of annual cold period duration in region. These tendencies

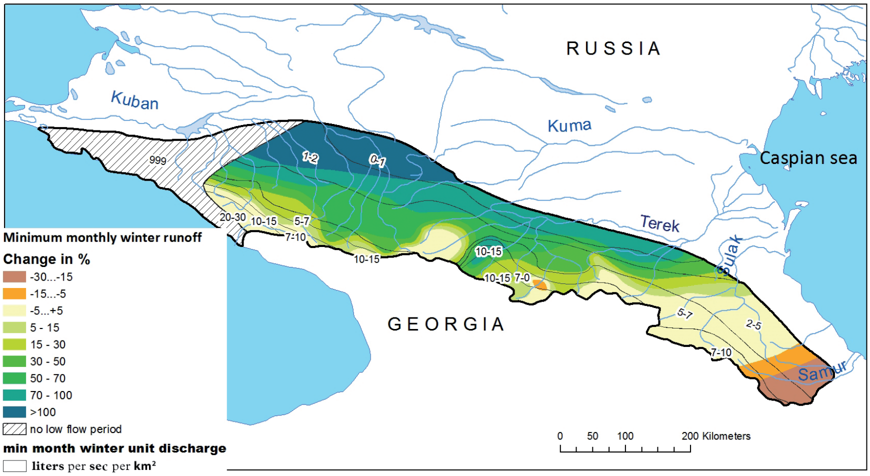

Fig. 3. Spatial distribution of winter minimum monthly unit discharge in the North Caucasus (averaged for 1978-2010), and its change compared to the previous period (1945-1977)

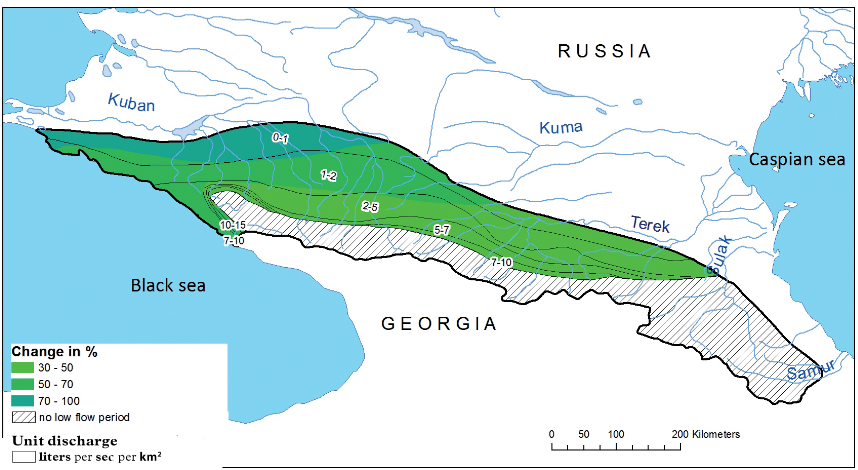

Fig. 4. Spatial distribution of summer minimum monthly unit discharge in the North Caucasus (averaged for 1978-2010), and its change compared to the previous period (1945-1977)

lead to a decrease in soil freezing depth, registered on agrometeorological stations in all regions of European Russia. Groundwater resources have been significantly more replenished during last decades compared to previous period due to melt water losses on infiltration (Kireeva et al. 2015). A respective increase in winter minimum monthly discharge is most intensive in the North of study area (>100 %) (Fig. 3). Within the foothills it amounts to 50-100%. In mountainous area long-term oscillation of winter minimum monthly discharge strongly depends on local factors, such as geological structure. In the upper reaches of some tributaries of Terek and Kuban river positive trends are still not observed, while in neighboring macrovalleys long-term variations of winter minimum monthly discharges correlate with the corresponding variations in the foothills and on plain. However, a decrease in positive tendency rate is observed throughout the study area with movement from plain to alpine zone. On the highest elevation belts, where the temperature is still strongly negative in winter for frequent thaws generation, winter minimum monthly discharge remains stable on the long-term scale. In the most arid Southeastern part of study area the negative trend in precipitation result in decrease of minimum monthly discharges by 15–30%.

The rate of the increase in summer minimum monthly discharge regularly grows from central foothill part of Northern Caucasus (30-50%) to the Western plain territory (70-100%) (Fig. 4).

TRENDS IN MAXIMUM RIVER DISCHARGES

The water-abundant period is observed from April/May to September in the North Caucasus. The fundamental wave or the runoff hydrograph, formed by snow and ice melting is overlain with sharp peaks of rain floods that usually form annual maximums of discharges. Maximum river discharges are usually associated with flood hazard (Shiklomanov et al. 2007; Frolova et al. 2017). However, tendencies in maximum water level tendency which results in out-of-bank flow does not always correlate with tendencies of maximum discharge in North Caucasus, owing to sedimentation processes and anthropogenic factors (Rets and Kireeva 2010; Frolova et al. 2017; Vishnevskaya et al. 2016; Kotlyakov et al. 2016). Accordingly, changes in maximum river runoff can be referred to as climatic prerequisites of modification of present-day flood hazard. Maximum annual river discharges tend to increase in the Western part of the North Caucasus. In Kuban river basin 7 of 23 (30%) analyzed time-series show positive trend in maximum instantaneous discharge at 5% significance level (Table 1), while 2 of 23 (9%) – negative. On the contrary, in the Eastern part – Terek river basin (Table 2) – negative trend in maximum instantaneous discharge is prevalent: 8 of 21 (38%) of time series. Positive trend in Terek river basin is characteristic of 9.5% of analyzed gauging stations (2 of 21).

Table 1. Statistically significant trends in maximum river discharges in Kuban river basin revealed by Spearman test

River	Gauging station	p-value	Observed trend
Kuban	Kosta Hetagurova	0.012	positive
Kuban	Armavir	0.288	none
Kuban	st. Ladozhskaya	0.124	none
Ullu-Kam	aul Hurzuk	0.236	none
Teberda	Teberda	0.540	none
Maruha	Maruha	0.112	none
Nevinka	h. Ust-Nevinskij	0.380	none
Bolshoj Zelenchuk	st. Zelenchukskaya	0.002	positive
Urup	st. Udobnaya	0.950	none
Urup	h. Steblitskij	0.093	none

Laba	h. Doguzhiev	0.000	positive
Malaya Laba	s. Burnoe	0.003	positive
Bolshaya Laba	nizhe Aziatskogo mosta	0.004	positive
Fars	st. Dondukovskaya	0.009	positive
Belaya	pgt Kamenomostskij	0.036	negative
Dah	st. Dahovskaya	0.029	negative
Kurdzhips	st. Nizhegorodskaya	0.982	none
Psekups	Goryachij Kluch	0.116	none
Afips	st. Smolenskaya	0.044	positive
Shebsh	s. Shabanovskoe	0.253	none
Ubinka	st. Severskaya	0.374	none
Adegoj	st. Shapsugskaya	0.867	none
Adagum	Krimsk	0.429	none

Table 2. Statistically significant trends in maximum river discharges in Terek river basin revealed by Spearman test

River	Gauging station	p-value	Observed trend
Terek	Vladikavkaz	0.025	negative
Terek	Kotlyarevskaya	0.251	none
Terek	Stepnoe	0.023	negative
Ardon	Tamisk	0.363	none
Tseya	Buron	0.003	negative
Fiagdon	Tagardon	0.461	none
Gizeldon	Dargavs	0.002	positive
Kambileyevka	Ol'ginskoye	0.050	negative
Belaya	Kora-Urusdon	0.000	negative
Malka	Kamennomostskoye	0.535	none
Malka	Prokhladnaya	0.013	negative
Baksan	Zayukovo	0.033	negative
Chegem	Nizhny Chegem	0.172	none
Cherek	Kashkhatau	0.165	none
Cherek Balkarsky	Babugent	0.174	none
Nalchik	Belaya rechka	0.000	negative
Sunzha	Karabulak	0.941	none
Sunzha	Grozny	0.025	positive
Assa	Nesterovskaya	0.893	none
Fortanga	Bamut	0.642	none
Belka	Gudermes	0.151	none

CONCLUSION

A directed increase in mean annual river runoff and summer minimum monthly discharge is observed in North Caucasus. The main reason of increase in water abundance of winter period is more often winter thawing due to overall warming of the winter period. The most pronounces changes occurred in the western part of the plain territory. In mountainous part, especially in the areas of certain geological structures expansion, the analyzed characteristics of river runoff remain stable. In the most arid Southeastern part a decrease in river runoff during low-flow periods is detected. Positive trend in maximum runoff is observed for one third of gauging stations in Kuban river basin that can be interpreted as a favorable climatic background for an increase in flood hazard. An opposite tendency is observed in Terek river basin for almost 40% of the gauging stations. It is an urgent need for the local economy to adapt to the new conditions.

ACKNOWLEDGEMENTS

This work was supported by the Russian Science Foundation (project no. 17-77-10169).

REFERENCES

Alekseev G.V., Ananicheva M.D., Anisimov O.A., Ashik I.M., Bardin M. Yu., Bogdanova E.G. and others (2014). The second assessment report of Roshydromet on climate change and its consequences on the territory of the Russian Federation. State Scientific Center of the Russian Federation «Arctic and Antarctic Research Institute» Federal Service of Russia for Hydrometeorology and Environmental Monitoring.

Bazelyuk A.A. and Lurie P.M. (2014). Catastrophic floods in southern Russia: Causes and impact assessment. In: River flows: spatio-temporal variability and hazardous hydrological phenomena. Collection of works of the Third Conference Room Research and Education Center. November 13, 2014, Moscow, Department of hydrology. M.V. Lomonosov Moscow State University, IWP RAS, pp. 44-60.

Dzhamalov R., Frolova N., Kireeva M., Rets E. (2014). Present-day surface and subsurface water resources of European Russia: conditions, use and forecast Hydrology in Changing World: Environmental and Human Dimensions. Proc. of FRIEND-Water 2014, IAHS Publ 363, 2014. pp. 215-220.

Frolova N. L., Kireeva M. B., Magritckiy D. V., Bolgov M. B., Kopylov V. N., Hall J., Semenov V. A., Kosolapov A. E., Dorozhkin E. V., Korobkina E. A., Rets E. P., Akutina Y., Dzhamalov R. G., Efremova N. A., Sazonov A. A., Agafonova S. A., Belyakova P. A. (2017). Hydrological hazards in Russia: origin, classification, changes and risk assessment. Natural Hazards, 88, 1, pp.103–131.

Grishenko N.S., Shevchenko G.V. Marchenko A.A. (2003). Preventing harmful effects of water from the spring floods and rain floods on the territory of floodplains (lakes) of the Russian Federation. Proc. rep. Proc. Congress of workers in Water Resources. Moscow, 191-192, 2003.

Kireeva M., Frolova N., Rets E. et al. (2015) The role of seasonal and occasional floods in the origin of extreme hydrological events. Proc. IAHS., 369, pp. 37–41.

Kotlyakov V. M., Koronkevich N. I., Desinov L. V., Dolgov S. V., and Vishnevskaya I. A. (2016). Catastrophic flood in the russian town krymsk (north caucasus, 6-7 july, 2012) - analysis of natural and anthropogenic causes. Journal of Contemporary Management. Academic Research Centre of Canada. 5, 4, pp. 1–11.

Lurie P. M. (2002). Water resources and water balance of the Caucasus. SPb .: Gidrometeoizdat.

Malneva I. V. and Kononova N. K. (2012). The activity of mudflows on the territory of Russia and the near abroad in the 21st century. Geo Risk, (4), pp. 48-54.

Melnikova T.N. (2011). The maximum runoff of rain floods in the rivers of the North-Western Caucasus. Bulletin of the Adyghe State University. Series 4: Natural and Mathematical and Technical Sciences, 3.

Melnikova T.N. (2010). The norm of the annual flow of the rivers of the North-Western Caucasus and the features of its territorial distribution. Bulletin of the Adyghe State University. Series 4: Natural and Mathematical and Technical Sciences, 2.

Resources of Surface Waters of the USSR (1973). Vol.8, Lenengrad. 446 (in Russian).

Rets E., Chizhova J., Budantseva N., Frolova N., Kireeva M., Loshakova N., Tokarev I., Vasil'chuk Y. (2017a). Evaluation of glacier melt contribution to runoff in the north Caucasus alpine catchments using isotopic methods and energy balance modeling. GEOGRAPHY, ENVIRONMENT, SUSTAINABILITY 11, 3, pp. 4–19.

Rets E., Chizhova J. N., Loshakova N., Tokarev I., Kireeva M. B., Budantseva N. A., Vasil'chuk Y. K., Frolova N., Popovnin V., Toropov P., Terskaya E., Smirnov A. M., Belozerov E., and Karashova M. (2017b). Using isotope methods to study alpine headwater regions in the northern Caucasus and Tien Shan. Frontiers of the Earth Science 11, 3, pp. 531–543.

Rets E. and Kireeva M. (2010). Hazardous hydrological processes in mountainous areas under the impact of recent climate change: case study of Terek River basin. Global Change: Facing Risks and Threats to Water Resources: proc. of the Sixth World FRIEND Conference. IAHS Publ. 340. 2010. Pp. 126–134.

Semenov V.A. and Korshunov A.A. (2008). Zoning of Russia territory in terms of dangerous river floods in the context of recent climate change. Water resources management under extreme conditions conference proceedings. Electronic resource. Moscow 3-6 June.

Seynova I. B. (2008). Climatic and glaciological conditions of debris flow formation in the Central Caucasus at a stage of regress of the little ice age. In: Debris Flows: Disasters, Risk, Forecast, Protection (ed. by S. S. Chernomorets). Pyatigorsk, Russia., pp. 121–124

Shahgedanova M., Nosenko G., Kutuzov S., Rototaeva O., and Khromova T. (2014). Deglaciation of the Caucasus Mountains, Russia/Georgia, in the 21st century observed with ASTER satellite imagery and aerial photography. The Cryosphere, 8(6), 2367-2379.

Shahgedanova M., Popovnin V., Aleynikov A., Petrakov D.A., Stokes C.R. (2007). Long-term change, interannual and intra-seasonal variability in climate and glacier mass balance in the central greater Caucasus. Annals of Glaciology, 46: 355–361.

Shiklomanov A.I., Lammers R.B., Rawlins M.A., Smith L.C., Pavelsky T.M. (2007). Temporal and spatial variations in maximum river discharge from a new Russian data set. Journal of Geophysical Research: Biogeosciences, 112(G4).

Toropov P.A., Aleshina M.A., Kislov A.V., Semenov V.A. (2018). Trends of climate change in the Black sea – Caspian region in the last 30 years. Moscow University Vestnik. Series 5. Geography, 2.

Vishnevskaya I.A., Desinov L.V., Dolgov S.V., Koronkevich N.I., Shaporenko S.I., Kireeva M.B., Frolova N.L., Rets E.P., Golubchikov S.N. (2016). Geographic and hydrological assessment of floods in the Russian Black Sea region. Izvestiya of the Russian Academy of Sciences. Geographic series, 1, pp. 131-146.

Voitkovskiy K.F. and Volodicheva N.A. (2004). Evolution of Elbrus glacial system. Geography, Society and Environment, 1: 377–395 (in Russian).

Zemp M., Frey H., Gärtner-Roer I., Nussbaumer S.U., Hoelzle M., Paul F., Haeberli W., Denzinger F., Ahlstrøm A.P., Anderson B., and Bajracharya S. (2015). Historically unprecedented global glacier decline in the early 21st century. Journal of Glaciology, 61(228), pp.745-762.

Received on November 15th, 2017 Accepted on July 31st, 2018

FIRST/CORRESPONDING AUTHOR

Ekaterina P. Rets is a Research Scientist at the Water Problems Institute of the Russian Academy of Science, PhD in Geography. Her research interests are mountain hydrology, hydrological modeling in alpine regions, water resources under the impact of climate change, and isotopic methods in mountain hydrology. She does a lot of field study in different mountainous regions. Hydrological observations in Djankuat glaciological station have been carried out under her supervision (in collaboration with Maria Kreeva) since 2007. She is an author of A-Melt hydrological model. She has published more than 15 peer-reviewed articles, is co-author of 3 books, including the Atlas "Modern resources of underground and surface waters of the European part of Russia: formation, distribution, use". She is a member of FRIEND Low Flow and Drought Group.

Alexander N. Safronov[1*], Nikolai F. Elansky[1], Andrey I. Skorokhod[1]
[1] Obukhov Institute of Atmospheric Physics RAS, Moscow, Russia
*** Corresponding author:** safronov_2003@mail.ru

DETECTION OF ATMOSPHERIC POLLUTION SOURCES BY USING CROSS-PLUME SCANNING METHOD AND MOBILE RAILWAY LABORATORY

ABSTRACT. In this study the power of the sulfur dioxide emissions from the Mid-Urals copper-smelting enterprise (MUCE) was estimated by using plume cross-scanning. The combination of the observational data obtained by the TROICA experiments and information obtained by satellite photos of the Earth's surface together with the ISCST3 dispersion model is promising for studies of the short-range atmospheric transport of chemically inactive pollutants. The results of ISCT3 model simulations indicate that the SO_2 emissions in terms of sulfur make up about 3–4% of the plant sulfuric acid production. Also the cross validation between ISCST3 and NOAA HYSPLIT dispersion models was carried out. The emission rate obtained at the NOAA HYSPLIT model simulation is 1.5 times higher than the emission rate calculated at the ISCST3 simulation. It was emphasized, that the using of mobile platforms on electric traction has advantages in studying the environmental situation in comparison with the measurement system, constructed on the stationary Environmental Protection Stations. The cross-plume scanning method to a lesser degree depends on the wind rose, the features of the landscape and a relative location of emission sources and sensors.

KEY WORDS: atmospheric pollution, mobile railroad laboratory, TROICA experiments, quasi-stationary plume, cross-plume scanning

CITATION: Alexander N. Safronov, Nikolai F. Elansky, Andrey I. Skorokhod (2018) Detection of Atmospheric Pollution Sources by Using Cross-Plume Scanning Method and Mobile Railway Laboratory. Geography, Environment, Sustainability, Vol.11, No 3, p. 71-82
DOI-10.24057/2071-9388-2018-11-3-71-82

INTRODUCTION

The TROICA international experiments (TRanscontinental Observations Into the Chemistry of Atmosphere) performed since 1995 have worldwide reputation (Crutzen et al. 1998), (Oberlander et al. 2002), (Tarasova et al. 2005), (Elansky et al. 2009).

The modern TROICA mobile railroad laboratory, which was manufactured in 2004 after a special design, is equipped with high-precision instruments intended for monitoring the gas and aerosol composition of the atmosphere and the radiative and meteorological characteristics and also for monitoring the soil, water, and vegetation pollution. At present, the laboratory is able of continuous real-time monitoring the concentrations of ozone (O_3), nitrogen oxides (NO and NO_2), carbon oxides (CO and CO_2), methane (CH_4) and a sum of non-methane hydrocarbons (NMHC), sulfur dioxide (SO_2), ammonia (NH_3), about 30 volatile organic compounds (VOCs), and radon (^{222}Rn) and its decay products, the mass and number concentrations of aerosol particles (including soot) in the size range from 2 nm to 15 µm, and the entire spectrum of meteorological parameters and solar-radiation characteristics with a high temporal resolution (from 10 s to 20 min), see (Berezina et al. 2013), (Skorokhod et al. 2017), (Vasileva et al. 2017). As a result of cooperation between a number of Russian and world scientific centers, a series of 15 international experiments on observations of the state of the atmosphere over vast Russian regions, from Moscow to Vladivostok and from Murmansk to Kislovodsk, was performed. The peculiar features of the spatial and temporal variations in atmospheric greenhouse gases and in chemically active substances, including ozone-destroying ones, were first obtained. The main factors determining the air quality were first revealed and systemized for different cities against their population, infrastructure, and character of the surrounding country. The causes of formation of extreme ecological situations, such as forest fires, methane leakages from the systems of natural gas transportation, transport of polluted air from neighboring countries, and increases in the oxidative properties of the atmosphere near electric power lines and other objects of power industry, are established.

The TROICA experiments along the Moscow circuit railroad gave unique information on the megapolis effect on the state of the environment; see (Elansky et al. 2010). Such information cannot be obtained on the basis of the traditional means of observations. The discussion about quality of the emission databases available for Russia, in particular EDGAR v4.2, and the comparison of these databases with the measurements carried out by our laboratory can be found in (Elansky et al. 2016) and (Eansky et al. 2018).
One of the important possibilities of this laboratory is the control over the implementation of International ecological agreements (the Kyoto and Montreal Protocoles, the Convention on the transboundary transport of pollutants, desertification of territories, etc.), substantiation of the distribution of quotas for emissions of greenhouse gases, and arbitration in the course of revealing the sources of atmospheric pollutants.

In the present work, an example of using of the TROICA mobile laboratory for revealing the sources of atmospheric pollutants is presented. The work includes the detailed study of the space–time distribution of the concentrations of pollutants in plumes under quasi-stationary conditions by the example of the studies of the sulfur dioxide concentration distribution near the city of Pervoural'sk.

DESCRIPTION OF THE WORK AND RESULTS

Quasi-stationary plumes

As is known, mobile laboratories performing studies of the atmospheric surface layer can be arranged on motor-car, aircraft, and railroad platforms. Due to the use of internal-combustion engines, the laboratories equipped on motor-car platforms provide no possibility of measurements under background conditions.

The aircraft laboratories have advantages and disadvantages. On the one hand, as a rule, they are capable of performing measurements of the concentrations of pollutants at heights exceeding 4000–5000 m, i.e., above the atmospheric mixing layer. On the other hand, their spatial resolution is low, about 1.6–2.2 km, due to high velocities of the flights (the cruising speed of the majority of aircraft laboratories is 600–800 km/h); this estimated resolution relates to the situation when the instrumentation installed in the aircraft laboratories is the same as that used now in the TROICA experiments and allows measurements with the 10-s intervals.

Notice that the resolution of the instrumentation installed at the mobile railroad laboratory is about 110–160 m at a mean train velocity of 40–60 km/h. Therefore, the TROICA experiments give the unique possibility of studying the dispersion scattering with a spatial resolution of about 100 m.

Thus, the TROICA mobile railroad laboratory has evident advantages over the mobile laboratories installed on motor-car and aircraft platforms. Let us compare the possibilities of the stationary observation stations and of the TROICA mobile railroad laboratory as applied to studies of the atmospheric plumes.

In the case of the cross wind, the TROICA measurements allow for obtaining the cross-section of the distribution of pollutants from an emission source. The situation when the time of one measurement in a plume is much less than both the time of the variations in the plume concentrations and the time of the variations in the atmospheric properties is typical.

$$\begin{cases} t_0 \ll \tau_{em} \\ t_0 \ll t_{atm} \end{cases}$$

where t_0 is the time period of one registration of an enhanced concentration in a plume; τ_{em} is the characteristic time of the variations in the emission power; t_{atm} is the time of the variations in the atmospheric properties

Hereafter, such plumes are termed the quasi-stationary ones. The authors make a special emphasis on the principal impossibility of obtaining the space–time distribution of pollutants and the spatial dynamics of the variations in the chemical composition inside quasi-stationary plumes on the basis of the network of stationary ground-based observation stations. The system of stationary observations is based on the passive downwind scanning. To obtain the spatial distribution of pollutants in a plume, the record time at the observation station should exceed the characteristic time of variations in the atmospheric parameters. However, for this time period, the power of the emission source and the chemical composition of the plume may change. Notice that each of the approaches, i.e., monitoring with the network of ground-based observation stations and monitoring with mobile laboratories, has its advantages and disadvantages with a view to studies of dispersion processes.

The disadvantage of the stationary observation systems is a strong effect of the local conditions in the areas of location of stations, including the wind rose, lay of land, and local windward emission sources.

At the same time, the platform vibrations and excesses in the "background" characteristics near motorways and railroads over the background ones in remote areas should be attributed to disadvantages of mobile laboratories intended for monitoring the atmospheric state. However, for the TROICA expeditions, in the case when the mobile laboratory moves along electrified railroads, the excesses in the concentrations of the main pollutants under study are insignificant and do not influence the general pattern of distributions of the pollutants.

When the TROICA carriage-laboratory moves along an electrified railroad and is coupled just after the locomotive, it allows for obtaining information on the undisturbed atmospheric layer not affected by the train pollutants, because the constructional features of the laboratory provide air sampling from the counter airflow through the air inlets located at the top of the carriage-laboratory over the top of the majority of the Russian electric locomotives.

Summing up the aforesaid, we can state that the TROICA mobile railroad laboratory gives a unique possibility for studying the processes of transport of atmospheric pollutants.

General characteristic of the emission source

Along the Trans-Siberian Railroad, the industrial zones and large-scale complexes of most cities are located in the immediate vicinity of the railroad. Therefore, it is of interest to solve the "inverse" problem of determination of the location and power for an emission source from the data on the cross-sections of the plume. We solved this problem by using the standard Gaussian methods. Notice that the Gaussian methods (OND-86, ISCST3) are applicable for distances up to 30–50 km from an emission source and for weakly-uneven territories with dispersed buildings.

By using the SQL search system, the extreme value (35.1 ppb) for the sulfur dioxide concentration measured in the course of the TROICA-8 *East* expedition was taken from the TROICA-DB. The NOAA HYSPLIT model of the back trajectories for heights of 100, 500, 1000 m (a.g.l) was used in the framework of isobaric approximation of vertical mixing for the primary analysis of the transport of air masses enriched with sulfur dioxide near the city of Pervoural'sk. Details about NOAA HYSPLIT model see in (Draxler and Hess 1998), (Draxler 2006), (Stein et al. 2016), (HYSPLIT Model Guide). Basing on analyses of the back trajectories, of the pollutant concentration distribution along the mobile-laboratory route (Fig. 1), and of the data of video cameras installed in the laboratory, we concluded that the emissions of pollutants are not associated with the work of the Pervoural'sk industrial objects but are fully determined by emissions from industrial objects located to the south-west of the observation site. Fig. 1 presents the distributions of nitric oxide, nitrogen dioxide, and sulfur dioxide along the TROICA route; these distributions show that, at a point in time when the sulfur dioxide concentration in the plume was maximal. the plume concentrations of nitric oxide and nitrogen dioxide were already at the background level.

Cartographic studies of the expected emission sources located to the south of Pervoural'sk allowed for making the unambiguous conclusions that the observed anomalous increase in the sulfur dioxide concentration is associated with ejections of the Mid-Urals copper-smelting enterprise (MUCE) (town Revda, 56.85˚N, 59.91˚E). Notice that the main types of the MUCP products are black copper, sulfuric acid, oleum, tripoliphosphate, and xanthogenate.

The spatial distribution of pollutants by the Gaussian model of scattering

Let us use the *ISCST3* Gaussian model to calculate the spatial distribution of pollutants (ISCST3 1995). According to the model, the complete equation giving the spatial distribution can be expressed as follows (1)-(2):

$$C=\frac{QKV}{2\pi\cdot u_s\sigma_y\sigma_2}\times\exp\left(-0.5\frac{y^2}{\sigma_y^2}\right)$$

where: *C(x,y,z)* (μg/m³) is the pollutant concentra-tion at a point with coordinates; *(x,y,z)* (g/s) is the ejection power for a substance; *K*=1·10⁶ is the scaling factor; *V* is the characteristic of vertical scattering; $ó_y ó_z$(m) are the vertical and horizontal standard deviations, м; u_s(m/s) is the wind velocity at the source effective height.

The *ox* axis is directed downwind from the emission source, the *oy* axis is perpendicular to the *ox* axis and lies in the horizontal plane, the *oz* axis is vertical. Under conditions with no dry deposition, the vertical-mixing coefficient is as follows:

$$V=\exp\left[-0.5\left(\frac{z-h_e}{\sigma_z}\right)^2\right]+\exp\left[-0.5\left(\frac{z+h_e}{\sigma_z}\right)^2\right]$$
$$+\sum_{k-1}^{\infty}\left(\begin{array}{l}\exp\left[-0.5\left(\frac{H_1}{\sigma_z}\right)^2\right]+\exp\left[-0.5\left(\frac{H_2}{\sigma_z}\right)^2\right]\\+\exp\left[-0.5\left(\frac{H_3}{\sigma_z}\right)^2\right]+\exp\left[-0.5\left(\frac{H_4}{\sigma_z}\right)^2\right]\end{array}\right)$$

Here, $H_1=z-\left(2kz_i-h_e\right)$,

$H_2=z+\left(2kz_i-h_e\right), H_3=z-\left(2kz_i+h_e\right)$,

and $H_4=z+\left(2kz_i-h_e\right)$;

h_e is the emission-source effective height; z_i is the height of mixing.

The initial data necessary for the emission calculations, namely, the wind velocity and direction, temperature, and pressure, are obtained from the WMO#28440 (Ekaterinburg, meteo.infospace.ru) and

NOAA (www.arl.noaa.gov/ready/amet.html) meteorological stations and from the database on the temperature profiles measured with the MTP-5 instrument during the TROICA expeditions. The atmospheric boundary layer state was characterized by the vertical temperature profile. Fig. 2 gives the vertical temperature profile measured by the MTP-5 instrument near the point of maximal sulfur dioxide concentration. Fig. 2 also characterizes the height dependence of the atmospheric state (the stability class by Pasquill).

It is seen that, at low heights (up to 250 m), the atmosphere is unstable; at heights of 250–300 m, the atmospheric state is neutral (D); and, at heights above 550 m, the atmospheric is of low stability (E). Thus, the form of the plume depends strongly on the pollutant-emission effective height and on the height level of pollutant propagation. If the distance from the point of registration of an anomalously-high pollutant concentration to the pollutant source is not long (10–12 km), it can be considered that, during the pollutant propagation, the pollutant has no time for rising to a height of more than 250 m. Therefore, we take that the atmosphere within the plume is somewhat instable (class C according to Pasquill).

The subsequent calculations were performed by the *ISCST3* method. To calculate the emission-source effective height h_e, the Brigg coefficients (F_b and F_m), the distance (x_f) from the pollutant source to the point of the maximum pollutant concentration, and the wind velocity (u_s) at the effective height were calculated. The dispersions ($ó_y$) and ($ó_z$) along the axis oriented perpendicularly to the plume in the horizontal plane and along the axis oriented upward, respectively, were calculated by the Pasquill-Gifford formulas, see (Briggs 1971), (Briggs 1972).

In the calculations, the following additional parameters of an industrial pollutant source were a priori taken: the smokestack height (h_s) is about 120 m, the smokestack diameter (d_s) is 4.5 m, the gas temperature (T_s) is 150^0C, and the emission rate (v_s) is 10.0 m/s.

The percentage Δ of the sulfur emissions in the enterprise total sulfur production was calculated on the basis of the data for 2004 when 483 442 tons of sulfuric acid was produced. The results of calculations with the *ISCT3* model are presented in Table 1. It is seen that SO_2 emissions in terms of sulfur make up about 3–4% of the enterprise sulfuric acid production. The experimental data and the values calculated with the ISCT3 model for different classes of atmospheric stability were presented in Fig.3. Notice that the figure gives the transverse dispersion projected on the route trajectory, i.e., considering the angle between the wind and route directions.

Notice that the choice of the stability class C proved to be justified, because the dispersions for the stability classes D and E turned out to be smaller than those measured in the course of the TROICA expeditions. This means that, really, the upward flows of the warmed pollutant did not reach the height layers located above 350–400 m, where stable atmospheric conditions occur.

The spatial-temporal SO_2 distribution in the vicinity of town Pervoural'sk

In most cases, simple accumulation of information without consideration of its spatial distribution does not allow the performance of a sufficiently accurate analysis of ecological situation. A great body of data, which is typical for monitoring, is usually difficult for perception until data are visualized on the map. Mapped data allow for revealing the regularity in the distribution of objects or phenomena and their variations in space and time.

Therefore, one of the main aims of the modern geoinformatics is the creation of an integrated database that accumulates the advanced geoinformation technologies. The geoinformation system (GIS) applied in this work consists of the ArcInfo 9.3 together with the GoogleMap space photos and the raster regional itineraries related to reference marks by using the Reoreferencing/ArcInfo standard technology.

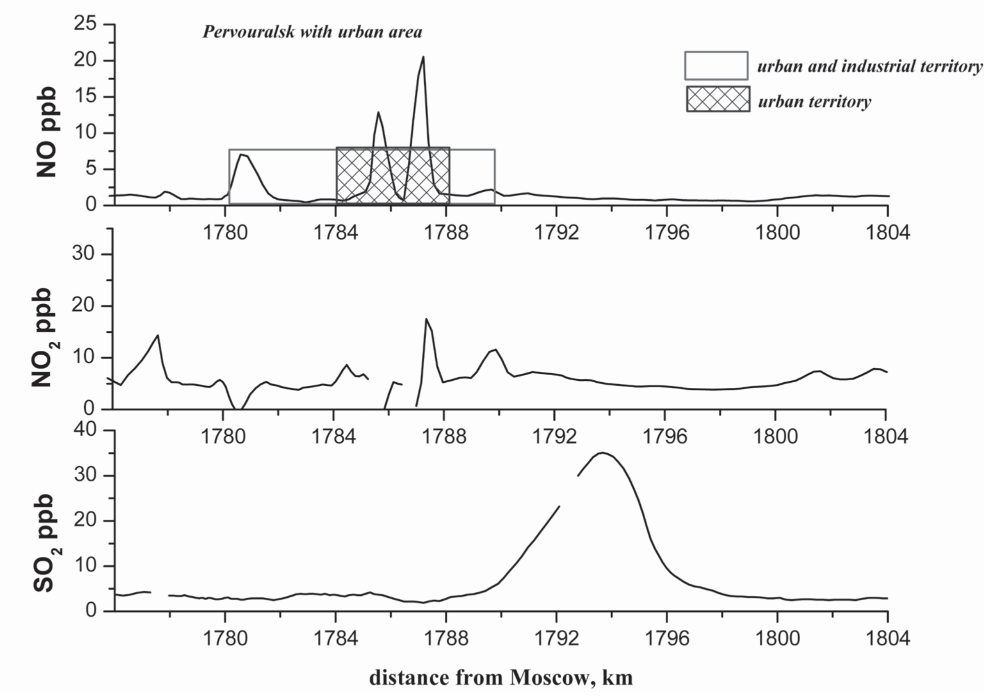

Fig. 1. NO, NO_2 and SO_2 surface concentrations along Trans-Siberian railway in the vicinity of town Pervoural'sk according to mobile laboratory measurements in March, 2004

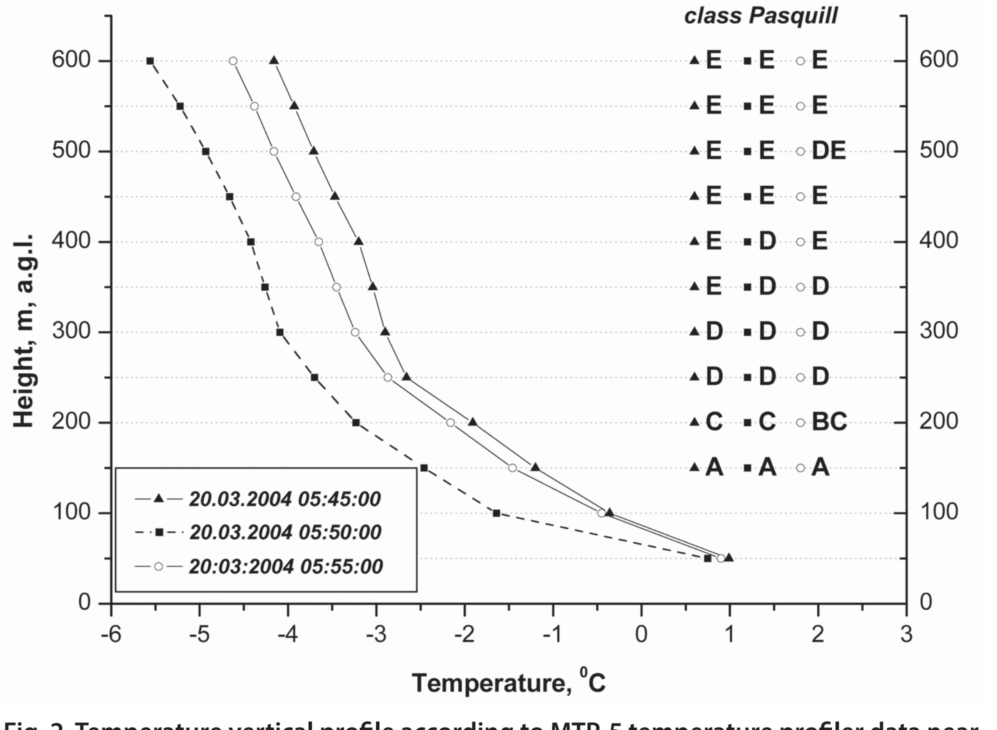

Fig. 2. Temperature vertical profile according to MTP-5 temperature profiler data near sulfur dioxide maximum point

Table 1. Results of calculations on model ISCST3

Model ISCST3		Stability class according to *Pasquill*					
parameter	dimension	A	B	C	D	E	F
u_s	m	3.3	3.3	3.6	4.1	6.7	11
$Ó_y$	m	1527	1163	813	539	403	269
$Ó_z$	m	5000	1385	508	136	79	47
F_b	m^4/s^3	178	178	178	178	178	178
F_m	m^4/s^2	324	324	324	324	324	324
x_f	m	946	946	946	946	515	639
h_e	m	380	380	362	333	206	175
V	–	38.33	10.98	4.24	0.40	0.07	0.00
Q	g/s	384	282	205	435	1707	35152
	t/year	12064	8855	6460	13673	53702	1105514
$\Delta_{\%}$	%	3.8	2.8	2.1	4.3	17	350

As a cartographic basis of Fig. 4, Google Map satellite-borne photography of the Earth's surface is taken. The Mid-Urals copper-smelting enterprise (MUCE) plume of sulfur dioxide concentration distribution calculated with the above-mentioned *ISCST3* model was mapped. The histogram of Fig. 4 designed on the basis the TROICA-8 *East* expedition data gives additional information on the SO2 distribution. It shows that the *ISCST3* model allows a good spatial description of observational data for the 10-km vicinities of pollutant sources.

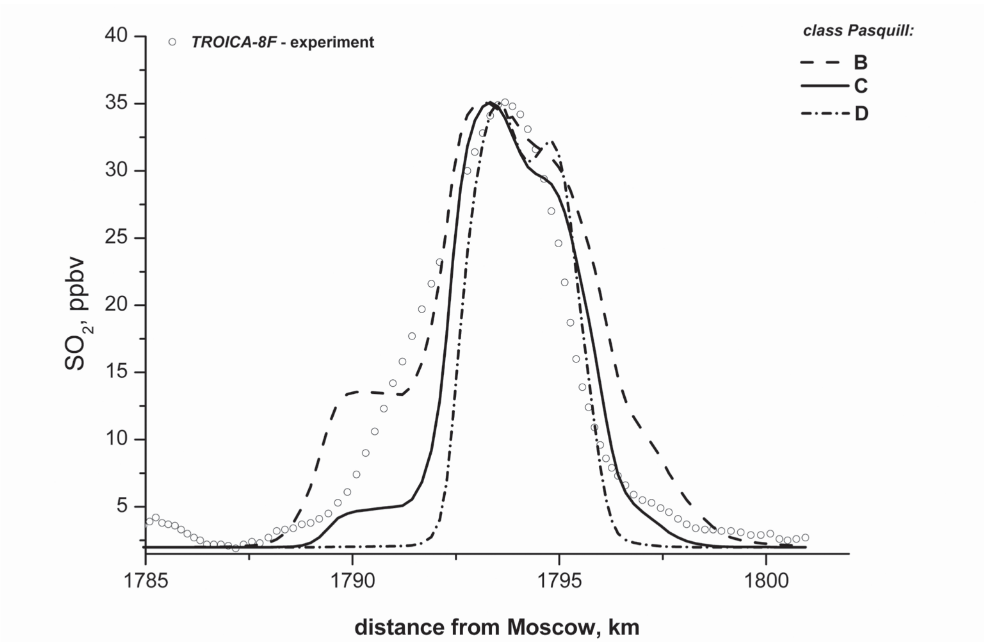

Fig. 3. Experimental data and values calculated on *ISCST3* model for different atmosphere stability classes

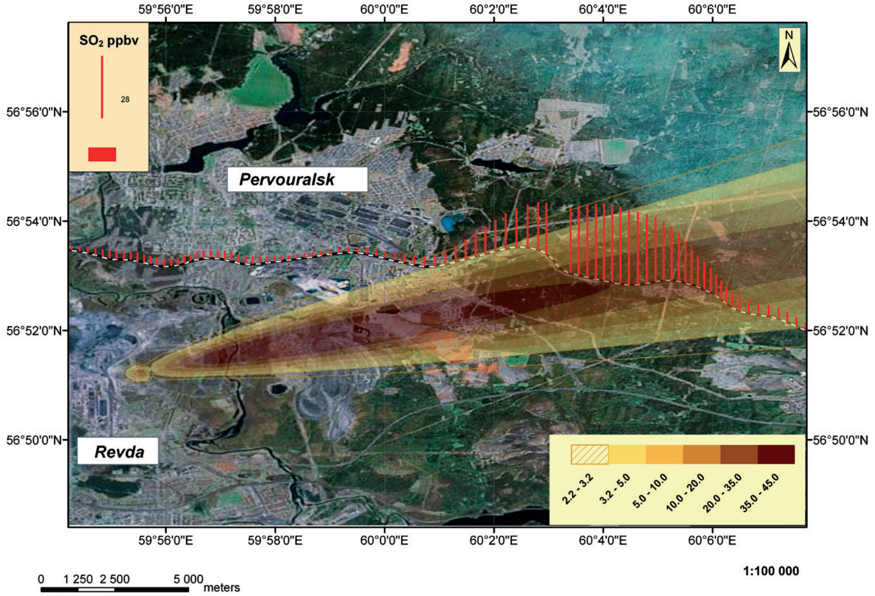

Fig. 4. The SO_2 plume from от Mid-Urals copper-smelting enterprise calculated on *ISCST3* model and shown on satellite image (GoogleMap)

For comparison, the result of the dispersion NOAA HYSPLIT model application to calculations of the spatial distribution of emitted pollutants is given in Fig. 5. It is seen that significant atmospheric pollution expends over a distance of 100–160 km. The estimation of the pollutant-emission power with the dispersion NOAA hysplit model on the basis of the hourly-mean pollutant concentration measured in the 100–200 m (a.g.l.) atmospheric layer leads to a value of 350 g/s. This value is somewhat higher than the value 205 g/s calculated with the ISCST3 model. The difference between these results is possibly caused by the application of the hybrid dispersion TH-part model (the Top Head and Lagrange approximations for the horizontal and vertical directions, respectively) to the calculations with the NOAA HYSPLIT model. The TH-part model underestimates the vertical mixing at small distances from pollutant-emission sources.

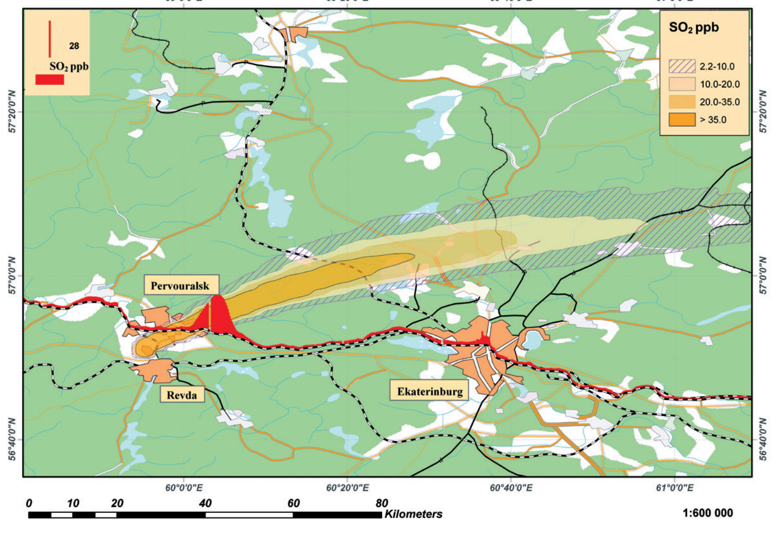

Fig. 5. SO_2 carrying-out spatial distribution calculated by NOAA HYSPLIT dispersion model

CONCLUSIONS

A procedure allowing the retrieval of the locations and powers of sources of atmospheric pollutants from the concentrations and directions of the atmospheric short-range plumes of chemically inactive pollutants monitored by the mobile railroad laboratory is developed. As an example, the power of the sulfur dioxide emissions from the Mid-Urals copper-smelting enterprise (MUCE) is estimated. It is shown that, for estimation of the powers of harmful emissions from the polluting sources located in flat regions at a distance up to 50 km from the Trans-Siberian Railroad, the ISCST3 computational model combined with the detailed satellite-borne photography of the Earth's surface can be successfully applied. It is noted that a combination of the observational data obtained by the TROICA experiments and taken from the geoinformation system (ArcInfo) and of the satellite-borne photos of the Earth's surface (GoogleMap) with the ISCST3 dispersion model is promising for studies of the short-range atmospheric transport of chemically inactive pollutants.

The cross-plume scanning method by using a mobile platform provides a number of advantages over the standard method of assessing of the environmental situation by means of a network of stationary stations. This method to a lesser degree depends on the wind rose, the features of the landscape and a relative location of emission sources and sensors.

REFERENCES

Berezina E.V., Elansky N. F., Moiseenko K.B., Belikov I.B., Shumsky R.A., Safronov A.N. and Brenninkmeijer C.A.M. (2013). Estimation of nocturnal 222Rn soil fluxes over Russia from TROICA measurements. Atmos. Chem. Phys., Vol.13, pp.11695-11708, doi:10.5194/acp-13-11695-2013.

Briggs G. A. (1971). Some recent analyses of plume rise observation, In: Proceedings of the Second International Clean Air Congress, Ed. H. M. Englund and W. T. Berry, Academic Press, Washington, U.S.A., pp. 1029-1032.

Briggs G.A. (1972). Discussion: chimney plumes in neutral and stable surroundings. Atmospheric Environment, Vol.6, pp.507-510, doi:10.1016/0004-6981(72)90120-5

Crutzen P.J., Elansky N.F., Hahn M., Golitsyn G.S., Benninkmeijer C.A.M., Scharffe D.H., Belikov I.B., Maiss M., Bergamaschi P., Röckmann T., Grisenko A.M., Sevostyanov V.M. (1998). Trace Gas Measurements Between Moscow and Vladivistok Using the Trans-Siberian Railroad. Journal of Atmospheric Chemistry, Vol.29, pp.179–194, doi:10.1023/A:1005848202970

Draxler R.R. (2006). The Use of Global and Mesoscale Meteorological Model Data to Predict the Transport and Dispersion of Tracer Plumes over Washington, D.C. Weather and Forecasting, Vol.21, No. 3., pp.383-394, doi:10.1175/WAF926.1.

Draxler R.R. and Hess G.D. (1998). An Overview of the Hysplit_4 Modeling System for Trajectories, Dispersion, and Deposition. Australian Meteorological Magazine. Vol.47, pp.295-308.

Elansky N.F., Belikov I.B., Berezina E.V., Brenninkmeijer C.A.M., Buklikova N. N., Crutzen P.J., Doherty S., Elansky S.N., Elkins J.V., Elokhov A.S., Golitsyn G.S., Gorchakov G.I., Granberg I.G., Grisenko A.M., Holzinger R., Hurst D.F., Iordansky M.A., Kozlova A.A., Kopeikin V.M., Kuokka S., Lavrova O.V., Lisitsyna L.V., Obvintseva L.A., Oberlander E.A., Obvintsev Yu.I., Pankratova N.V., Postylyakov O.V., Putz E., Romashkin P.A., Safronov A.N., Shenfeld K.P., Skorokhod A.I., Shumsky R.A., Tarasova O.A., Turnbull J.C., Vartiainen E., Weissflog L.. Zhernikov K.V. (2009). Atmospheric composition observations over the Northern Eurasia using the mobile laboratory (Troica experiments). Obukhov Institute of Atmospheric Physics, Russian Academy of Science, International Science and Technology Center, European Union, pp.1-75.

Elansky N. F., Belikov I. B., Golitsyn G. S., Grisenko A. M., Lavrova O. V., Pankratova N. V., Safronov A. N., Skorokhod A. I., Shumsky R. A. Observations of the atmosphere composition in the Moscow megapolis from a mobile laboratory (2010). Doklady Earth Sciences, Vol.432, No 1, pp.649-655, doi:10.1134/S1028334X10050211.

Elansky N.F., Lavrova O.V., Skorokhod A. I., Belikov I. B. Trace gases in the atmosphere over Russian cities (2016) Atmospheric Environment, Vol.143, pp.108-119, doi:10.1016/j.atmosenv.2016.08.046

Elansky N.F., Ponomarev N. A., Verevkin Y. M. Air quality and pollutant emissions in the Moscow megacity in 2005–2014 (2018). Atmospheric Environment, Vol.175, pp. 54-64, doi:10.1016/j.atmosenv.2017.11.057

HYSPLIT Model Guide (The Hybrid Single Particle Lagrangian Integrated Trajectory model), desciption available on-line http://www.arl.noaa.gov/ready/hysplit4.html

ISCST3, Industrial Source Complex Short Term dispersion model, U.S. Environmental Protection Agency (EPA), User's guide for the industrial source complex (ISC3) dispersion models, Volume II – description of model algorithms, Office of Air Quality Planning and Standards Emissions, Monitoring, and Analysis Division Research Triangle Park, North Carolina 27711, EPA-454/B-95-003b, September 1995. Available on-line: https://www3.epa.gov/scram001/userg/regmod/isc3v2.pdf

Oberlander E. A., Brenninkmeijer C.A.M., Crutzen P.J., Elansky N.F., Golitsyn G.S., Granber I.G., Scharffe D.H., Hofmann R., Belikov I.B., Paretzke H.G. and van Velthoven P.F.J. (2002). Trace gas measurements along the Trans-Siberian railroad: The TROICA 5 expedition. // Journal of Geophysical Research: Atmospheres, Vol.107, Issue D14, doi:10.1029/2001DJ000953.

Skorokhod A. I., Berezina E. V., Moiseenko K. B., Elansky N. F., and Belikov I. B. (2017). Benzene and toluene in the surface air of northern Eurasia from TROICA-12 campaign along the Trans-Siberian Railway. Atmos. Chem. Phys., Vol.17, pp.5501-5514, doi:10.5194/acp-17-5501-2017.

Stein A. F., Draxler R. R., Rolph G. D., Stunder B.J.B., Cohen M.D., Ngan F. (2015). NOAA's HYSPLIT Atmospheric Transport and Dispersion Modeling System. Bulletin of the American Meteorological Society, Vol.96, No.12, doi:10.1175/BAMS-D-14-00110.1.

Tarasova O.A., Brenninkmeijer C.A.M., Assonov S.S., Elansky N.F. and Hurst D.F. (2005). Methane variability measured across Russia during TROICA expeditions. Environmental Sciences, Vol. 2, No. 2-3, pp.241-251, doi: 10.1080/15693430500384713

Vasileva A., Moiseenko K., Skorokhod A., Belikov I., Kopeikin V., and Lavrova O. (2017). Emission ratios of trace gases and particles for Siberian forest fires on the basis of mobile ground observations. Atmos. Chem. Phys., Vol.17, pp.12303-12325, doi:10.5194/acp-17-12303-2017.

Received on April 23rd, 2018 Accepted on July 31st, 2018

AUTHORS

Alexander N. Safronov is scientific researcher in the Laboratory of Atmospheric Gaseous Species (LAGS) at the A.M. Obukhov Institute of Atmospheric Physics RAS. In 1982 he graduated with honors from Faculty of Experimental and Theoretical Physics of the Moscow Engineering Physics Institute. Then he worked during 1982 – 1987 at the National Research Center "Kurchatov Institute" as a researcher investigating the generated spontaneous emission in the Free Electron Laser (FEL). In 1987 he has also graduated the Department of Mechanics and Mathematics of the Lomonosov Moscow State University. In 1990 – 1996 he was an assistant professor at the Department of Physics of the Moscow State University of Fine Chemical Technologies. A.N. Safronov has obtained in 1994 his PhD degree in Physical and Mathematical Sciences (in the Section of the Theoretical Physics). The theme of his dissertation was "The investigation of transient and quasitransition radiation". From 2002 till present he is a researcher at the A.M. Obukhov Institute of Atmospheric Physics. In 2015-2016 he also was a collaborator in the Nuclear Safety Institute (IBRAE) of RAS. His scientific interests are transient and quasitransition radiation, atmospheric composition in background and urban regions, air quality, atmospheric spectroscopy, database creation, GIS system using, CTM simulations, dynamic processes in the atmosphere, nuclear safety and philosophy. He is an author (and co-author) of 30 publications in Russian and international journals.

Nikolai F. Elansky is Head of Department at the A.M. Obukhov Institute of Atmospheric Physics RAS. He is doctor of Physical and Mathematical Sciences since 1998, he is Corresponding Member of the RAS since September 18, 2013. Elansky is Author (and co-author) of 180 publications in Russian and foreign editions. His research interests are in the fields of investigation of small impurities in the atmosphere, organization of measurements of atmospheric composition and solar radiation, statistical data analysis, numerical simulation of photochemical and dynamic processes in the atmosphere. He is organizer and supervisor of the observational system for tropospheric ozone and nitrogen dioxide, which is part of the global atmospheric monitoring networks GAW and NDSC; participant of Russian-American space projects: METEOR-3 / TOMS; METEOR-3 / SAGE-3. Head of many national and international projects, in particular ECCA, TRIDES, TROICA. The scientific leader of the work on the creation of a mobile railway laboratory.

He is member of the International Commission on Atmospheric Ozone, chairman of the section on atmospheric ozone at the National Geophysical Committee, participant of several academic and interdepartmental commissions, expert working groups. He was awarded with the Certificate of Honor of the Russian Academy of Sciences. In 2004 he got «Environmental Hero» from the Department of Commerce and NOAA USA.

Andrey I. Skorokhod currently works as Head of Laboratory of Atmospheric Gaseous Species (LAGS) at the A.M. Obukhov Institute of Atmospheric Physics RAS. He is an expert in atmospheric chemistry of lower troposphere. In 1992 he graduated from Department of Oceanology of Geographical Faculty of Lomonosov Moscow State University. Then worked at the State Oceanography Institute, Moscow as a post-graduate student and researcher investigating marine water and ice chemistry and salinity for seas surrounding Russia. In 1996 defended his PhD Thesis work about chemistry and salinity of the Caspian Sea waters. Since 1999 started to work at the A.M. Obukhov Institute of Atmospheric Physics RAS studying and observing atmospheric chemistry and air pollution. Since that time he has been leading several large-scale scientific projects about trace gases and aerosols in Moscow, Central Siberia and other parts of Russia and Northern Eurasia. Since 2014 Andrey has headed scientific program on greenhouse and reactive trace gases observations over the Arctic Ocean.

Igor Esau[1*], Victoria Miles[1]
[1] Nansen Environmental and Remote Sensing Centre/Bjerknes Centre for Climate Research, Bergen, Norway
*** Corresponding author:** igore@nersc.no

EXOGENOUS DRIVERS OF SURFACE URBAN HEAT ISLANDS IN NORTHERN WEST SIBERIA

ABSTRACT. Urban temperature anomalies, frequently referred to as the urban heat islands (UHIs), are of the most distinct and influential climatic factors with significant impact on urban life and environment. However, UHIs in high latitudes are still studied only fragmentary. There is a knowledge gap related to the urban temperature distinction with respect to local temperature anomalies of natural surface types. This study extends upon our recent high latitude regional-scale climatic survey in 28 cities in the Northern West Siberia (NWS) region. Based on MODIS land surface temperature (LST) products covering 15 years between 2001 and 2015, it was revealed that all 28 cities have significant surface urban heat islands (SUHIs). The strong statistical dependence (r = 0.73) on endogenous factors such as city size and the population was found. It was suggested that exogenous factors such as the background LC types could be significant as well. This study presents the analysis of the exogenous factors shaping the apparent SUHI intensities. The major contribution to the SUHI was revealed for water, sparse vegetation, grassland, and shrubland. There are no clear dependence between the partial SUHI intensity and the area fraction occupied by the given LC type. The mechanisms and pathways of the SUHI maintenance cannot be inferred solely from the remote sensing data. Further understanding requires numerical experiments with turbulence-resolving models.

KEY WORDS: Surface Urban Heat Island, Remote sensing, MODIS, Siberia, Exogenous factors of urban climate, Sustainable urban development

CITATION: Igor Esau, Victoria Miles (2018) Exogenous Drivers Of Surface Urban Heat Islands In Northern West Siberia. Geography, Environment, Sustainability, Vol.11, No 3, p. 83-99
DOI-10.24057/2071-9388-2018-11-3-83-99

INTRODUCTION

Microclimates of anthropogenic and natural landscapes can significantly deviate from the regional climate. Anthropogenic landscapes dominate urban and industrial areas where the economic and cultural values of our societies are concentrated. These values induce the need to characterize urban microclimates and to distinguishes them from microclimates of the surrounding natural landscapes. An urban microclimate is typically warmer than that outside of the city margins. This phenomenon is widely referred to as an urban heat island (UHI), or, more specifically, as a surface urban heat island (SUHI) when the land surface temperature (LST) is considered (Voogt and Oke 2003). It should be noted that even the most rigorous studies are somewhat vague on definition of urban and rural temperature observations (Lowry 1977); as they might be affected by the urban boundary layer footprint (Tomlinson et al. 2012).

Following urban climate literature, the UHI intensity could be defined as a temperature difference

$$\Delta T = T_u - T_r \tag{1}$$

between the urban and rural sites. The choice of proper sites is however never trivial. Both urban and natural microclimates are geographically fragmented. Both T_u and T_r vary strongly from site to site. Stewart (2011) proposed a set of reasonable criteria to organize inter-comparable surface air temperature (SAT) measurements in the UHI studies. Those criteria are however not universal and would probably not meet the needs of many practical tasks.

Satellite observations and remote-sensing data sets open an opportunity to study urban microclimate with spatially dense and regular meteorological data. In this case, T_u , T_r and ΔT could be understood correspondingly as the urban and rural LST and the SUHI intensity. Schwartz et al. (2011) compared 11 approaches for quantifying SUHI with the Moderate Resolution Imaging Spectroradiometer (MODIS) LST data for European cities. The study showed that the resulting SUHI intensity is strongly sensitive to the choice of both urban and rural pixels as well as the calculation methods.

Effective utilization of the urban microclimate information in decision-making processes is impossible without understanding of the UHI driving factors, mechanisms and variability. Such studies require internally homogeneous, intercomparable ΔT data sets to retrieve the effects of different endogenous factors, i.e. those induced by the urban characteristics itself, and *exogenous* factors, i.e. those induced by the characteristics of the surrounding natural background. The endogenous factors change T_u. Among the most common endogenous factors, one may find dependences on the percent of impervious surface area (ISA) (e.g. Li et al. 2018), the city area and population (e.g. Oke 1973; Sun and Lin 2005; Mokhov 2009; Shastri et al. 2017). For example, a high correlation between T_u from the MODIS LST and ISA was shown in Minneapolis (USA) (Yuan and Marvin 2007). Smoliak et al. (2015) took this correlation into account redefining the UHI as the urban-airport temperature difference. Their approach separates the anthropogenic flux contribution but is inconsistent with observations requirements for the natural background temperatures. A wider study by Imhoff et al. (2010) concluded that the ISA alone could explain up to 70% of the total LST variance in 38 the most populous US cities. Zhang et al. (2010) found that 60% of the total LST variance could be explained by the ISA for the cities within a high-latitude forest zone.

The exogenous factors induce changes in T_r. In many cases, the endogenous factors alone cannot characterize the urban microclimate and the anthropogenic contribution in its formation. Hu and Jia (2010) found expansion of the positive temperature anomalies with land use – land cover changes in China. They noted that the temperature observations are very sensitive to the placement of a meteorological station. Zhao et al. (2014) studied major North American cities and concluded that the exogenous factors, such as the local background climate, strongly influence the UHI intensity. The urban temperature anomalies, ΔT, were-largely explained by variations in the air-land heat exchange within the atmospheric boundary layer – canopy – upper soil system. This efficiency is largely controlled by the physical climatic factors of the surrounding natural background, which include aerodynamic surface roughness, soil heat capacity, surface albedo and evapotranspiration properties. As the physical factors are difficult and expensive to measure and quantify, geographical climatic factors, e.g. land cover (LC) types, are more widely applied (e.g. He et al. 2010). Yang et al. (2017) reviewed the influence of background landscape on the SUHI intensity in 332 Chinese cities across several climate zones. In the study, LC types were retrieved from satellite observations and used to identify the profound effects of the natural microclimatic factors on the LST. The most significant impact was attributed to vegetation classes such as forest, grassland and cultivated land. The overall effect was that the UHI in humid forested landscapes is less intensive than in open dry ones.

There are good reasons to expect that the exogenous factors are similarly or even more effective in scaling the SUHI intensity in high latitudes. There are often more contrasting landscapes of dark coniferous forest and open grassland. The natural local temperature differences could be large and persistent (Li et al. 2015), while snow cover may exacerbate differences in the surface radiative balance (Lemonsu et al. 2008; Dudorova and Belan 2015; Mori and Sato 2015). There is strong competition between sensible and latent fluxes for additional heating, whereas the balance could be skewed by small changes in soil moisture (Brunsell et al. 2011; Barichivich et al. 2014). Moreover, the additional heat is usually trapped near the surface in the stably stratified atmosphere, raising the temperature more than it would be observed at lower latitudes (Davy and Esau 2016; Davy et al. 2017).

The SUHI in the boreal regions have received some attention only in recent years. Before the Miles and Esau (2017) study, hereafter referred to as ME17, the published remote sensing studies had not extended north of 60°N (Zhang et al. 2010; Peng et al. 2012; Clinton and Gong 2013). There were however a few available in situ studies addressing the UHI in the high-latitude cities (Magee 1999; Hinkel and Nelson 2007; Varentsov et al. 2014; Konstantinov et al. 2015). The most recent in situ study by Konstantinov et al. (2018) have addressed the UHI in 3 cities in Northern Western Siberia (NWS). Both the ME17 and Konstantinov et al. (2018) studies revealed rather large intensity of the urban LST and air temperature anomalies with peak values exceeding 10K. The seasonally averaged SUHI intensities are however less extreme. They vary between 0.5K to 2.5K in most cases in both seasons. Moreover, the SUHI in NWS demonstrates a rather unusual behaviour, with larger wintertime and nocturnal intensities.

In this study, we investigate the *exogenous* factors affecting, and therefore, contributing to the large scatter and unusual behaviour of the SUHI intensities found in the 28 NWS cities. Although such exogenous factors of the SUHI received little attention in literature, there is a growing demand to assess them and determine their role in shaping urban microclimates. This demand is driven by the observed and suggested SUHI impact on related physical, ecological and socio-economic processes (Makhrovskaya et al. 1977; Lapenis et al. 2005; Khrustalyov and Davidova 2007; Heleniak 2009; Grebenets et al. 2012; Streletskiy et al. 2012; Shiklomanov et al. 2016; Esau and Miles 2016). There are strong physical reasons to expect that the cold continental climate in NWS exacerbates the microclimatic distinction, trapping heat in a shallow urban boundary layer of the stably stratified lower atmosphere (Davy and Esau 2016; Davy et al. 2017). This study is based on the same data sets as ME17, but its focus shifts to the spatial composition with respect to selected land cover types. The data represent the period between 2001 and 2015.

MATERIALS AND METHODS

The study area

The NWS region has the largest concentration of small and medium cities in severe continental climate across several bioclimatic zones of high latitudes. This region includes the territory of two administrative districts (okrugs): Yamalo-Nenets Autonomous Okrug and Khanty–Mansi Autonomous Okrug. The NWS landscape is flat and homogeneous. However, at the city scales, the land cover could be rather heterogeneous and fragmented. The surface elevations are typically less than 100 meters above the sea level. The low, flat surface and large surface humidity result in widespread paludification of the region; in some parts, swamps cover up to 80%. Forest covers only 36% of the area.

Climate of the region is of the Dfc type (cold, fully humid climate with snow) according to the Koeppen-Geiger classification (Kottek et al. 2006). The mean winter surface temperature and amount of snow decrease in the northeastern direction, according to the Russian National Atlas (http://национальныйатлас.рф). Winters are cold with the stable snow cover from October through April (200 to 230 days per annum). The mean January temperatures vary between –22°C and –29°C. The mean July temperatures are distributed more uniformly with a south-north temperature decrease from +17°C (in the cities along the middle Ob river) to +14°C (in the northernmost cities). The mean annual surface air temperatures are between –2°C to –9°C. At the same time, permafrost remains isolated, sporadic and discontinuous due to significant snow depth (about 150 cm by the end of the season), according to the International Permafrost Association (https://ipa.arcticportal.org/). The cloud cover in the region is moderate (60%) with a large number of the clear-sky days (1600 hours of the annual sunshine), particularly in the winter season. Thus, the regional climate is beneficial to the application of remotely sensed data sets.

The MODIS LST data products

This study utilizes the LST data from the Moderate Resolution Imaging Spectroradiometer (MODIS), which provides an opportunity for the region-scale analysis of the SUHI. The MODIS data has high calibration accuracy in multiple thermal infrared bands designed for retrievals of the LST and atmospheric properties (Wang 2008). The LST products from the MODIS sensors aboard the Terra (EOS AM) and Aqua (EOS PM) satellites have been already widely used for the urban climate studies (e.g., Imhoff et al. 2010; Clinton and Gong 2012; Peng 2012). It has been shown that the MODIS LST have high correlations with the in situ measured soil temperature for different northern land cover types (Muster et al. 2015) and with the surface air temperature measured at the height of 2 m above the ground (Comiso 2003; Jin and Dickinson 2010; Hachem et al. 2012). Although the MODIS LST is observed only under the clear-sky weather conditions, it is generally representative for climatic LST studies (Chen et al. 2017), especially when the gap filling in larger areas is applied (Yang et al. 2017; Metz et al. 2017). We continue the discussion of the LST – SAT differences in the high latitudes in the next section.

This study considers the thermal anomaly associated with urban areas using the Terra/MODIS LST product MOD11A2. MOD11A2 is an 8-day LST product by averaging from two to eight days of the clear sky MOD11A1 daily product and has 12 Science Data Sets (SDS) layers (Li 2013). A split-window algorithm is used for calculating the LST. The day/night LST method retrieves land-surface temperature and band emissivity simultaneously from pairs of daytime and night-time MODIS data scenes in seven TIR bands. The LST composites were downloaded from http://reverb.echo.nasa.gov/. The data were re-projected from the Sinusoidal projection to the UTM Zone 42N projection system with the WGS84 datum. The data were also reformatted from HDF-EOS to GeoTIFF and converted from °K to °C. According to the product quality control flag, the utilized data have an average LST error ≤ 2°C.

This study considers data collected between 2001 and 2015. The analysis has been carried out for winter (December, January and February, DJF) and summer (June, July and August, JJA) seasons. We processed day and night LST data for the Terra/MODIS overpass times at approximately 10:30 and 22:30 local time.

The SUHI definition

The SUHI intensity, ΔT, is defined by Eq. 1 in this study. The ME17 study defined the urban temperature, T_u, as the maximal temperature of the urban pixels. The urban pixels were associated with the city area (polygon) given by the administrative city boundaries. The city edge polygons were downloaded from the Russian Demographic Database (http://www.grid.unep.ch/russia/). Because administrative city boundaries differed from the true extents, each polygon was manually corrected using ArcGIS base maps.

The rural temperature, T_r, was defined as the average temperature of the surrounding, non-urban pixels in a 2 km buffer around the city area. Rural pixels were classified as natural surfaces of different LC types. Averaging did not account for the LC types of the rural pixels. But we excluded all pixels related to the urban or artificial surfaces and water pixels, because these surfaces have significant impact on the mean rural LST. The approach was partially adopted from that by Zhou et al. (2013). Thus, the resulting represented the difference between the maximum temperature of the city and the mean temperature of minimally developed land outside the city. Daytime and nighttime SUHI were calculated separately for winter and summer seasons. They were further averaged to obtain the seasonal mean values. Such SUHI are methodologically similar to the SUHI in the earlier studies by e.g. Peng et al. (2012) and Zhou et al. (2015).

Investigation of the exogenous factors requires a redefinition of the type-specific SUHI intensity as the temperature difference between the maximal urban temperature, T_u, and the temperature average over all pixels of a given LC type, l. Thus, Eq. 1 will be interpreted as

$$\Delta T_l = T_u - T_l \tag{2}$$

If the fraction of the buffer, which is covered by the LC type l, is f_l where

$$\sum_l f_l = 1 \quad ,$$

then one may recover

$$\Delta T = \sum_l f_l \Delta T_l = T_u - \sum_l f_l T_l = T_u - T_r \tag{3}$$

where $f_l \Delta T_l$ is the partial contribution of the l-th LC type to the total SUHI intensity. The type-specific SUHI intensity does not necessarily need to be positive. According to the conclusion of Li et al. (2015), the SUHI might be negative relative to the boreal forest LC types.

The land cover data set

This study is based on the LC types from the Climate Change Initiative (CCI) data provided by the European Space Agency (ESA). The data are publicly available. The CCI LC data have the spatial resolution of 300 m. The LC types were obtained from the annual global time series from 1992 to 2015. In this study, we use the data for 2015. The land cover was extracted from CCI LC raster and converted to polygons. The original CCI LC types were aggregated into new 9 more general LC types. Table 1 provides an overview of the CCI LC types that were found around the NWS cities, and aggregated types used in this study. All GIS and remote-sensing data were processed using ArcGIS 10.3 software.

The 28 NWS cities

The study considers 28 NWS cities. The list of cities is given in Table 1. Fig. 1 shows the NWS region with the cities, SUHI intensity and background mean seasonal LST. The majority of the considered settlements exhibit SUHI intensities in the range from 1.5 K to 3.0 K with the extreme wintertime SUHI anomaly in Surgut exceeding 5 K. The seasonally averaged summer SUHI intensities in these cities have small and even negative values in the most northern cities.

The impact of exogenic factors on the SUHI was quantified through calculation of the LST differences between the urban LC type and the specific LC types found in the 2 km buffer around administrative boundaries of each city. This method is given by Eq. 2 and Eq. 3. Fig. 2 gives a visual example of the method applied to the small-size city of Pokachy. It shows the city polygon and the surrounding 2 km buffer covered by different aggregated LC types in 300 x 300 m^2 squares. The numbers show the mean summer (positive) and winter (negative) LST for different LC types. This figure reveals that all LC types have lower LST than the urban area. However, there are significant differences between the LC types. The area is largely covered with sparse vegetation and wetlands. Wetlands are considerably warmer than the other LC types, reducing the specific SUHI by almost 1 K.

Composition of the LC types surrounding the cities

The natural background of the NWS cities is dominated by three LC types: wetland; grassland; and sparse vegetation. Only a few cities are in the background with a large fraction of woodland (Beloyarsky, Purpe, Nyagan and Sovetskiy) and shrubland (Nefteyugansk, Nadym, Labytnangi). Fig. 3 presents the fractions of the LC types for each city. The natural background of many cities

Table 1. The CCI LC types

ID	Aggregated LC types	Original CCI LC type description
10	Cropland	Cropland, rainfed
11	Grassland	Herbaceous cover
30	Cropland	Mosaic cropland (>50%) / natural vegetation (tree, shrub, herbaceous cover) (<50%)
40	Woodland	Mosaic natural vegetation (tree, shrub, herbaceous cover) (>50%) / cropland (<50%)
60	Spare vegetation	Tree cover, broadleaved, deciduous, closed to open (>15%)
70	Spare vegetation	Tree cover, needleleaved, evergreen, closed to open (>15%)
80	Spare vegetation	Tree cover, needleleaved, deciduous, closed to open (>15%)
90	Woodland	Tree cover, mixed leaf type (broadleaved and needleleaved)
100	Shrubland	Mosaic tree and shrub (>50%) / herbaceous cover (<50%)
110	Grassland	Mosaic herbaceous cover (>50%) / tree and shrub (<50%)
120	Shrubland	Shrubland
122	Shrubland	Shrubland deciduous
130	Sparse vegetation	Grassland
140	Spare vegetation	Lichens and mosses
150	Spare vegetation	Sparse vegetation (tree, shrub, herbaceous cover) (<15%)
152	Spare vegetation	Sparse shrub (<15%)
160	Wetland	Tree cover, flooded, fresh or brakish water
180	Wetland	Shrub or herbaceous cover, flooded, fresh/saline/brakish water
190	Artificial land	Urban areas
200	Bare areas	Bare areas
201	Bare areas	Consolidated bare areas
210	Water bodies	Water bodies

is largely covered by one or two LC types. It makes the corresponding SUHI dependent on the local climate of that specific LC type, and therefore, intercomparison becomes sensitive to selection of the cities with similar LC types. A few cities found on a more diverse background. This applies mostly to the older cities (Salekhard/Labytnangi, Khanty-Mansiysk).

Exogenic contribution to the SUHI intensity

We calculated the partial contribution of each aggregated LC type to the total SUHI intensity for the considered 28 cities in the NWS region. The LC type data (Fig. 3) were used to obtain the fractional area, f_l, and the LST data (e.g. as in Fig. 2) – to obtain the LST anomaly, ΔT_l, specific for the given LC type. The method is given in Eq. 3. Fig. 4 shows that some LC types can locally have nearly the same or even higher LST as the urban proper itself.

The apparent SUHI is the most pronounced on the background of spare vegetation and grassland. In some cities, shrubland has also contributed in the SUHI. The contributions of woodland, wetland and water types are

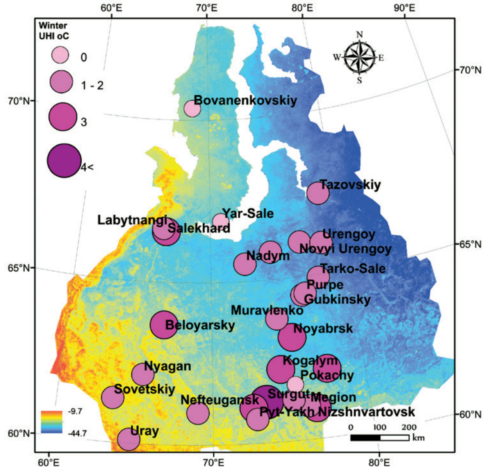

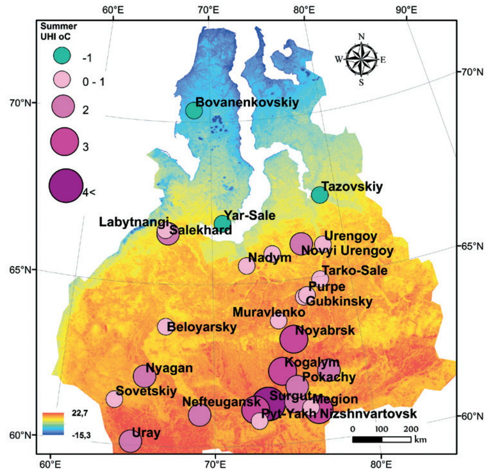

(a) (b)

Fig. 1. Map of the Northern Western Siberia with the SUHI in the 28 cities: (a) the mean winter background LST (colour shading) and SUHI (coloured circles); (b) the mean summer background LST and SUHI. The summer season includes June, July and August, whereas the winter season includes December, January and February

Table 2. Studied cities in the northern West Siberia region and their relevant characteristics

City name	Pop. (x10^3)	Area (km^2)	Long. (deg.)	Lat. (deg.)	SUHI JJA (K)	SUHI DJF (K)	LST JJA (°C)	LST DJF (°C)
Beloyarsky	49	33	66,68	63,71	1,45	2,59	15,63	-25,68
Bovanenkovskiy	4	0,5	68,54	70,36	0,00	0,00	7,84	-26,17
Gubkinsky	26	18	76,46	64,44	0,80	1,66	15,22	-28,06
Khanty-Mansyisk	93	22	69,02	61,01	1,50	2,19	16,72	-22,81
Kogalym	61	79	74,54	62,25	2,89	3,33	16,07	-26,54
Labytnangi	26	12	66,42	66,66	1,19	1,89	13,40	-26,68
Langepas	43	19	75,18	61,26	1,92	1,83	16,40	-26,00
Megion	49	6	76,11	61,04	1,33	1,59	17,14	-24,16
Muravlenko	33	14	74,53	63,79	1,21	1,64	16,01	-27,18
Nadym	46	10	72,53	65,54	1,32	1,78	14,65	-27,13
Nefteugansk	126	30	72,60	61,09	2,62	2,79	17,19	-24,76
Nizshnevartovsk	266	76	76,55	60,94	3,30	3,94	17,21	-25,26
Novyi Urengoy	116	64	76,83	66,04	1,56	2,02	15,16	-28,74
Noyabrsk	107	69	75,45	63,19	3,20	2,69	15,26	-26,75
Nyagan	56	22	65,40	62,14	2,41	2,19	16,13	-23,49
Pangody	11	8	74,52	65,87	1,14	1,55	14,09	-28,82
Pokachy	17	10	75,60	61,74	1,93	0,43	17,22	-26,07
Purpe	10	9	76,70	64,49	0,67	1,06	15,59	-27,87

Pyt-Yakh	41	23	72,82	60,74	1,17	1,72	16,52	-24,60
Raduzhnyi	43	123	77,47	62,11	2,37	3,03	15,91	-27,26
Salekhard	48	17	66,60	66,53	2,28	3,29	12,86	-26,27
Sovetskiy	28	14	63,57	61,37	1,38	1,16	16,60	-22,46
Surgut	332	54	73,41	61,25	3,64	5,97	17,69	-22,97
Tarko-Sale	21	7	77,79	64,92	0,93	0,93	14,82	-29,23
Tazovskiy	7	6	78,71	67,48	0,28	0,79	12,19	-29,16
Uray	40	31	64,77	60,12	1,54	1,30	17,08	-21,56
Urengoy	11	8	78,36	65,97	1,02	0,73	13,49	-29,55
Yar-Sale	7	1	70,83	66,87	0,00	0,00	11,38	-27,60

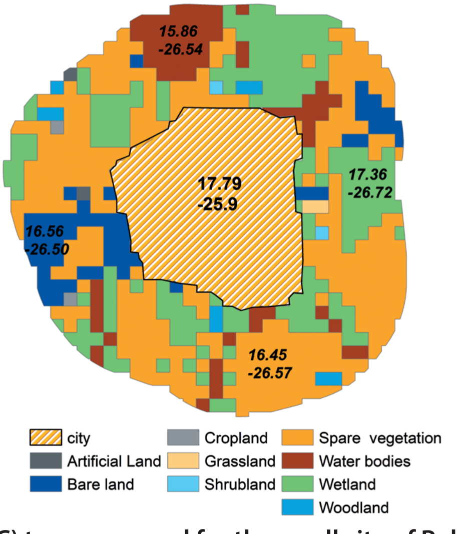

Fig. 2. Land cover (LC) types mapped for the small city of Pokachy. The colour coding shows the different aggregated LC types. The numbers indicate the summer (positive) and the winter (negative) mean LST for the given LC type in the buffer. Details could be found in the text

much smaller (or even negative) than would be expected from their land fraction cover. To further look at these relationships, we studied the SUHI intensity dependence on each LC type. Fig. 5 reveals that there is no clear dependence for each given LC type. At the same time, both the averaged SUHI and the scatter of ΔT_i strongly vary with the LC type. The non-vegetated LC types support the largest SUHI scatter, whereas grassland and cropland support the smallest scatter.

Discussion on the local climates of the LC types

The local climates are shaped by the thermal and aerodynamical features of the surface, by soil moisture and evapotranspiration from the vegetation canopy. Low surface albedo of boreal forest and shrubland, particularly in winter, creates sharp LST contrasts with other LC types. The differences of upper soil moisture shift the balance between latent and sensible heat fluxes sharing a limited amount of incoming heat. Boreal woodland and shrubland, particularly the dark coniferous forest, absorb a larger share of incoming solar radiation than the lighter urban surfaces and other natural LC types (Bonan et al. 1992; Bonan 2008). The surface albedo (from MODIS) of snow covered grassland is 0.7 in the region, whereas it is only 0.5 in the forest area and less than 0.4 without the snow cover (Atlaskina et al. 2015). Lee et al. (2011) and Li et al. (2015) demonstrated that the boreal forest is generally warmer than other surface types. Thus, the boreal forest reduces the apparent SUHI if the urban area itself does not includes significant forest patches. Spatial heterogeneity of vegetation trends in the region was studied in Miles and Esau (2016). The role of warmer water surface and wetlands becomes important in the northernmost settlements where it reduces the apparent SUHI intensities in Bovanenkovskiy, Yar-Sale and Tazovskiy in summertime, and in Megion and Novyi Urengoy in wintertime.

The winter SUHI is less sensitive to the LC types in the urban buffer. The direct anthropogenic heating in the cold climate cities may reach 50 W m^{-2} and even more locally in severe climate conditions of more densely populated cities (Flanner 2009). This anthropogenic flux exceeds the natural urban heat forcing and supports the winter SUHI in the NWS cities despite less contrasting snow-covered surface.

Discussion on the LST – SAT differences

Recent comprehensive assessments of the LST – SAT differences by Yang et al. (2017) and Nielsen-Englyst et al. (2018) help to understand the physical factors and seasonality of the LST deviations. As Zilitinkevich and Esau (2005) have shown, these differences remain small in convective and near-neutral atmosphere, which can be associated with the positive surface heat balance. The differences rapidly increase in stably-stratified atmosphere, which can be associated with the negative surface heat balance (Esau et al. 2012; Davy and Esau 2014). Thus, increasing atmospheric stability leads to progressively larger cold bias in the LST with respect to the SAT. The periods of diurnal and seasonal cycle, which

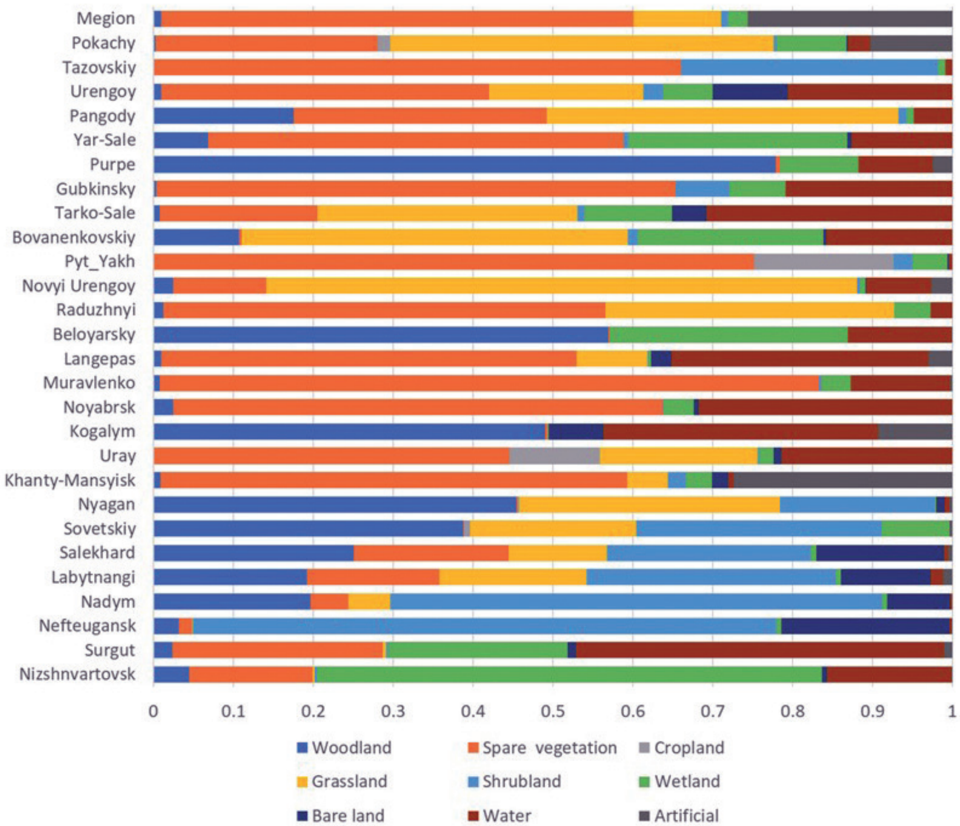

Fig. 3. Composition of the aggregated CCI LC types in the 2 km buffers around the 28 cities in the NWS

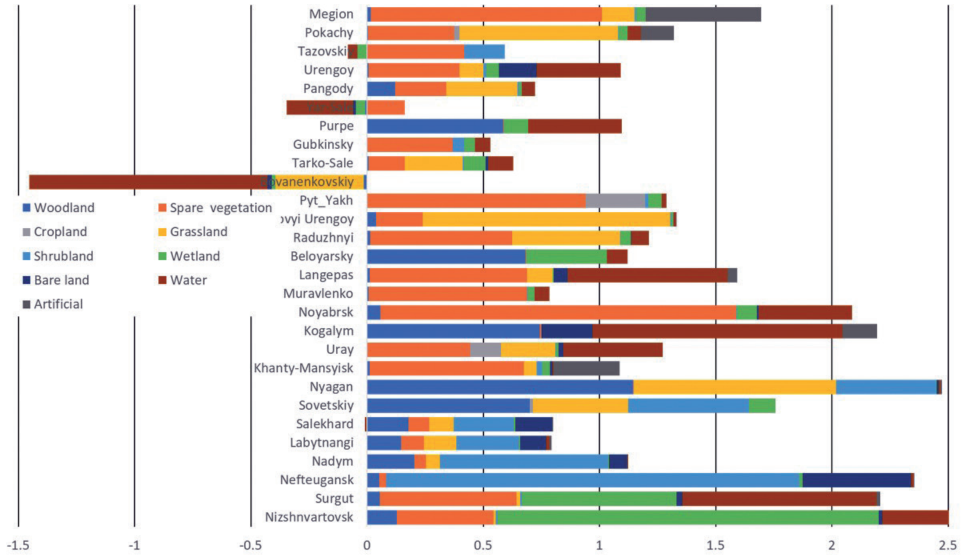

(a) Summer SUHI

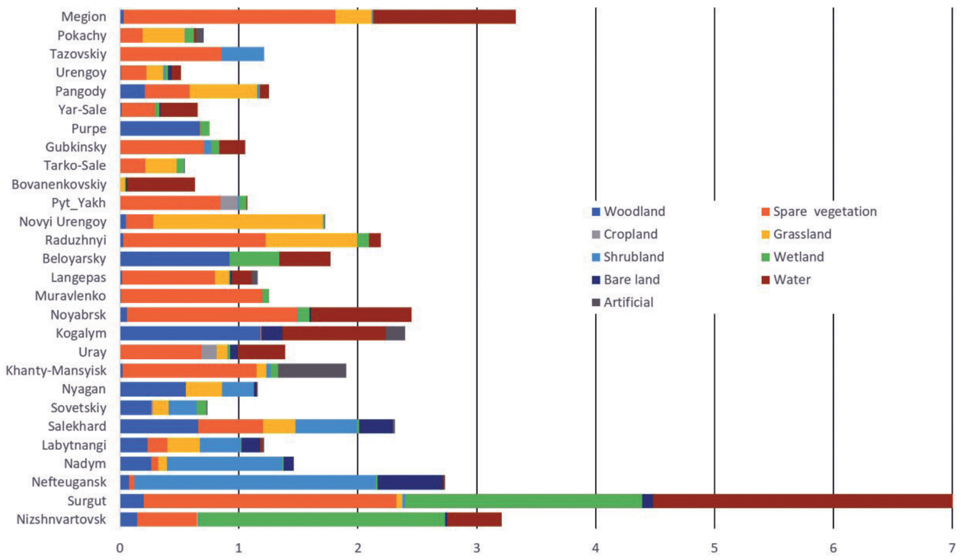

(b) Winter SUHI

Fig. 4. Partial contributions, $f_i \Delta T_i$, of the aggregated LC types into the total SUHI intensity, ΔT for the 28 cities in the NWS region. The contribution is given in Kelvins. The negative values indicate that the specific LC types are locally warmer than the urban area

are dominated by the stable stratification, will show the negative LST bias.

We compared the MODIS LST of the urban pixel and the nearly collocated SAT observations at the WMO station 23848 (Nefteyugansk airport) over the period 2006-2014. The analysis revealed that the summertime LST was 0.0 K (2007) to 2.5 K (2012) higher than the SAT. The average LST – SAT difference was +1.2 K. The wintertime LST of the urban pixel was 1.0 K (2010) to 7.5 K (2012) lower than the SAT. The average difference was -2.9 K. The urban LST is higher than that of the natural background in both seasons (see ME17 and Table 2). Therefore, the SAT comparison with the natural pixels would constitute the smaller LST – SAT

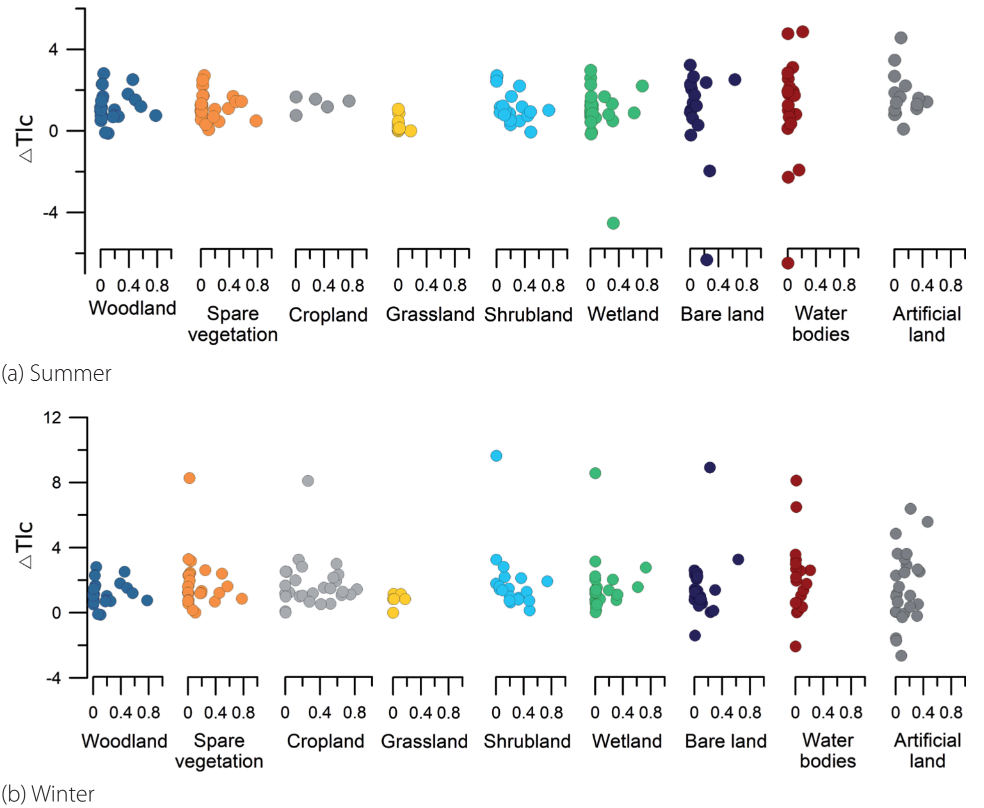

Fig. 5. Dependence of the partial SUHI intensity, ΔTι [K], on the buffer fraction covered with the given LC type for the 28 cities in the NWS

differences in the summertime and even larger difference in the wintertime.

There are no pairs of close urban-rural SAT observations in the region. Therefore, we can only speculatively extrapolate our understanding to the SUHI – UHI relationships. The SUHI in this study is unlikely to be significantly different from the more traditional urban canopy UHI in summertime. Moreover, the summertime SUHI should not exhibit significant sensitivity to the stratification over the different land use – land cover types. On the contrary, the wintertime SUHI is expected to be much colder than the corresponding UHI. The region of this study is known for its persistent negative surface heat balance and frequent clear-sky anti-cyclonic weather (e.g. Konstantinov et al. 2018). Considering sites with similar winter conditions from the Nielsen-Englyst et al. (2018) study, we expect the wintertime LST over open natural landscapes to be 2-3 K lower than the LST in the urban area. This question needs further investigation.

CONCLUSIONS

This study presents the analysis of the exogenous factors responsible for the apparent SUHI in the 28 cities in Northern West Siberia. It considered the quantitative contribution of local climates, specific for the aggregated LC types in the 2 km buffer of the urban administrative area. The study utilized the MODIS LST data product for the period of 2001-2015. The CCI LC types were aggregated in 9 coarser LC types in this study.

The MODIS LST analysis in ME17 revealed significant and persistent warm LST anomalies in the cities. ME17 found a strong statistical dependence (R^2 = 0.73) on the single endogenies factor, namely, the size of city population. It was suggested that the background LC types, such as boreal forest, could play a significant role in scaling of the SUHI. Here, we studied and quantified that suggestion. No clear dependence between the partial SUHI intensity and the area fraction occupied by the given LC type was found. Nevertheless, the major contribution to the apparent SUHI was revealed for water, spare vegetation, grassland and shrubland.

Different partial SUHI intensity can explain relatively small summer LST anomalies in the high latitude cities as compared to their counterparts in lower latitudes. Indeed, the NWS cities are surrounded by dark natural vegetation (forest and shrub), as cropland is practically not present. The higher urban albedo counteracts warming, making the LST differences less significant. The mechanisms and pathways of the SUHI maintenance cannot be solely inferred from the remote sensing data. Their further understanding requires numerical experiments with turbulence-resolving models.

The large and persistent SUHI in the NWS cities may have significant ecosystem as well as socio-economic impacts. Esau et al. (2016) showed that the vegetation productivity generally increasing in and around those 28 cities. Following analysis of the NWS climate change, it is reasonably to expect that the SUHI will further reduce the bearing capacity of frozen soils. The work of Zhou et al. (2004) suggests that shifts in the vegetation phenological cycle should be also observed. Such an expected impact calls for concrete in depth investigations of the SUHI effects in each city as well as for urban planning and policy measures to minimize those effects.

ACKNOWLEDGEMENTS

This work was supported by the Belmont Forum and Norwegian Research Council project HIARC: *Anthropogenic Heat Islands in the Arctic: Windows to the Future of the Regional Climates, Ecosystems, and Societies (no. 247468).*

REFERENCES

Atlaskina K., Berninger F., de Leeuw G. (2015). Satellite observations of changes in snow-covered land surface albedo during spring in the Northern Hemisphere. The Cryosphere. Vol. 9. P. 1879-1893.

Barichivich J., Briffa K.R., Myneni R., van der Schrier G., Dorigo W., Tucker C.J., Osborn T.J., Melvin T.M. (2014). Temperature and snow-mediated moisture controls of summer photosynthetic activity in northern terrestrial ecosystems between 1982 and 2011. Remote Sens. Vol. 6. P. 1390-1431.

Bonan G.B., Pollard D., Thompson S.L. (1992). Effects of boreal forest vegetation on global climate. Nature. Vol. 359. P. 716-718.

Bonan G.B. (2008). Forests and Climate Change: Forcings, Feedbacks, and the Climate Benefits of Forests. Science. Vol. 320. P. 1444-1449.

Brunsell N.A., Mechem D.B., Anderson M.C. (2011). Surface heterogeneity impacts on boundary layer dynamics via energy balance partitioning. Atmos. Chem. Phys. Vol. 11. P. 3403-3416.

Chen X., Su Z., Ma Y., Cleverly J., Liddell M. (2017). An Accurate Estimate of Monthly Mean Land Surface Temperatures from MODIS Clear-Sky Retrievals. J. Hydrometeorol. Vol. 18. P. 2827-2847.

Comiso J. C. (2003). Warming Trends in the Arctic from Clear Sky Satellite Observations. J. Climate. Vol. 16. P. 3498-3510.

Clinton N., Gong P. (2013). MODIS detected surface urban heat islands and sinks: Global locations and controls. Remote Sens. Env. Vol. 134. P. 294-304.

Davy R., Esau I., Chernokulsky A., Outten S., Zilitinkevich S. (2017). Diurnal asymmetry to the observed global warming. Int. J. Climatol. Vol. 37. P. 79-93.

Davy R., Esau I. (2014). Surface air temperature variability in global climate models. Atmos. Sci. Letters. Vol. 15. P. 13-20.

Davy R., Esau I. (2016). Differences in the efficacy of climate forcings explained by variations in atmospheric boundary layer depth. Nature Comm. Vol. 7. Art. ID. 11690.

Davy R., Esau I., Chernokulsky A., Outten S., Zilitinkevich S. (2017). Diurnal asymmetry to the observed global warming. Int. J. Climatol. Vol. 37. P. 79-93.

Dudorova N., Belan B. (2015). Thermal balance of the underlying surface in Tomsk during 2004–2005. Atmos. Ocean Optics. Vol. 28. No. 4. P. 318-327.

Esau I., Davy R., Outten S. (2012). Complementary explanation of temperature response in the lower atmosphere. Env. Res. Letters. Vol. 7. Art. ID. 044026.

Esau I., Miles V. (2016). Warmer urban climates for development of green spaces in northern Siberian cities. Geogr. Env. Sustain. Vol. 9. P. 48-62.

Esau I., Miles V.V., Davy R., Miles M.W., Kurchatova A. (2016). Trends in normalized difference vegetation index (NDVI) associated with urban development in northern West Siberia. Atmos. Chem. Phys. Vol. 16. P. 9563–9577.

Flanner M.G. (2009). Integrating Anthropogenic Heat Flux with Global Climate Models. Geophys. Res. Lett. Vol. 36. No. 2. Art. ID. L02801.

He J. F., Liu J. Y., Zhuang D. F., Zhang W., Liu M. L. (2007). Assessing the effect of land use/land cover change on the change of urban heat island intensity. Theor. Appl. Climatol. // Vol. 90. P. 217-226.

Hachem S., Duguay C. R., Allard M. (2012). Comparison of MODIS-derived land surface temperatures with ground surface and air temperature measurements in continuous permafrost terrain. The Cryosphere. Vol. 6. P. 51-69.

Heleniak T.E. (2009). The role of attachment to place in migration decisions of the population of the Russian North. Polar Geography. Vol. 32. P. 31-60.

Hinkel K.M., Nelson F.E. (2007). Anthropogenic heat island at Barrow, Alaska, during winter: 2001–2005. J. Geophys. Res. Vol. 112. Art. ID. D06118

Hu Y., Jia G. (2010). Influence of land use change on urban heat island derived from multi-sensor data. Int. J. Climatol. Vol. 30. P. 1382-1395.

Grebenets V.I., Streletskiy D., Shiklomanov N. (2012). Geotechnical safety issues in the cities of polar regions. Geography Env. Sustainability. Vol. 5. P. 104-119.

Imhoff M.L., Zhang P., Wolfe R.E., Bounoua L. (2010). Remote sensing of the urban heat island effect across biomes in the continental USA. Remote Sensing Env. Vol. 114. P. 504–513.

Jin M., Dickinson R. E. (2010). Land surface skin temperature climatology: benefitting from the strengths of satellite observations. Enviromen. Res. Lett. Vol. 5. ID. 044004

Khrustalyov L., Davidova I. (2007). Forecast of climate warming and account of it at estimation of foundation reliability for buildings in permafrost zone. Earth Cryosphere. Vol. 11. P. 68-75. (in Russian)

Konstantinov P.I., Grishchenko M.Y., Varentsov M.I. (2015). Mapping Urban Heat Islands of Arctic Cities Using Combined Data on Field Measurements and Satellite Images Based on the Example of the City of Apatity (Murmansk Oblast). Izvestiya, Atmos. Ocean. Phys. Vol. 51. P. 992–998.

Konstantinov P., Varentsov M., Esau I. (2018). A high density urban temperature network deployed in several cities of Eurasian Arctic. Environ. Res. Lett. Vol. 13. ID. 075007.

Kottek M., Grieser J., Beck C., Rudolf B., Rubel F. (2006). World Map of the Köppen-Geiger climate classification updated. Meteorol. Zeitschrift. Vol. 15. P. 259–263.

Lapenis A., Shvidenko A., Shepaschenko D., Nilsson S., Aiyyer A. (2005). Acclimation of Russian forests to recent changes in climate. Global Change Biology. Vol. 11. P. 2090-2102.

Lee X., Goulden M.L., Hollinger D.Y. et al. (2011). Observed increase in local cooling effect of deforestation at higher latitudes. Nature. Vol. 479. P. 384-387.

Lemonsu A., Bélair S., Mailhot J., Benjamin M., Morneau G., Harvey B., Chagnon F., Jean M., Voogt J. (2008). Overview and First Results of the Montreal Urban Snow Experiment 2005. J. Appl. Meteorol. Climatol. Vol. 47. P. 59-75.

Li Z.-L., Tang B.-H., Wu H., Ren H., Yan G., Wan Z., Trigo I.F., Sobrino J.A. (2013). Satellite-derived land surface temperature: Current status and perspectives. Remote Sensing Env. Vol. 131. P. 14–37.

Li Y., Zhao M., Motesharrei S., Mu Q., Kalnay E., Li S. (2015). Local cooling and warming effects of forests based on satellite observations. Nature Comm. Vol. 6. Art. ID. 6603.

Li B., Liu Z., Nan Y., Li S., Yang Y. (2018). Comparative Analysis of Urban Heat Island Intensities in Chinese, Russian, and DPRK Regions across the Transnational Urban Agglomeration of the Tumen River in Northeast Asia. Sustainability. Vol. 10. ID. 2637

Lowry W. P. (1977). Empirical Estimation of Urban Effects on Climate: A Problem Analysis. J. Appl. Meteorol. Vol. 16. P. 129-135.

Magee N., Curtis J., Wendler G. (1999). The Urban Heat Island Effect at Fairbanks, Alaska. Theor. Appl. Climatol. Vol. 64. P. 39-47.

Makhrovskaya A.V., Vaytens M.Y., Panov L.K., Belinskiy A.Y. (1977). Urban planning and construction in the kola north (Part I). Polar Geography. Vol. 1. P. 205-216.

Metz M., Andreo V., Neteler M. (2017). A New Fully Gap-Free Time Series of Land Surface Temperature from MODIS LST Data. Remote Sens. Vol. 9. P. 1333

Miles V.V., Esau I. (2016). Spatial heterogeneity of greening and browning between and within bioclimatic zones in northern West Siberia. Environ. Res. Lett. doi:10.1088/17489326/11/11/115002

Miles V., Esau I. (2017). Seasonal and Spatial Characteristics of Urban Heat Islands (UHIs) in Northern West Siberian Cities. Remote Sensing. Vol. 9. Art. ID. 989

Mokhov I.I. (2009). Links between urban heat island intensity and its size and urban population. Doklady RAS. Vol. 427. P. 530-533.

Mori K., Sato T. (2015). Evaluating the Role of Snow Cover in Urban Canopy Layer on the Urban Heat Island in Sapporo, Japan with a Regional Climate Model. J. Meteorol. Soc. Japan. Vol. 93. P. 581-592.

Muster S., Langer M., Abnizova A., Young K., Boike J. (2015). Spatio-temporal sensitivity of MODIS land surface temperature anomalies indicates high potential for large-scale land cover change detection in Arctic permafrost landscapes. Remote Sens. Environ. V. 168. P. 1-12.

Nielsen-Englyst P., Høyer J.L., Madsen K.S., Dybkjær G., Tonboe R., Alerskans E. (2018). In situ observed relationships between skin temperatures and 2m air temperatures in the Arctic. The Cryosphere Discussions. doi: 10.5194/tc-2018-150

Oke T.R. (1973). City size and the urban heat island. Atmos. Env. Vol. 7. P. 769-779.

Peng S., Piao S., Ciais P., Friedlingstein P., Ottle C., Bréon F.-M., Nan H., Zhou L., Myneni R.B. (2012). Surface Urban Heat Island Across 419 Global Big Cities. Env. Sci. Technol. Vol. 46. P. 796-703.

Schwarz N., Lautenbach S., Seppelt R. (2011). Exploring indicators for quantifying surface urban heat islands of European cities with MODIS land surface temperatures. Remote Sensing of Env. Vol. 115. P. 3175-3186.

Shastri H., Barik B., Ghosh S., Venkataraman C., Sadavarte P. (2017). Flip flop of day-night and summer-winter surface urban heat island intensity in India. Scientific Reports. Vol. 7. ID. 40178

Shiklomanov N.I., Streletskiy D.A., Swales T.W., Kokorev V.A. (2016). Climate change and stability of urban infrastructure in Russian permafrost regions: prognostic assessment based on GCM climate projections. Geograph. Rev. P. 1-18.

Smoliak B.V., Snyder P.K., Twine T.E., Mykleby P.M., Hertel W.F. (2015). Dense Network Observations of the Twin Cities Canopy-Layer Urban Heat Island. J. Appl. Meteorol. Climatol. Vol. 54. P. 1899-1917.

Stewart I.D. (2011). A systematic review and scientific critique of methodology in modern urban heat island literature. Int. J. Climatol. Vol. 31. P. 200-217.

Streletskiy D.A., Shiklomanov N., Grebenets V. (2012). Changes of foundation bearing capacity due to climate warming in northwest Siberia. Earth Cryosphere. Vol. 16. P. 22-32. (in Russian)

Sun C.-Y., Lin H.-T. (2005). Urban heat island intensity in subtropical Taiwan. Proc. World Sustainable Building Conf. Tokyo. 27-29 Sep. P. 2296-2301.

Tan M., Li X. (2015). The effects of settlement size on urban heat islands in fairly uniform geographic areas. Habitat Int. Vol. 49. P. 100-106.

Tomlinson C. J., Chapman L., Thornes J. E., Baker C. J. (2012). Derivation of Birmingham's summer surface urban heat island from MODIS satellite images. Int. J. Climatol. Vol. 32. P. 214-224.

Varentsov M.I., Konstantinov P.I., Samsonov T.E., Repina I.A. (2014). Investigation of the urban heat island phenomenon during polar night based on experimental measurements and remote sensing of Norilsk city. Sovremennye Problemy Distantsionnogo Zondirovaniya Zemli iz Kosmosa. Vol. 11. P. 329–337 (in Russian).

Voogt J., Oke T. (2003). Thermal remote sensing of urban climates. Remote Sens. Environ. Vol. 86. P. 370-384.

Wang W., Liang S., Meyers T. (2008). Validating MODIS land surface temperature products using long-term nighttime ground measurements. Remote Sensing Env. Vol. 112. P. 623–635.

Yang Y., Cai W., Yang J. (2017). Evaluation of MODIS Land Surface Temperature Data to Estimate Near-Surface Air Temperature in Northeast China. Remote Sens. Vol. 9. P. 410.

Yuan F., Marvin E. B. (2007). Comparison of impervious surface area and normalized difference vegetation index as indicators of surface urban heat island effects in Landsat imagery. Remote Sens. Environ. Vol. 106. No. 3. P. 375–386.

Zilitinkevich S., Esau I. (2005). Resistance and Heat Transfer Laws for Stable and Neutral Planetary Boundary Layers: Old Theory, Advanced and Re-evaluated. Q. J. R. Meteorol. Soc. Vol. 131. P. 1863-1892.

Zhang H., Zhang F., Zhang G., He X., Tian L. (2016). Evaluation of cloud effects on air temperature estimation using MODIS LST based on ground measurements over the Tibetan Plateau. Atmos. Chem. Phys. Vol. 16. P. 13681-13696.

Zhang P., Imhoff M.L., Wolfe R.E., Bounoua L. (2010). Characterizing urban heat islands of global settlements using MODIS and nighttime lights products. Canadian J. Remote Sensing. Vol. 36. No. 3. P. 185-196.

Zhao L., Lee X., Smith R.B., Oleson K. (2014). Strong contributions of local background climate to urban heat islands. Nature, Vol. 511. P. 214-219.

Zhou L., Dickinson R.E., Tian Y., Fang J., Li Q., Kaufmann R.K., Tucker C.J., Myneni R.B. (2004). Evidence for a significant urbanization effect on climate in China. Proc. Nat. Acad. Sci. USA. Vol. 101. 9540–9544.

Zhou B., Rybski D., Kropp J.P. (2013). On the statistics of urban heat island intensity. Geophys. Res. Lett. Vol. 40. 5486–5491.

Zhou D., Zhao S., Zhang L., Sun G., Liu Y. (2015). The footprint of urban heat island effect in China. Sci. Reports. Vol. 5. P. 11160.

Received on October 27th, 2017 Accepted on July 31st, 2018

AUTHORS

Igor Esau graduated in meteorology and climatology in 1992 from the Tomsk State University. He received a Ph.D. in 1996 at the Institute for Numerical Mathematics of the Russian Academy of Science and in 2003 at the Uppsala University in Sweden. Since 2003, he is working at the Nansen Environmental and Remote Sensing Centre in Norway (www.nersc.no) where he presently leads a Climate Processes group. His main fields of interest include: the role of the planetary boundary layer in the earth's climate system; numerical modeling of the atmospheric turbulence; and societal effects of the micro-climate processes. The most significant recent publication: Davy R., Esau I. (2016). Differences in the efficacy of climate forcings explained by variations in atmospheric boundary layer depth, Nature Communications, Vol. 7, 11690, doi:10.1038/ncomms11690

Victoria Miles graduated the St. Petersburg Forestry Academy in 1993. She received a Ph.D. in 1998 at the St. Petersburg State University. Since 2002, she is working at the Nansen Environmental and Remote Sensing Centre in Norway (www.nersc.no) where she studies climate processes with the methods of the satellite remote sensing image analysis and geo-information systems. Her main fields of interest include: forest studies; high-latitude vegetation and land use mapping; glaciological processes. The most significant recent publication: Miles V. and Esau I. (2017) Seasonal and Spatial Characteristics of Urban Heat Islands (UHIs) in NorthernWest Siberian Cities. // Remote Sensing, 9, 989

Varvara V. Akimova [1,2*]
[1] Faculty of Geography, Lomonosov Moscow State University, Moscow, Russia
[2] Center for Strategies of Regional Development, Institute of Applied Economic Research, Russian Presidential Academy of National Economy and Public Administration, Moscow, Russia
[*]**Corresponding author:** atlantisinspace@mail.ru

SOLAR ENERGY PRODUCTION: SPECIFICS OF ITS TERRITORIAL STRUCTURE AND MODERN GEOGRAPHICAL TRENDS

ABSTRACT. The study deals with the socio-economic geographical analysis of the solar energy production — one of the most rapidly developing industries of the world energy complex. The aim of the study is to identify and explain main features of the territorial structure of solar energy production and assess its role and place in the world. The paper also investigates the factors that affect the development of solar energy production itself as well as the deployment of individual solar panels or solar power stations. The study carried out is based on the review of datasets and official documents which enable to draw a conclusion that the result of an intensive development of solar energy production is its dynamic spatial expansion visible in the emergence of new poles of growth which largely changes the territorial structure of the industry, transforming it from a monocentric to polycentric.

KEY WORDS: renewable sources of energy, solar energy, photovoltaics, solar thermal energy

CITATION: Varvara V. Akimova (2018) Solar energy production: specifics of its territorial structure and modern geographical trends. Geography, Environment, Sustainability, Vol.11, No 3, p. 100-110
DOI-10.24057/2071-9388-2018-11-3-100-110

INTRODUCTION

During the last few years solar energy production has evolved from an alternative to the main or even basic energy industry. More and more countries are considering solar energy production as a guarantee of national energy security, especially in the light of the worldwide transition to the concept of sustainable development. Undoubtedly, solar energy production is one of the most rapidly growing industries of the world energy complex. During the last few years its overall installed capacity increased by 5.8 times (Jäger-Waldau 2016). No other industry in the world, including telecommunications and computers, had such impressive growth. Great potential for the development of solar energy production is attributed to such global factors as the need to ensure national energy security, growing concern about the environmental consequences of the use of fossil energy sources, full scale innovative activity in the field of alternative energy sources and constant price reduction of electricity generated by solar power systems as a result of innovation and technological advancement. If 20 years ago 1 kWh cost 1 euro, now it costs 5-7 cents and sometimes even less (SolarPower Europe 2016). Moreover, solar energy production seems to be quite attractive to investors in terms of much lower capital and operating costs than traditional energy sources as well as being able to operate on-grid/grid-connected or off-grid.

What is more, solar energy production, being a relatively new phenomena, in its geographical context seems to break many conventional rules. Therefore, the aim of this article is to analyse the specifics of its territorial structure as well as the factors that affect the development and deployment of solar energy production. In order to do so several questions were raised and analysed accordingly: 1) brief analysis of the technical and economic characteristics of solar energy production as a complex of several subindustries; 2) identification of the main features and trends of the world solar energy production; 3) identification of the regional specifics of the development of the world photovoltaics and solar thermal energy (including concentrating solar energy systems (CSP)).

MATERIALS AND METHODS

The vast majority of the works dedicated to solar industry have mainly economic or technical context and cannot be applied to geographical matters, which makes this study unique as it is concentrated on the geographical specifics rather than the most traditional for this topic – economic ones. The data is fragmented due to the fact that solar energy production is still a very young industry, and as a result, there are no clear criteria for what kind of production might be attributed to solar industry, and there is no direct statistical information on the structural components of it. This article is based on the official statistical data and annual reports from international organizations engaged in solar energy field such as the International Energy Agency (IEA), SolarPower Europe (former European Photovoltaic Industry Association (EPIA)), European Solar Thermal electricity Association (ESTELA), National renewable energy laboratory (NREL), US Energy Information Administration (EIA), PV Insider, news-portal CSP today, GTM Research, etc. Therefore, the data accumulated and used for this research is valid and up-to-date. SolarPower Europe and ESTELA organizations update the yearly reports every June-July. After their release the existing authentic data bank created by the author is updated accordingly. The prices of different parts of solar modules are monitored every week so as to be able to notice the main trends. Moreover, many news sites are monitored once in two weeks period to gain data about the commission of new solar power stations. That is why every point in this article is hard born and is a result of a thorough research and consideration. The methods used are statistical and comparative analysis allowing studying the problem at hand from different angles.

RESULTS AND DISCUSSION

To start with, we need to clarify that solar energy production is in fact a combination of two subindustries: 1) solar thermal energy, represented by the technology of converting solar energy into heat (solar collectors) and technology of concentrating solar power (CSP) and its subsequent converting into electricity Solar concentrators are designed to generate electricity on a commercial scale, representing a new generation of solar collectors. They are collectors of a focusing type. Large mirrors concentrate sunlight to an extent that the water turns to steam, thus releasing enough energy to rotate the turbine (Mills 2004); 2) photovoltaics (PV) — the direct conversion of solar energy into electricity using devices containing solar cells made from semiconductor materials (for example, silicon) with special properties (the basic principle of photovoltaic cells is the appearance of the electrical current when exposed to light between two semiconductors with different electrical properties that are in contact with each other). Each of these subindustries has its own specifics and unique features of geographical distribution.

The development of the solar energy production in the world is accompanied by its spatial expansion. If in the early stages of the development of solar energy production its territorial structure had a pronounced «euromonocentric» character, the now happening process of the emergence of new poles of growth led to the appearance of a polycentric model of its territorial structure. In this model three main centres are distinguished: *European* — led by Germany (which for the past ten years has retained the status of world leader), Spain (the leader in concentrating solar energy), Italy and, more recently, Great Britain; *American* — with the United States and *Asian* — where the main poles of growth are two countries — China (since 2015, the world leader in total installed photovoltaic capacity (43 GW) and Japan (where, as a result of the shutdown of all operating nuclear reactors (in connection with the accident at the nuclear power plant Fukushima-1 in 2011) since 2012 there appears to take place a real «solar boom», designed to fill the deficit of energy capacity) (Akimova and Tikhotskaya 2014).

Along with the dynamic development of large centres, a mass of less significant ones appears, contributing to a change in the structure of the location of the industry's facilities. In the future, it is possible that these new centres will become the locomotive of the development of the world's solar energy production. In North America the «solar club», which until recently had only one member — the United States, was joined by Canada, in Europe – Germany, Italy, France and Spain were joined by the United Kingdom and Belgium, in the future this "club" can also welcome Bulgaria, Czech Republic and Romania.

In countries of South America and Africa, solar power has yet to become widespread, but in the long term these countries represent one of the main regions for the development of this industry due to the existence of high energy demand, high level of solar radiation over a large part of the territory and an environmental factor. For example, in Chile and South Africa, the total installed photovoltaic capacity has already exceeded 1 GW.

Despite the spatial expansion, solar energy production is characterized by a high degree of territorial concentration at various levels, which shows in the dominance of individual countries and their regions. For example, at the level of macroregions – 45% of photovoltaic capacity is concentrated in Europe, 73% of solar thermal (without CSP (concentrated solar power)) — in the Asia-Pacific region, 50% of concentrated solar power – in Europe.

At country level there appears to be a similar situation: the leader in photovoltaics is China, which accounts for 19% of total power capacity, in solar thermal — China (about 70%), in concentrated solar power — Spain (50%).

Nevertheless, the main trend of recent years in photovoltaics is the shaping up of a small group of leading countries while leveling up the intercountry differences within this group. Thus, China accounts for about 19% of the world's global photovoltaic power, but Germany, which is in the second place, lags only slightly behind — 17% of global capacity, Japan has 15% and the United States 11%. This trend in photovoltaics is confirmed by the calculated Herfindahl-Hirschman index for a set of countries with total installed photovoltaic capacity of more than 1 GW — 1124, which indicates a moderate degree of concentration on this market, the emergence of new players and the gradual expansion of the industry beyond the main centres of its origin.

Solar thermal (STE) and concentrating solar energy (CSP) production, on the contrary, have a very high index value — 5028 for STE, 3659 for CSP.

This trend is particularly noticeable at the in-country level, where the core is formed by 3-4 regions, in some cases 1-2. For example, Gansu, Qinghai, Jiangsu, Inner Mongolia in China (Fig. 1), California, North Carolina and Arizona in the USA (Fig. 2, 6), Extremadura and Andalusia in Spain (Fig.

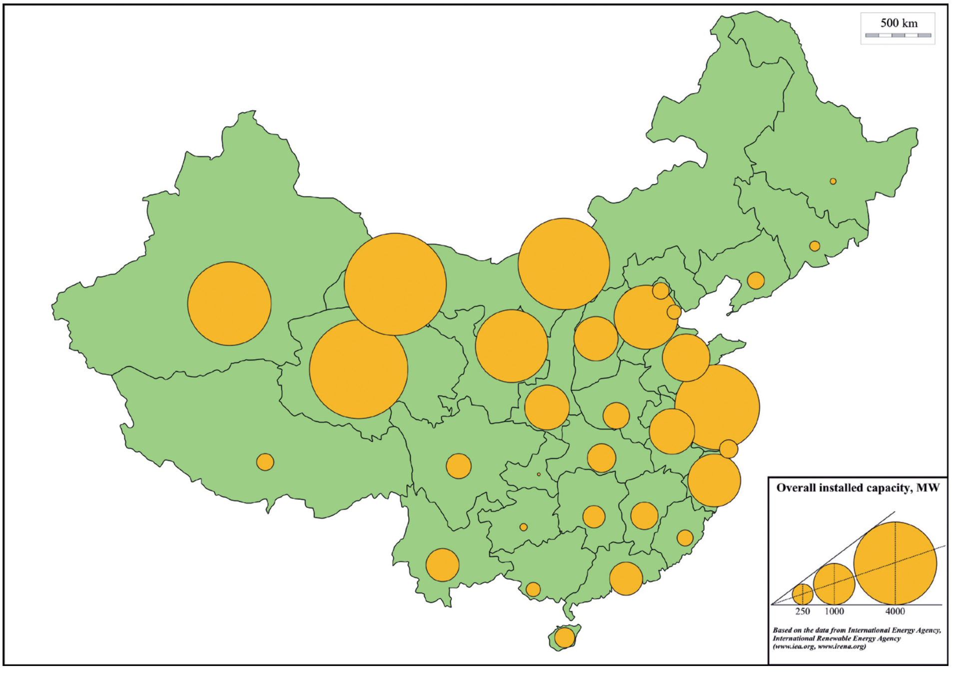

Fig. 1. Photovoltaics in China

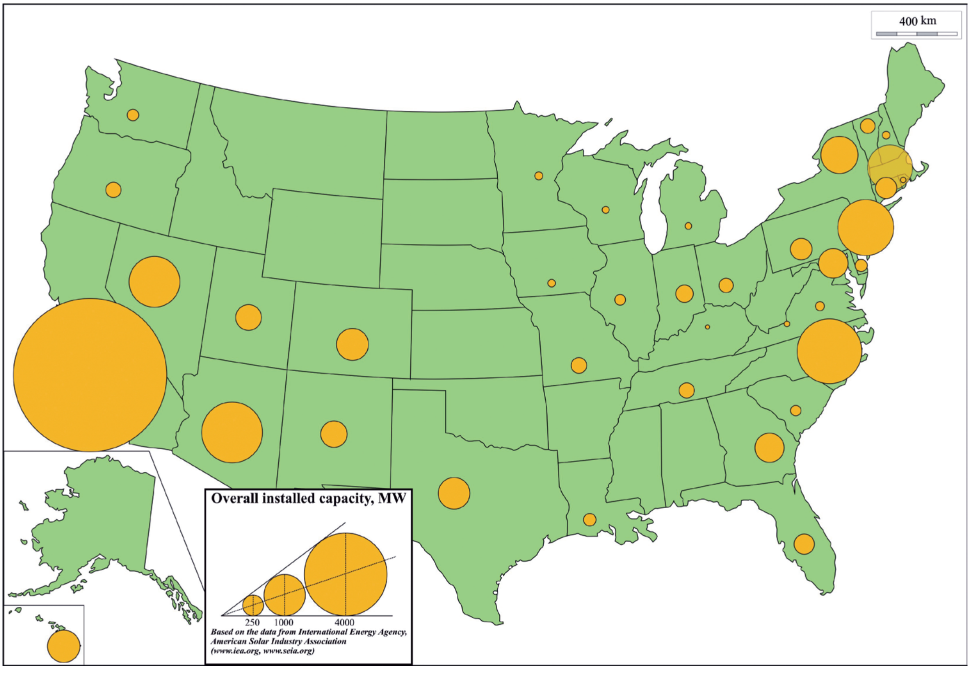

Fig. 2. Photovoltaics in the USA

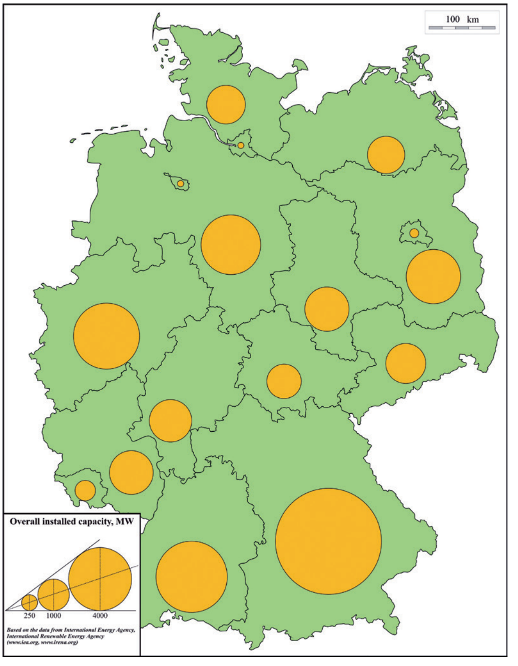

Fig. 3. Photovoltaics in Germany

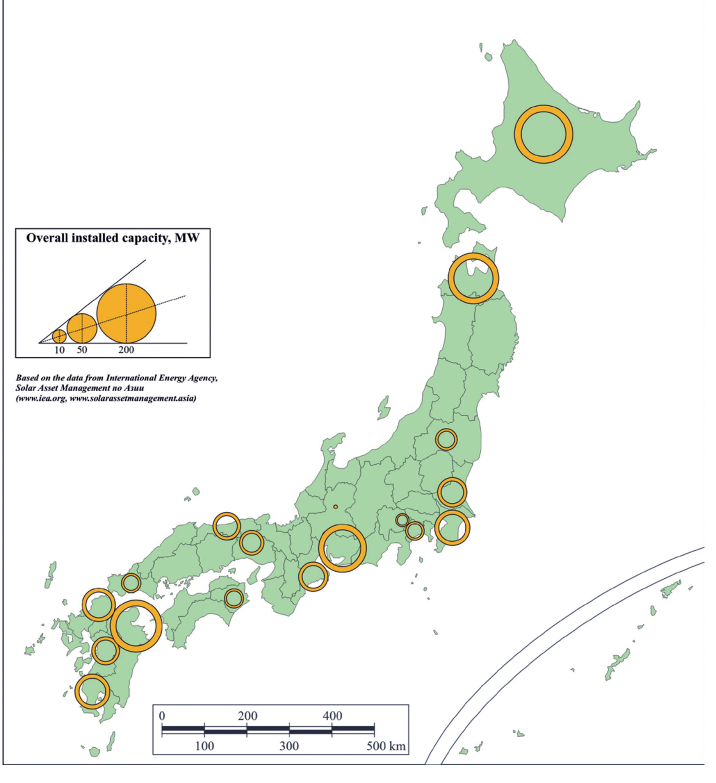

Fig. 4. Photovoltaics in Japan

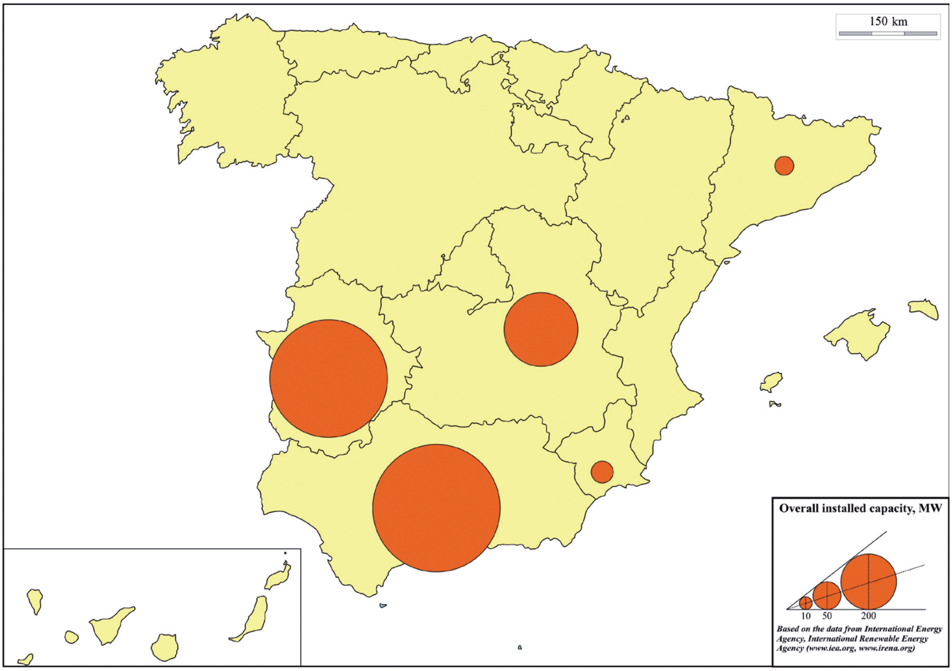

Fig. 5. Concentrated solar energy production in Spain

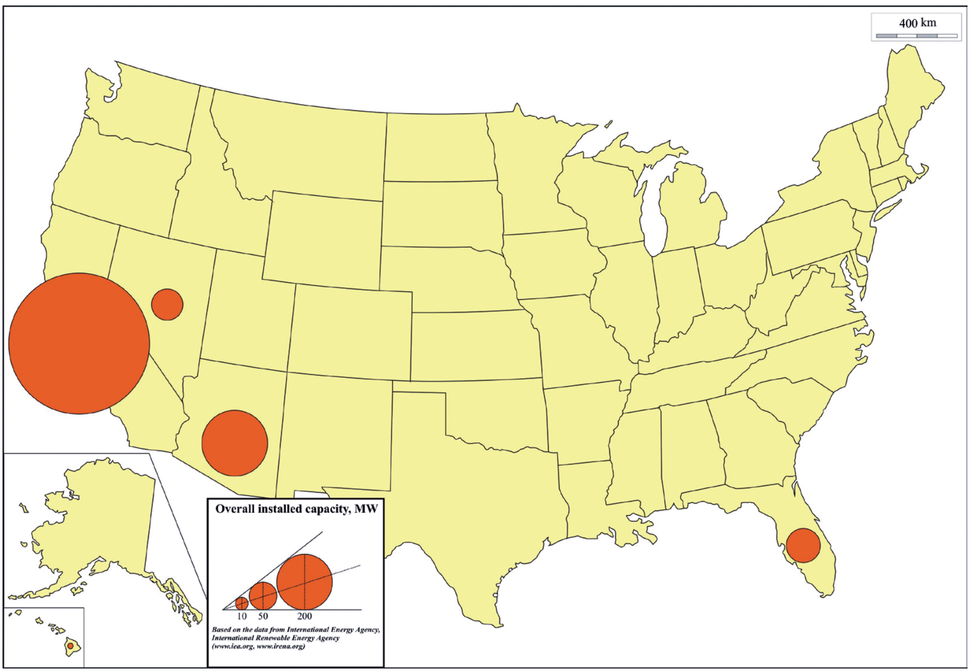

Fig. 6. Concentrated solar energy production in the USA

5), Bavaria, Baden-Württemberg and North Rhine-Westphalia in Germany (Fig. 3), Oita, Aichi, Aomori and Hokkaido in Japan (Fig. 4), etc.

A profound complex research revealed that nowadays the most important feature of the territorial development of solar energy production is its rapid development in Asian countries, so to say "drift to the East". During the period 2012-2015 share of Asian countries in the world photovoltaic capacity increased from <20% to 38%, and in solar thermal power — from 68% to 74%, while the share of European countries fell significantly from 69% to 42% and from 17% to 11%, respectively. A similar change in the "development vector" was observed in the production of components and equipment for the industry, as well as in the service sector (design, monitoring, advertising, etc.), i.e. in sectors where often the same companies operate. Now the main centre is China, with which fiercely compete European and American companies. Unsurprisingly China occupies a leading position due to the fact that the solar technology, that first appeared in the developed countries of Europe and the United States, in Chinese version is much cheaper (the price difference is 20-25%), which is due to the following factors:

• *economies of scale*. Chinese plants have significantly higher production capacity and output than the plants of other countries. The largest plant that produces solar modules in China has a capacity of 3.2 GW, while the largest plant in Europe and the US — only 650 MW.

• *proximity to suppliers of cheap raw materials*. Leading Chinese companies were the first to use local suppliers of cheap raw materials, which made it possible to reduce the cost of materials compared to other competitors in the world.

• *specialization in the production of standard modules*. Chinese companies give preference to the production of standard basic products (multicrystalline modules with a size of 60x60). In comparison, Western and Japanese companies have historically operated in the market segments, providing a larger range of sizes and technologies of solar modules.

As a result, China accounts for more than 60% of the world's production of photovoltaic cells, 70% of solar modules. It can be assumed that the producers of solar modules in China will soon force out all other producers on the market due to the collapse of prices for their products (Masson et al. 2014; Greentech Media Research 2015; PV Insider 2015).Therefore, European and American companies have nothing else to do but search for new high-tech solutions to overcome this situation, for example, by specializing in the production of thin-film solar modules with a lower conversion efficiency, but also with less capital costs.

Europe and the United States still retain their leading positions on the polysilicon market, as its production is extremely complicated technological process (Bernreuter 2014; Platzer 2012). Taking into consideration the decline in the price of polysilicon, China still cannot produce both high-quality and cheap product at the same time, as a consequence, cannot ensure the production of polysilicon in sufficient volume to also dominate in this production segment.

China is the undisputed leader on the solar collector market. Surprisingly, it specialises in the production of the most sophisticated and technologically advanced, while Europe and the United States are actively developing the production of the simplest and the cheapest flat solar thermal collectors. This is due to the fact that European and American companies cannot withstand price competition with China in the production of technologically complex collectors, which, due to their technical characteristics, are most effective for use in China itself (in addition, they have lower requirements of financial investments during their life cycle compared with gas analogs, which predetermines their popularity in the country) (Mauthner and Weiss 2015; European solar thermal electricity association 2016).

Concentrated solar energy production is still very young and the leaders on the global market are yet to be settled and vary depending on the technology used and design applied. In general, we can conclude that at the moment only two countries retain leading positions — Spain and the United States (Renewables 2016; CSP Today 2016), the companies of those have a very high level of vertical integration due to the high capital investments of CSP systems. The domination of these countries can be put down to the complexity of the technology and, as a consequence, the necessity to have a strong technological base and R & D centers specialized in this segment of the solar energy production. Nevertheless, concentrating solar energy production is a promising sector for developing countries. The reasons are economic and geographical. Concentrating solar energy production is most effective when placed in areas of the tropical belt with a high level of solar radiation, it benefits from economies of scale and does not need expensive photovoltaic materials.

It was determined that there is no single determining factor of location, acting for each country. Determinative factor varies from country to country, in accordance with the socio-economic and political specifics of these countries. It should be recognized that there are a number of different factors: the cost of other energy sources, population density, national energy pricing strategies, geographic location (latitude), the structure of government subsidies, global trends, etc. — and each of them plays its role. For example, due to the still relatively high cost of solar electricity, institutional factors play a big role in the development of solar energy production: the political climate in the country, the desire or unwillingness of the authorities to promote the development of the industry, the level of awareness of the population about this technology, etc. In all countries with high level of the development of solar energy production the state support measures are used to improve the competitiveness and investment attractiveness of the industry. The most common measures to support and encourage the development of solar energy production in the European Union and the United States include: 1) an obligation to establish a fixed tariff for electricity generated by solar installations; 2) subsidies for every kilowatt * hour of electricity generated (in the form of tax rebates or direct payments); 3) investment subsidies (grants, loans, favorable tax incentives) to compensate for the high capital investments in the construction of renewable energy facilities, such as solar energy production; 4) establishing a standard that obliges manufacturers or distributors of electrical energy to produce a certain percentage of renewable energy. Such measures are widely used in the European Union; 5) measures to encourage investors by facilitating access to credit at a reduced rate; 6) setting goals of public commissioning of solar power by 2020 and 2030 and the targets for the development of a certain percentage of electricity from alternative sources by a certain year; development and adoption of a financial support programme to achieve its goals; 7) unlimited connection to networks of local solar energy production facilities etc (Couture and Gagnon 2009; Mendonça 2007).

Nevertheless, there is one single factor for each country, which played a decisive role in the development of solar energy production, and is not necessarily the most obvious one. For example, solar radiation is no longer a decisive factor for the development of photovoltaics due to the evolution of solar technologies, which allows solar modules to generate electricity even when it is cloudy by using both direct and scattered solar radiation. In addition, hybrid plants can always be used. At the same time, it should be noted that within one of subindustries of solar energy production for different sectors (industrial and individual) factors can be different.

1) The consumer, demand, high incomes of the population — played a decisive role in the development of individual solar energy production in the countries of the European region (the United Kingdom, Italy, Belgium, France, Germany, Czech Republic, Austria, Switzerland), as well as in Israel;

2) State policies — contributed to the development of individual solar power in India, Japan, industrial — in Bulgaria, Romania and Germany;

3) The existence of national material and production base, as well as the need for the electrification of rural and hard-to-reach remote areas — China, Canada, Turkey, Mexico, Brazil (all — individual solar energy production);

4) External influence (energy crises, collapse in other sectors of the fuel and energy complex) — the USA (all segments of solar energy production), Japan (industrial solar energy production);

5) Availability of sparsely populated areas with high levels of solar radiation — industrial solar energy production — Spain, Chile, Morocco, Algeria, China.

CONCLUSION

The study presents novel comprehensive geographical analysis of world solar energy production, in which special focus was given to its territorial structure.

1. This study proved that solar energy production is indeed one of the most promising industries of the world energy complex. In just 5 years — from 2010 to 2015 — its global capacity increased almost 6 times (in comparison: wind power — by 2,2, bioenergy — 1,7 geothermal — 1,2 times).

2. Accelerated development of solar energy production is predetermined by: a) enormous power, inexhaustibility and general availability of solar energy, b) high ecological safety of the industry, c) constant and rapid improvement of its economy (solar modules have fallen in price by more than 250 times since 1977, the price of solar kilowatt-hour from 2010 by 4 times, etc.).

3. The combination of traditional resource vector (using the energy coming from the Sun) and new technologies has allowed solar energy production to compete with traditional hydrocarbon energy and gradually start winning state and individual consumer preferences, thus beating its main competitor — wind energy. At the moment, the geography and development of solar energy production cannot be viewed solely through the prism of its placement and the balance of power in relation to the finished product — a solar installation. Solar energy production — is a single set of industries from mining to installing solar panels that performs a fundamental function in society — the production of heat and electricity of solar origin.

4. The result of active development of solar energy production is its dynamic spatial expansion transforming its territorial structure from monocentric to polycentric with three main centers: Europe (Germany, Spain, Italy, the UK), North America (USA) and Asia (Japan and China).

5. An important feature of the territorial development of the world's solar energy production is its rapid growth in Asian countries (in China, Japan and South Korea) — the so-called «drift to the East".

6. However, a high level of territorial concentration is still present, that manifests itself in the domination of a small number of countries and their regions. For example, at the intra-country level, the nucleus is formed by only 3-4 regions, sometimes just 1-2.

7. At the same time, there is no single, common for all countries, location factor at the mesolevel. Depending on the socio-economic and political specifics of the country, the determining location factor also changes.

REFERENCES

Akimova V. V., Tikhotskaya I. S. (2014). New Japanese «miracle» ... Solar! Asia and Africa today. No 9, pp. 18-25 (in Russian).

Bernreuter J. (2014). The 2014 Who's Who of Solar Silicon Production: Players, Technologies, Supply/Demand, prices. Global Market Perspectives through 2017, Bernreuter Research [online] Available at www.bernreuter.com/en/shop/polysilicon-market-reports/2014-edition/report-details.html [Accessed 17.02.2018].

Couture T. and Gagnon Y. (2009). An analysis of feed-in tariff remuneration models: Implications for renewable energy investment. Energy Policy, 38 (2), pp. 955-965.

CSP Today global tracker (2016). CSP Today [online]. Available from: www.social.csptoday.com/tracker/reports [Accessed 17.02.2018].

European solar thermal electricity association (2016) [online]. Available from: www.estelasolar.eu [Accessed 11.01.2018].

Greentech media research (2015) [online]. Available from: www.greentechmedia.com/research [Accessed 07.01.2018].

Jäger-Waldau A. (2016) PV status report 2016: Research, Solar Cell Production and Market Implementations of Photovoltaics, European Commission, Joint Research Centre, Institute for Energy and Transport, Italy, 2016. 90 p.

Masson G., Rekinger M., Orlandi S. (2014). Global market outlook for photovoltaics 2014-2018, EPIA. [online] Available at http://www.solarniasociace.cz/tmp/44_epia_gmo_report_ver_17_mr.pdf [Accessed 17.06.2016].

Mauthner F., Weiss W. (2015). Solar Heat Worldwide Markets and Contribution to the Energy Supply 2014, IEA Solar Heating & Cooling Programme [online] Available at https://www.iea-shc.org/data/sites/1/publications/Solar-Heat-Worldwide-2015.pdf [Accessed 19.02.2018].

Mendonça M. (2007). Feed-in Tariffs: Accelerating the Deployment of Renewable Energy. London: EarthScan. 172 p.

Mills D. (2004). Advances in solar thermal electricity technology, Solar Energy, 76, pp. 19–31.

Platzer M. (2012). U.S. Solar Photovoltaic Manufacturing: Industry Trends, Global Competition, Federal Support, Congressional Res. Service (CRS) Report for Congress. [online] Available at http://www.eenews.net/assets/2012/05/02/document_pm_01.pdf [Accessed 27.02.2018].

PV Insider (2016) [online]. Available from: www.analysis.pv-insider.com/ [Accessed 27.02.2018].

Renewables 2016 (2016). Global status report. Ren 21 Renewable Energy Policy Network for the 21st Century [online] Available at http://www.ren21.net/wp-content/uploads/2016/06/GSR_2016_Full_Report.pdf [Accessed 13.03.2018].

Solarpower Europe (2016) [online]. Available from: http://www.solarpowereurope.org/home/ [Accessed 08.02.2018].

Received on March 15th, 2018 Accepted on July 31st, 2018

FIRST/CORRESPONDING AUTHOR

Varvara V. Akimova studied Social and Economic Geography at the Lomonosov Moscow State University, graduated with honour in 2014 and obtained the Specialist's degree (Diploma). In October 2017 she completed PhD programme at the Department of social and economic geography of foreign countries of the faculty of Geography, Moscow State University. In March 2018 she received her PhD degree in Geography. The focus of her studies is in alternative energy, solar energy complex, oil and gas sector.

Eludoyin Adebayo Oluwole[1*], Yetunde Mary Adelere[2], Olusegun Olufemi Awotoye[3]
[1] Department of Geography, Obafemi Awolowo University, Ile-Ife, Nigeria
[2] Institute of Ecology and Environmental Studies, Obafemi Awolowo University, Ile-Ife, Nigeria
[3] Department of Crop Protection and Environmental Biology, Obafemi Awolowo University, Ile-Ife, Nigeria
[*]**Corresponding author:** oaeludoyin@yahoo.com

CHARACTERISTICS AND QUALITY OF SOILS UNDER SELECTED FARMING PRACTICES IN SOUTHWESTERN NIGERIA

ABSTRACT. This study compared soil properties and quality under five different farm practices in a part of the southwest Nigeria. The study indicated that fewer soil properties accounted for more percentage change in total variance at the fallow and mono-cropping plots than at the forest, crop rotation and alley farming systems. It also showed that soils under fallow and mono-cropping systems exhibited the lowest quality values among the farm practices system studied. The study recommends improved soil management approaches in plots under mono-cropping practices, and extensive soil recovery programmes for fallow lands.

KEY WORDS: Agricultural practices; Soil physical and chemical attributes, Soil quality index; *Plinthic luvisol*.

CITATION: Eludoyin Adebayo Oluwole, Yetunde Mary Adelere, Olusegun Olufemi Awotoye (2018) Characteristics and quality of soils under selected farming practices in southwestern Nigeria. Geography, Environment, Sustainability, Vol.11, No 3, p. 111-125
DOI-10.24057/2071-9388-2018-11-3-111-125

INTRODUCTION

The physio-chemical properties of soils have been attributed to natural and anthropogenic causes; the natural causes being mostly related to the underlying bedrocks, and the anthropogenic causes to land management practices (Wienhold et al. 2004; Yoo et al. 2006; Verachtert et al. 2009). Many studies on the indices of soil degradation, including nutrient losses, deterioration in soil quality and soil pollution, showed that poor farmland management can pose significant threats to food security in many regions of the world (Malhi et al. 2001; Lavelle et al. 2001; Liebig et al. 2004).

The effects of soil quality on food security can be overwhelming in countries where adequate agricultural technology and environmentally sustainable practices are limited. Recently, the Food and Agriculture Organization of the United Nations (FAO 2010) advocated for advancement of conservation agriculture practices – practices which involves minimal mechanical soil disturbance, minimum tillage and no-tillage systems, direct seeding, mulching, crop rotations and mixed farming. Such advocate is probably because farming activities have become sensitive to the need for environmental sustainability. Whereas, developed countries, such as the United Kingdom through research-support policies offer guide to farmers on environmental sustainability (Tilman et al. 2001; Withers and Lord 2002; European Environment Agency 2003; Carabias-Martinez et al. 2003; Horsey 2006; Lane et al. 2006; DEFRA 2009; Eludoyin 2013), many farmers in the sub-Saharan Africa countries, including Nigeria, still practice indigenous land management schemes, despite changing climatic factors, competition for land for non-agricultural purposes and many other factors (Scholes et al. 1994, Luoga 2000).

In many sub-Saharan Africa, including Nigeria, practices such as continuous cropping, mono-cropping and mixed cropping are common; relatively new and more organized practice is the alley cropping system. The alley cropping system is an agroforestry practice of hedgerows with annual crops, and was probably introduced to the Nigerian agricultural practices in the 1970s through the International Institute for Tropical Agriculture, Ibadan (Kang et al. 1981). The hedgerows (typically *Gliricidia sepium* and *Leucaena leucocephala*) are usually pruned before planting the annual crop, and then periodically to prevent shading of the crops from sunlight (Oyedele et al. 2009). Whereas many studies have shown that many parts of the southwest Nigeria are characterized by fragile soils with poor nutrient status and quality, and that which require care in their management (Lal 2005; Oenema et al. 2006), recent studies have suggested that the assumed poor soil quality may be corrected if information on the practices of farming in the area is improved, as is elsewhere – when compared with agricultural productive heavy clay soils of the *Stagni-vertic* or *Stagni-eutric* Cambisols soil groups in the southwest England (Harrod and Hogan 1981) and drained soils (Eludoyin 2013).

The objectives of the present study are (i) to compare the soils under five common farming practice systems (alley cropping, crop rotation, mono-cropping, fallow or shifting cultivation) with that of relatively undisturbed forested sub-region in the study area; and (ii) determine the quality of the soils under selected farm practice systems using the soil quality index (SQI) approach. The SQI approach has been found relevant to soil assessment in tropical areas (Doran and Parkin 1994; Bremer and Ellert 2004; Bastida et al. 2008; Ezeaku 2011; Awotoye et al. 2011; Armenise et al. 2013; Ibrahim et al. 2014; Mukherjee and Lal 2014). The main hypothesis is that soil characteristics and quality vary significantly with farming practices in the area. The study is aimed at contributing to the discussion that land management rather, than natural factors are main causes of the poor soil quality and productivity in the sub-Saharan Africa.

STUDY AREA

The study area, plots of farmlets in of Leventis Farms are in the southwestern Nigeria (7° 40′N - 7° 48′ N, 4° 10′E - 4° 45′ E) (Fig. 1), and underlain by the Iwo soil association (Smyth and Montgomery 1962) or Plinthic luvisols of FAO/UNESCO (1974)'s classification. The World Reference Base for Soil Resources of FAO (2006) classified the Plinthic luvisols as Fe-rich, humic, and capable of changing irreversibly to a layer with hard nodules, a hardpan or irregular aggregates on exposure to repeated wetting and drying. The Plinthic luvisols soil covers about 60 million ha, globally, and is associated with the rainforest area where it supports food and tree crops (Ekanade 1991; FAO 2006). The study area is underlain by the basement complex geology, rich in gneisses and schists. The schist belt in Ilesa area is a black-arc basin where there is a subduction of an ocean slab into the mantle while the gneisses have resulted from part of the rocks that have metamorphosed into banded gneisses from which granite gneisses were derived (Oyinloye 1998). Both schists and gneisses, being metamorphic–having been subjected to varying degrees of pressure and temperature- are associated with slow weathered and fragile soils.

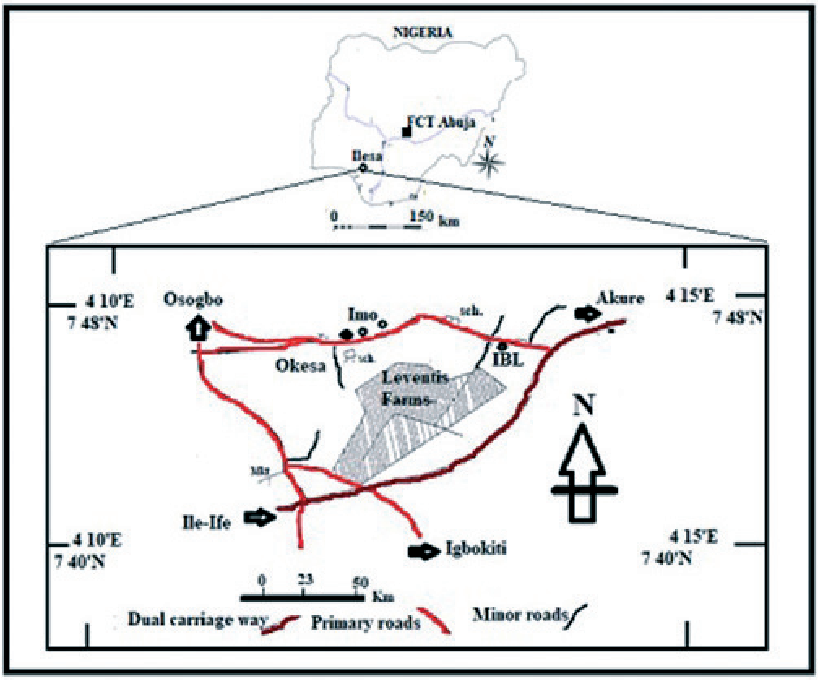

Fig. 1. The study area in Leventis Farms, Ilesa, Osun State, southwest Nigeria

Annual rainfall in southwest Nigeria averages 2500 mm with over 90% of occurring between April and October; average monthly temperatures vary between 22.5°C and 31.2°C while average relative humidity is about 76.1 %, annually. The general relief of the area is plain, varying between 360 m and 400 m above the mean sea level.

The Leventis Farms was created in 1988, and the Farms with the 'control' site had been under the indigenous farming system which was characterized by a mix of fallow or shifting cultivation, mixed cropping and crop rotation based on the perception of individual farmers. Since 1988, when the farmlands were cleared for cultivation, the 'control' site was left fallow and allowed to regrow as forest (secondary regrowth). In other words, until the use of the farmlands as experimental sites, the area was under similar farming (at individual farmer's discretion, however) practices.

MATERIALS AND METHODS

Data collection

First, plots under different farming practice systems (alley cropping, mono-cropping, crop rotation and a fallow that has been part of a shifting cultivation practice) were identified in the entire experimental fields in the study area. Also, part of the Farms that is relatively undisturbed and treated as an agro-forestry system (since 1988) was identified for selection as 'control'. Identified plots are as follows:

a. Alley plot: about 4 years old and comprised of hedgerows intercropped with *Zea mays*. The hedgerows were 2 m apart, and the *Zea mays* was planted in a single row between them.

b. Mono-cropping plot has been under cultivated for 10 years, also with *Zea mays*

c. Fallow plot: about 3 years old. Dominant plant species were *Chromoleana odorata, Sida acuta, Mucuna pruriens and Pennisetum purpureum*

d. Crop rotation was cultivated with melon, maize and cassava, in order of cultivation, based on the lifecycle of the crops; and

e. the 'Control', the relatively undisturbed forest plot (since 1988) with species of *Gmelina arborea, Acacia nilotica, Tectona grandis, Azadirachta indica, Elaeis guineensis, Ficus exasperate, Parkia biglobosa; grasses were Chromoleana odorata, Pennisetum purpureum* that appear are well maintained.

A 45 by 45 m spread-out portion was randomly carved out at the centre of each plot, and further delineated into three (15 by 15 m subplots). Each of the subplots was further divided into 3 by 5 grids for soil sampling, such that soil samples (a triplicate-composite sample for physiochemical analysis and another with a 5.5 by 10 cm cylindrical corer) were obtained from each grid. Subsequently, 45 composite soil samples each were obtained with the aid of soil auger, each at 0 – 15 cm, 15 – 30 cm soil layers in each of the five plots and another 45 samples using the cylindrical corer for determination of soil bulk density. The soil samples were collected in labelled black polyethylene plastic bags, and taken for laboratory analysis at the Soil Laboratory, Department of Soil and Land Resources and Management, Obafemi Awolowo University, Ile-Ife, Nigeria.

Laboratory analysis

The composite soil samples were first were divided into two subsets; one set for determination of particle-size distribution by Hydrometeric method in a Bouyoucos cylinder (as described by Gee and Bauder 1986), and the other air-dried, sieved (2 mm) and analysed for pH, soil organic matter (SOM), total N, organic carbon (OC), available P (AP), exchangeable Ca^{2+}, Mg^{2+}, K^+ and Na^+, cation exchange capacity (CEC), NO_{3-} and $NH_{4'}$, exchangeable acidity (EA) and SO_4^{2-}. The pH was determined as pH in H_2O and pH in KCl with a standardized pH meter (Page et al. 1986), SOM by the loss on ignition method (Motsara and Roy 2008) and OC by Walkley-Black method (Walkley and Black 1934). The total N was determined after digestion with Technicon AAII (Technicon Instrument Corporation 1971) while concentrations of AP were determined at 640 nm wavelength of an Atomic Absorption Spectrophotometer (AAS) (Bray and Kurtz 1945). The exchangeable Ca^{2+}, Mg^{2+}, K^+ and Na^+ were determined with AAS at their respective wavelength values while CEC was determined with Flame Photometer (Uehara and Gillman 1981). Concentrations of NO_{3-}N and NH_{4-}N were determined by weighing and centrifuging using Technicon AAII (Technicon Instrument Corporation 1971) whereas the EA was extracted with 1M KCl as described by Thomas (1982). Lastly, SO_4^{2-} was determined by weighing, filtration and centrifuging (Daji 1970).

In addition, bulk density was determined as described by the International Organisation for Standardisation, ISO 11272 (ISO 1998) as the ratio of oven-dried (after 24 hours at 105°C) soil samples to volume of the core (after the volume of materials greater than 2 mm and other organics that were removed had been subtracted) (1)

$$Bulk\ density = \frac{Ms}{Vt - Wt} \qquad (1)$$

Where
Ms = Mass of oven-dried soil
Vt = Total volume of the cylindrical core
Wt = Volume of solids greater than 2mm plus that of litter or vegetation taken in by the corer. The ***Wt*** was determined by water displacement method, such that volume of materials larger than 2 mm and removed organics were estimated from the volume of water displaced, in a water cylinder

Porosity was determined in terms of the percentage of the ratio of the bulk density and particle density (Brady and Weil 2008).

Data analysis

Data were analyzed in the IBM SPSS 12 for descriptive statistics, variance, Factor and Principal Component Analysis. Principal Component Analysis (PCA) was used to reduce the factors of the parameters, and to deduce those which significantly ($p \leq 0.05$) contributed to spatial variations in each field. The SQI was computed following the listed steps:

i. 'Minimum data sets' (MDS) were determined for each farm site. The MDS are variables which exhibits significant (95%) between-plots difference and possessed eigenvalue greater than 1.0 after rotated under the Varimax normalization procedure for PCA. The MDS were considered to have ranged in the 10% of the highest component loading, and be non-redundant (i.e. exhibits high correlation with other variables) (Armenise et al. 2013).

ii. The MDS were then transformed into unit scores ranging from 0 to 1 (1 represents the optimum level for the index), accounting for their contribution to soil functions, and scored as either 'more is better' (when increasing values suggest high quality) or 'less is better' (when increase in variable values is associated with declining quality) (Wymore 1993).

iii. Subsequently 'less is better' was used to assess the physical properties particle size (percentage sand, bulk density, acidity and porosity) whereas nutrients (including AP, total N, organic matter content and carbon) were assessed with the 'more is better' index.

iv. Scores were then used to generate the SQI values for each plot using equation 2

$$SQI = \sum_{i}^{n} W \times S \tag{2a}$$

W = the weighting factor

$$W = \frac{\% VE}{Sum\ of\ the\ \% VE} \tag{2b}$$

S_i = MDS score

VE = Variable Explained (for variables with at least 1.0 Eigenvalue)

Furthermore, mean stocks of selected nutrient variables were described as recommended by Kiely et al (2010) (equation 3)

$$Stock = bulk\ density \times N \times d \tag{3}$$

N = concentration of selected variable

d = soil depth at which samples were taken.

RESULTS

Soil characterisation

Table 1 shows the mean values and variations of selected variables at both 0 – 15 cm and 15 – 30 cm soil strata at the different farm plots. The soils are generally characterised by low acidity (pH value of 6 – 8), CEC (1.0 – 10 cmolc kg^{-1}), organic matter (1.1 – 5.1 g kg^{-1}), and by particle sizes varying from medium to coarse-texture sandy-clay-loam or loamy-sand soil types when plotted on the FAO soil texture chart (Jeffery et al. 2010). The soil bulk density was in the range of 1.1 – 1.6 g cm^{-3}. Also, the 15 – 30 cm soil layers was generally more acidic than the 0 – 15 cm layer, and pH values were generally higher at the forest plot than either the plots used for mono-cropping, rotation or fallow. Except for the percentage sand, silt and clay, exchangeable cations and other nutrients were more concentrated in the 0-15 cm layer than at 15 – 30cm layer, except for the plot for mono-cropping (for cation exchangeable capacity) and pH.

Fig. 2 shows that nitrogen stock at the 0 – 30 cm soil stratum was more at the fallow and forest plots while organic carbon stock was more at forest plot despite that the plot for alley cropping exhibited richer organic matter contents than the other cultivated soil plots. Available phosphorus was dominant among the selected chemical variables, although the results of the regression analysis done to establish significant prediction of one nutrient by the other only showed that the organic matter content is a significant predictor of the organic carbon and total N in the area (R^2 = 0.43 and 0.63, respectively, R^2 = 0.39 in the relationship between organic matter and available P) (Table 2).

Furthermore, Fig. 3 shows that fewer soil properties (out of the selected) also accounted for more fractions of the total variance at the fallow and mono-cropping plots (75% and 59%, respectively) that at the forest, crop rotation and alley cropping plots, suggesting lesser diversity in the nutrient inputs in the latter plots (fallow

Table 1. Mean distribution and coefficient of variation (%, in parenthesis) of selected variables across plots at the 0-15 cm and 15- 30 cm soil depths

	Alley cropping		Crop rotation		Fallow		Forest		Mono-cropping	
	0-15 cm	15 – 30 cm	0-15 cm	15 – 30 cm	0-15 cm	15 – 30 cm	0-15 cm	15 – 30 cm	0-15 cm	15 – 30 cm
% sand	70 (6)	72 (6)	78 (4)	74 (5)	75 (8)	78 (2)	65 (5)	63 (7)	86 (7)	77 (5)
% silt	8 (19)	10 (6)	7 (51)	6 (53)	5 (60)	6 (28)	8 (31)	12 (47)	7 (57)	5 (58)
% clay	22 (20)	18(26)	15 (43)	20 (16)	20 (29)	16 (16)	27 (22)	25 (6)	13 (42)	18 (33)
pH (water)	7.4 (7)	6(8)	6.5 (5)	5.8 (7)	7.1 (6)	6.4 (5)	8.4 (5)	6.6 (2)	7.6 (8)	6.4 (3)
pH (KCl)	6.5 (5)	5.5(7)	6.1 (7)	5.4 (7)	6.4 (5)	6.0 (3)	7.8 (5)	6.1 (3)	7.1 (7)	6.0 (3)
Exchangeable acidity (cmol$_c$ kg^{-1})	0.02 (50)	0.02(20)	0.03 (33)	0.03 (3)	0.02 (50)	0.02 (20)	0.01 (100)	0.01 (20)	0.01 (100)	0.01 (20)
Bulk density (g cm^{-3})	1.5 (20)	1.2(17)	1.6 (13)	1.2 (8)	1.4 (29)	1.4 (36)	1.2 (17)	1.1 (27)	1.5 (13)	1.3 (23)
Porosity (%)	5.5 (13)	5.4(7)	5.6 (32)	5.5 (11)	4.8 (14)	7.2 (29)	7.7 (29)	7.2 (141)	7.5 (23)	4.1 (7)
Cation exchange capacity (cmol$_c$ kg^{-1})	5.7 (24)	3(37)	5.3 (30)	3.3 (45)	5.8 (55)	3.5 (80)	11.3 (39)	5.7 (46)	4.7 (24)	4.8 (15)
K^+ (cmol$_c$ kg^{-1})	0.4 (8)	0.2(20)	0.4 (25)	0.2 (50)	0.4 (10)	0.2 (35)	0.4 (25)	0.2 (20)	0.3 (133)	0.2 (20)
Na^+ (cmol$_c$ kg^{-1})	0.2 (5)	0.1(200)	0.2 (100)	0.2 (20)	0.2 (50)	0.1 (20)	0.2 (10)	0.1 (30)	0.1 (20)	0.1 (10)
Ca^{2+} (cmol$_c$ kg^{-1})	4.1 (15)	2.3 (30)	3.2 (19)	1.9 (21)	3.1 (10)	1.5 (13)	5.6 (9)	3.1 (23)	3.2 (16)	1.7 (24)
Mg^{2+} (cmol$_c$ kg^{-1})	0.9 (22)	0.5 (20)	0.8(25)	0.4 (25)	0.9 (4)	0.5 (4)	0.9 (11)	0.5 (20)	0.8 (13)	0.9 (6)
NH^{4+}- N (cmol$_c$ kg^{-1})	0.1 (200)	0.2 (50)	0.1 (10)	0.2 (50)	0.1 (30)	0.2 (50)	0.1 (10)	0.2 (50)	0.1 (40)	0.1 (100)
Total N (g kg^{-1})	1.4 (7)	0.7 (29)	1.3 (8)	0.8 (13)	2.5 (12)	0.9 (11)	2.4 (4)	1.0 (20)	0.8 (13)	0.5 (120)
Available P (cmol$_c$ kg^{-1})	4.5 (22)	3.8 (26)	3.9 (5)	3.3 (12)	3.0 (10)	2.5 (16)	4.1 (5)	3.7 (3)	3.4 (21)	2.8 (18)
Organic C (g kg^{-1})	2.2 (9)	0.7 (29)	1.2 (25)	1.0 (20)	1.4 (29)	1.3 (38)	3.4 (15)	2.1 (10)	1.3 (23)	1.6 (19)
Organic matter (g kg^{-1})	4.1 (10)	1.6 (25)	3.4 (18)	1.6 (31)	3.7 (11)	1.6 (25)	5.1 (14)	2.1 (24)	2.9 (34)	1.1 (27)
NO_{3-} - N (mg kg^{-1})	0.1 (30)	0.3 (33)	0.1 (30)	0.2 (50)	0.1 (20)	0.3 (33)	0.2 (20)	0.3 (33)	0.1 (100)	0.1 (100)
SO_4^{2-} - S (mg kg^{-1})	0.1 (10)	0.4 (3)	0.2(15)	0.4 (25)	0.2 (5)	0.4 (25)	0.2 (10)	0.4 (50)	0.3 (33)	0.2 (50)

and mono-cropping) than the former plots. Fig. 3. Distribution of the eigenvalues of variables that explained the highest fraction of the total variance across selected plots. Total variance explained is provided in parenthesis for each plot

Soil quality assessment

The results of the SQI indicated that whereas the forest plot showed higher SQI values than the other plots; fallow and monocropping plots with the lowest SQI

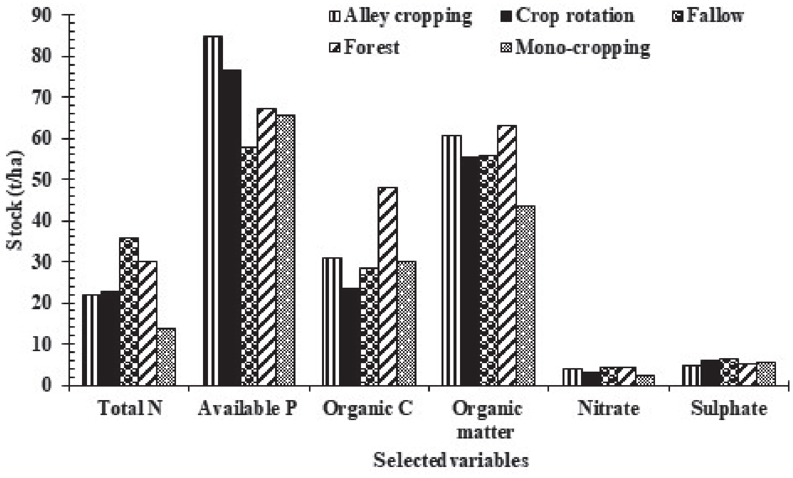

Fig. 2. Mean stock of selected soil variables under the different farm practices

Table 2. Relationship among selected soil nutrients in the study area

Organic matter				Organic carbon			Total N		Available P
Organic carbon	Total N	Available P	NO_{3-} -N	total N	Available P	NO_{3-} -N	Available P	NO_{3-} -N	NO_{3-} -N
1.17x+0.83 (R^2 = 0.47)	2.08x (R^2 = 0.63)	1.33x– 1.95 (R^2 = 0.39)	- 5.87x+ 3.78 (R2 = 0.17)	0.64x + 0.84 (R^2 = 0.33)	0.55x - 0.31 (R^2 = 0.20)	-0.47x + 1.71 (R^2 = 0.003)	0.30x + 0.18 (R^2 = 0.07)	-1.90x+1.57 (R^2 = 0.06)	0.24x + 3.2 (R^2 = 0.07)

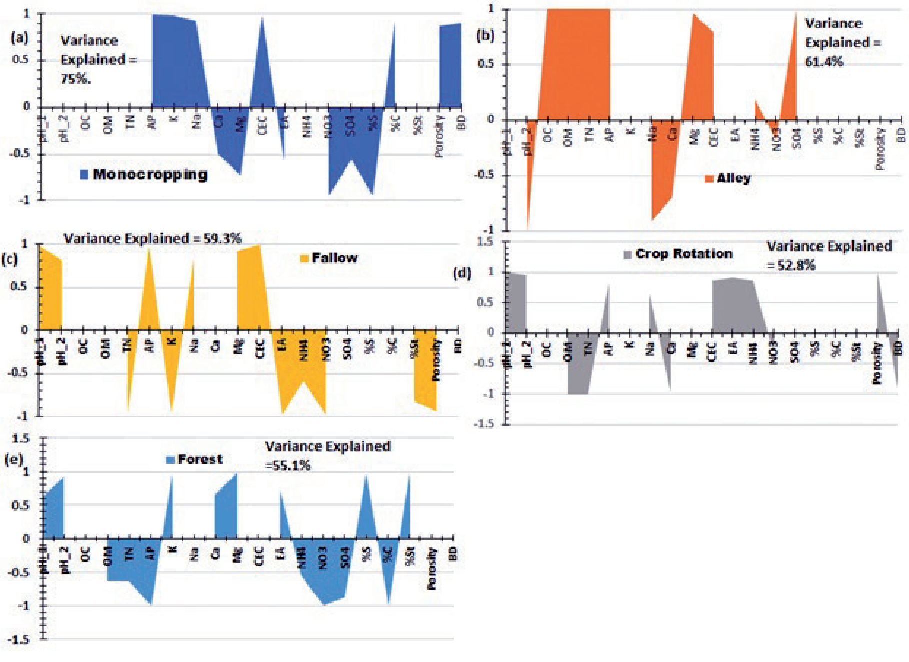

Fig. 3. Distribution of the eigenvalues of variables that explained the highest fraction of the total variance across selected plots. Total variance explained is provided in for each plot

values at both 0 -15 cm and 15 – 30 cm soil depth were with the poorest soil quality (Fig. 4). Whereas the alley cropping method produced a lower SQI aggregate than the soils under crop rotation at 0 – 15 cm, it appeared to be better at 15 – 30cm layer. Fig. 4. Soil quality index (SQI) scores and quality rank of selected farm practices

DISCUSSION

This study showed that the study area is generally characterized with above 60% of sandy soil components and less than 15% of silt, low acidity, CEC and organic matter, which are features of fragile or structurally weak soils (Bady and Weily 2002; Vijith et al. 2012). This result is not surprising as it previous studies (e.g. Lal 2005; Oenema et al. 2006) have argued

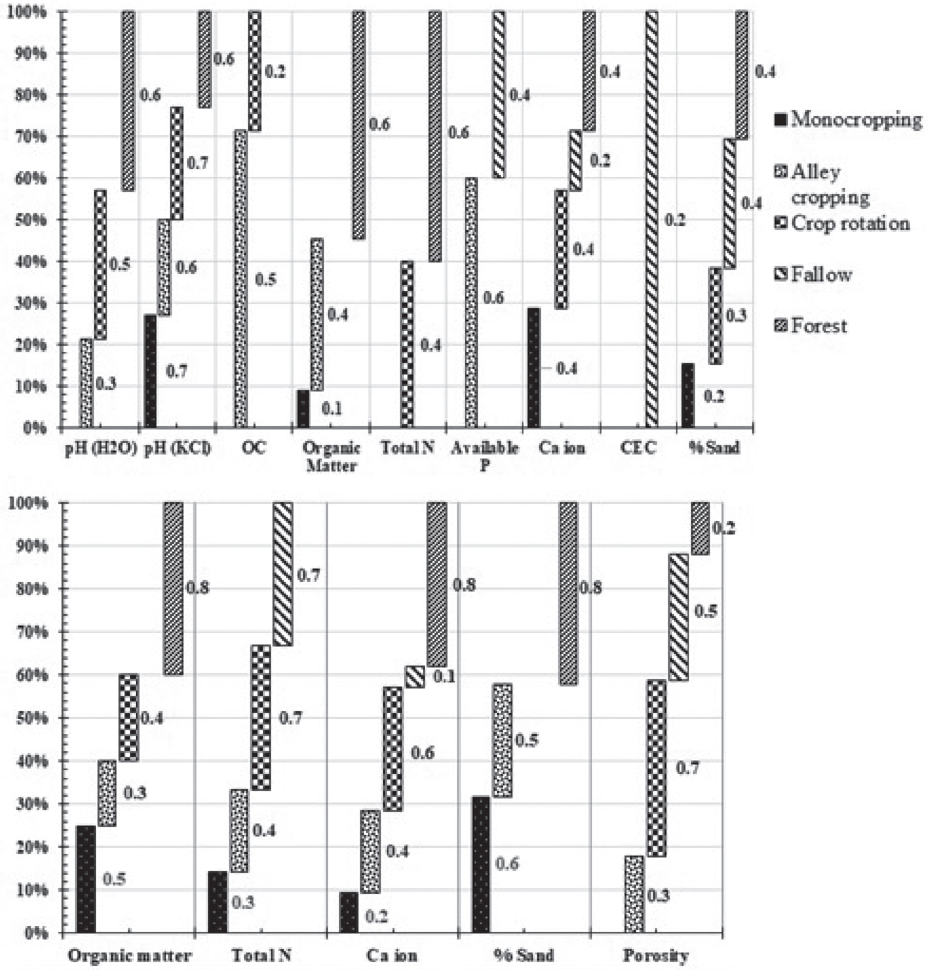

Farming practices	Average		0-15 cm		15 – 30 cm	
	Values	Rank	Values	Rank	Values	Rank
Fallow	1.3	5	1.2	5	1.3	5
Mono-cropping	1.5	4	1.4	4	1.6	3
Crop rotation	2.4	2	2.3	3	2.4	2
Alley cropping	2.2	3	2.4	2	1.9	3
Forest	2.8	1	2.8	1	2.8	1

Fig. 4. Soil quality index (SQI) scores and quality rank of selected farm practices

that the soils in the region, as typical of many tropical African soils, are fragile and requires care (especially for agricultural purposes). The soil attributes may have linked with the geology, which is gneiss – and schist – rich metamorphic rock of the basement complex geology that are characterized by slow weathered and fragile soils (Oyinloye 1998). The parts of the soils in the present study area is in the group of coarse-texture sandy-clay-loam or loamy-sand, and the results of the study showed that about 63%, 47% and 39% of the total nitrogen, organic carbon content and available P, respectively, in the soils were accounted for by the distribution of the organic matter. These results suggest that the soils in the area would benefit from sufficient use of organic matter. Soils with low organic matter contents often exhibit low carbon nitrogen and available P (van Breemen et al. 1983; Blackwell et al. 2010; Awotoye et al. 2011; Marschner 2012). Also, the stock (product of bulk density and concentration per soil depth) of the investigated variables (especially organic carbon, total nitrogen, nitrate and available P) in the soil indicated more deposits of available P and organic matter, and this suggests that the organic matter content contains more available P than organic carbon and total Nitrogen.

In terms of the soil quality, soils under the different farm practices exhibited different level of quality; the lowest rated being Fallow system. Existing studies (e.g. Mendoza-Vega and Messing 2005) have indicated that fallowing practice may have lost its sustainable relevance in the face of increasing urbanization and population-induced pressure on land resources, and as shorter (than the previously known 5-10 years) period of fallow now cause fallow land not to regain full restoration of its fertility. In addition, the second lowly rated practice, mono-cropping has been discouraged in many ecosystems because it is found to be characterized by lesser quantity of soil microbial biomass and soil enzymes than the more effective practices of alley cropping and crop-rotation (Acosta-Martinez et al. 2004; Tian et al. 2005; Liang et al. 2004). Mono-cropping is an important cropping practice in West Africa, and in the present study area, it was a 10-year period of the continuous maize cultivation. In general. forest, alley cropping, and crop rotation practices ranked 1 – 3, in the five practices examined in this study, suggesting that the soils under such practices exhibited quality better than those under fallow and mono-cropping practices. The results of the SQI obtained in this study is in line with the reports from other parts of Nigeria (e.g. Awotoye et al. 2011; Ezeaku. 2011; Ibrahim et al. 2014) that show the soils to be fragile and very reactive to management methods.

Main limitations of this study is the inability of the researchers to access long-term farm records, which studies have argued to be useful for assessing management roles (e.g. Minae et al. 2008; Rothamsted Research 2009; Eludoyin 2013; Eludoyin et al. 2017). The problem of poor historical data is not peculiar to the study area as Minae et al. (2008) argued that farm data systems in many sub-Saharan African countries comprise fragmented and disjointed multi-source that may greatly be subjective. In addition, the procedure for the SQI will be further investigated, especially since it involves some subjective ranking (e.g. categorization into 'less or more is better') (Bremer and Ellert 2004).

CONCLUSION AND RECOMMENDATIONS

The study compared soil properties and quality under five different farm practices in a part of the southwest Nigeria. The results showed disparity among the soils under the farm practices, and based on available records. The study showed that dominant cultivation practice system exacerbated the condition of the already fragile soils in the region. The results of the SQI also indicated that fallow and mono-cropping possessed the lowest quality values among the farm practices system studied. The main hypothesis that soil characteristics and quality vary significantly with farming practices in the area is accepted for this study. The study recommends improved soil management approach for the area, and extensive soil recovery programmes for the already depleted soils, because poor soil may herald difficulty for sustainable food production, given the unsound agricultural technology in many parts of the sub-Saharan Africa.

REFERENCES

Acosta-Martinez V., Zobeck T. M., Allen V. (2004). Soil microbial. chemical and physical properties in continuous cotton and integrated crop-livestock systems. Soil Sci. Soc. Am. J., 68, 1875–1884.

Adesina A. A. and Zinnah M. M. (1993). Technology characteristics, farmers' perceptions and adoption decisions: A Tobit model application in Sierra Leone. Agric. Econ., 9, 4, 297-311.

Andrews S.S., Karlen D.L., Cambardella C.A. (2004). The soil management assessment framework: a quantitative soil quality evaluation method. Soil Science Society of America Journal. 68, 1945–1962.

Andrews S.S., Mitchell J.P., Mancinelli R., Karlen D.L., Hartz T.K., Horwath W.R., Pettygrove G.S., Scow K.M., Munk D.S. (2002). On-farm assessment of soil quality in California's Central Valley. Agronomy Journal. 94, 12–23.

Armenise E., Redmile-Gordon M.A., Stellacci A.M., Ciccarese A., and Rubino P. (2013). Developing a soil quality index to compare soil fitness for agricultural use under different managements in the Mediterranean environment. Soil & Tillage Research, 130, 91–98.

Awotoye O.O., Ogunkunle C.O., and Adeniyi A.S. (2011). Assessment of soil quality under various land use practices in a humid agro-ecological zone of Nigeria. African Journal of Plant Science, 5, 10, 565-569.

Bastida F., Zsolnay A., Hernández T., and García C. (2008). Past, present and future of soil quality indices: A biological perspective. Geoderma, 147, 159–171.

Blackwell M.S.A., Brookes P.C., de la Fuente-Martinez N., Gordon H., Murray P.J., Snars K.E, Williams J.K., Bol R., and Haygarth P.M. (2010). Phosphorus Solubilization and Potential transfer to surface waters from the soil microbial biomass following drying–rewetting and freezing–thawing. In: Sparks, D.L. (Ed.) Advances in Agronomy, 106, 1-35.

Blake G. R. (1965). Bulk density. In: Black, C.A. (Ed.). Methods of Soil Analysis. Am. Soc. Agron, 9, 374-399.

Brady N.C. and Weil R.R. (2008). The nature and properties of soil (14th Ed.). Prentice Hall. Upper Saddle River, N.J., Chapter 4.

Bray H. R. and Kurtz L.T. (1945). Determination of total. organic, and available forms of phosphorus in soils. Soil Sci. 59: 39-45.

Bremer E. and Ellert K. (2004). Soil Quality Indicators: a review with implications for agricultural ecosystems in Alberta, Unpublished report for Alberta Environmentally Sustainable Agriculture Soil Quality Program, Alberta Agriculture, Food and Rural Development, Alberta, Canada, 38p.

Carabias-Martinez R., Rodriguez-Gonzalo E., Fernindez-Laespada M. E., Calvo-Seronero L., Sanchez-San R. F. J. (2003). Evolution over time of the agricultural pollution of waters in an area of Salamanca and Zamora (Spain). Water Research 37, 928-938.

Carlin B. P. and Louis T.A. (2009). Texts in Statistical Science, Bayesian methods for data analysis (3rd Edition). CRC Press, Taylor and Francis Group, USA, 520p.

Daji J. A. (1970). A Textbook of Soil Science. JK Publishers, Bombay India, 380 p.

Department for Environment, Food and Rural Affairs, DEFRA (2007). ECSFDI England Catchment Sensitive Farming Delivery Initiative Technical Services Team. ECSFDI Evaluation. Final Report Department for Environment, Food and Rural Affairs. Available at http://archive.defra.gov.uk/foodfarm/landmanage/water/csf/documents/ecsfdi-phase1-report.pdf, 34p.

Department for Environment, Food and Rural Affairs, DEFRA (2009). Protecting our Water, Soil and Air. A Code of Good Agricultural Practice for farmers, growers and land managers. DEFRA, 124 p.

Donald P. F., Pisano G., Rayment M.D., Pain D.J. (2002). The Common Agricultural Policy, EU enlargement and the conservation of European's farmland birds. Agriculture, Ecosystems & Environment, 89: 167-182.

Doran J.W. and Parkin T.B. (1994). Defining and assessing soil quality. SSSA special publication, 35, 3-3.

Ekanade O. (1991). Degradation of the physical elements of the rural environment resulting from tree crops cultivation in the Nigerian cocoa belt, Singapore Journal of Trop. Geo. 12, 2, 82-94.

Eludoyin A. O. (2013). Modelling the hysteretic patterns of solute concentration-discharge relationships and their significance for hydrological pathways at the farm scale, Doctoral Thesis, University of Exeter, Exeter, United Kingdom. Available at http://hdl.handle.net/10871/15374.

Eludoyin A.O., Griffith B., Orr R., Bol R., Quine T. A. and Brazier R.E. (2017). An evaluation of the hysteresis in chemical concentration-discharge (C-Q) relationships from drained, intensively managed grasslands in Southwest England. Hydrological Sciences Journal–Journal des Sciences Hydrologique, 62, 1243-1254.

European Environment Agency (2003). Europe's environment: the third assessment. Environmental Assessment Report No. 10 European Environment Agency, Copenhagen, 341 p.

Ezeaku P.I. (2011). Soil quality as influenced by land use and management in the southern guinea savanna of Nigeria, Nig. J. Soil & Env. Res., 9, 1-11.

Feder G., Just R. E., and Zilberman D. (1985). Adoption of agricultural innovations in developing countries: A survey. Econ. Dev. & Cult. Cha., 255-298.

Food and Agriculture Organization of the United Nations (FAO) (2005). The importance of soil organic matter. Key to drought-resistant soil and sustained food and production, Food and Agriculture Organization of the United Nations. 95 p.

Food and Agriculture Organization of the United Nations (FAO) (2010). Climate-smart agriculture, The Hague conference on agriculture, food policies, practices and financing for food security, adaptation and mitigation security and climate change, 3 October- 5 November 2010. Available at www.fao.org/climatechange, 48 p.

Gee G. W. and Bauder J. W. (1986). Particle-size analysis, In: Klute A. (Ed). Methods in Soil Analysis, Part 1, Physical and Mineralogical Methods, American Society of Agronomy and Soil Science Society of America, Madison, Wisconsin, USA, 383– 409.

Glanz J. (1995). Saving our soil: solutions for sustaining earth's vital resource. Boulder, USA.

Horsey S. (2006). Case studies aimed at reducing diffuse water pollution from agriculture in England. Department for Environment, Food and Rural Affairs, Water Quality Division: London, available at http://www.adlib.ac.uk/resources/000/245/958/dwpa-report.pdf, 103p.

Ibrahim Y. E., Nuraddeen A. M., and Abubakar A. R. (2014). Factors affecting soil quality maintenance in northern Katsina State, Nigeria. Science World Journal. 9, 4, 39-45.

Jeffery S., Gardi C., Jones A., Montanarella L., Marmo L., Miko L., Ritz K., Peres G., Römbke J., and van der Putten W. H. (Eds.). (2010). European Atlas of Soil Biodiversity. European Commission, Publications Office of the European Union, Luxembourg, 130p.

Kang B. T., Wilson G. F., Sipkens L. (1981). Alley cropping maize (Zea mays L.) and Leucaena (Leucaena leucocephala LAM) in Southern Nigeria. Plant Soil 63, 165–197.

Kiely G. McGoff N, Eaton J., Leahy P., Xu X., and Carton O. (2010). Soil C: Measuring and modeling of soil carbon stocks and stock changes in Iris soils. Environmental Protection Agency, EPA Report Strive Vol. 35, 132p.

Lal R. (1989). Conservation tillage and sustainable agriculture: tropics vs. temperate environment. Adv. Agron. 42, 85-197.

Lal R. (2003). Soil erosion and the global carbon budget. Environment International 29, 437-50.

Lal R. (2005). No-till farming and environment quality. In: Simpósio sobre Plantio direto e Meio ambiente; Seqüestro de carbono e qualidade da agua, pp. 29–37. Anais. Foz do Iguaçu, 18–20.

Lane S. N., Brookes C. J., Heathwaite A. L., Reaney S. M. (2006). Surveillant science: challenges for the management of rural environments emerging from the new generation diffuse pollution models. Journal of Agricultural Economics, 57: 239–257.

Lavelle P., Barros E. and Blanchart E. (2001). SOM Management in the Tropics: Why Feeding the Soil Macrofauna? Nutrient Cycling in Agroecosystems, 61, 1-2, 53–61.

Liebig M. A., Tanaka D. L., Wienhold B. J. (2004). Tillage and cropping effects on soil quality indicators in the northern Great Plains. Soil Till. Res., 78, 131–141.

Luoga E. J. (2000). Subsistence use of wood products and shifting cultivation within Miombo woodland of eastern Tanzania, with special notes on commercial uses. South African Journal of Botany 66, 72-85.

Malhi S.S., Grant C.A., Johnston A.M., Gill K.S. (2001). Nitrogen fertilization management for no-till cereal production in the Canadian Great Plains: A review. Soil Till. Res., 60, 101–122.

Marschner H. (2012). Marschner's mineral nutrition of higher plants. Academic press, San Diego, USA. 672 p.

Mclean E. O. (1965). Aluminum In: Black C.A. (Ed.). Methods of soil analysis, Part II. Am. Soc. Agron., Madison, Wisconsin. USA No. 9, 978-998.

Mendoza-Vega J. and Messing I. (2005). The influence of land use and fallow period on the properties of two calcareous soils in the humid tropics of southern Mexico. Catena, 60, 3, 279-292.

Mestdagh I., Lootens P., Cleemput V.E., and Carlier L. (2008). Variation in organic-carbon concentration and bulk density in Flemish grassland soils. J. Plant Nutr. Soil Sci. 169, 616–622.

Minae S., Baker D. and Dixon J. (2008). Status of farm data systems and farmer decision support in sub-Saharan Africa, FAO, Rome.

Motsara M. and Roy R. N. (2008). Guide to laboratory establishment for plant nutrient analysis Food and Agriculture Organization of the United Nations.

Mukherjee A and Lal R. (2014). Comparison of soil quality index using three methods. Plos One 9, 8, 1-15.

Oenema O., Janssen B. H., Smaling E., and Hoffland E. (2006). Nutrient management in tropical agroecosystems. Editorial. Agriculture, Ecosystems and Environment 116, 1–3.

Oyedele D. J., Awotoye O. O. and Popoola S. E. (2009). Soil physical and chemical properties under continuous maize cultivation as influenced by hedgerow trees species on an alfisol in South Western Nigeria. African Journal of Agricultural Research, 4, 7, 736-739.

Oyinloye A.O. (1998). Geology, geochemistry and origin of the banded and granite gneisses in the basement complex of the Ilesha area, southwestern Nigeria. Journal of African Earth Sciences 28 (4): 633 – 641.

Page A. L., Miller R. H., Keeney D. R. (1986). Methods of Soil Analysis. Part 2. Chemical and Microbial Properties, 2nd ed., Agron. Monog. 9. ASA and SSSA, Madison, WI.

Rothamsted Research (2009). Long-term Experiments: Guide to the classical and other long-term experiments, datasets and sample archive. Lawes Agricultural Trust, Rothamsted Research, Harpenden, UK, 52 p.

Scholes M. C., Swift M. J., Heal O.W., Sanchez P. A., Ingram J. S. I., and Dalal R. C. (1994). Soil Fertility Research in Response to the Demand for Sustainability. In: Woomer P. L., Swift M. J. (Eds.). The Biological Management of Tropical Soil Fertility. Wiley, Chichester, 1-14.

Technicon Instrument Corporation (1971). Nitrate and Nitrite in Water, Industrial Method No. 32– 69W. Technicon Instrument Corporation, Tarrytown, New York, USA.

Throop H. L., Archer S. R., Monger H. C., Waltman S. (2012). When bulk density methods matter: implications for estimating soil organic carbon pools in rocky soils. Journal of Arid Environments 77, 66-71.

Tian G., Kang B. T., Kolawole G. O., Idinoba P. and Salako F. K. (2005). Long-term effects of fallow systems and lengths on crop production and soil fertility maintenance in West Africa. Nutr. Cycl. Agroecosyst. 71, 139-150.

Tilman D., Cassman K. G., Matson P. A., Naylor R., Polasky S. (2002). Agricultural sustainability and intensive production practices. Nature 418, 671–677.

Uehara G. and Gillman G. (1981). The mineralogy, chemistry, and physics of tropical soils with variable charge clays. Westview Press, Boulder, Colorado, USA.

van Breemen N., Mulder J., and Driscoll C. T. (1983). Acidification and alkalinization of soils. Plant and soil, 75, 3, 283-308.

Verachtert E., Govaerts B., Lichter K., Sayre K. D., Ceballos-Ramirez J. M., Luna- Guido M. L., Deckers J., and Dendooven L. (2009). Short term changes in dynamics of C and N in soil when crops are cultivated on permanent raised beds, Plant Soil 320, 281–293.

Vijith H., Suma M., Rekha V. B., Shiju C., Rejith P. G. (2012). An assessment of soil erosion probability and erosion rate in a tropical mountainous watershed using remote sensing and GIS. Arab J Geosci, 5, 797–805.

Walkley A. and Black I. A. (1934). An Examination of the Degtjareff method for determining soil organic matter and a proposed modification of the chromic acid titration method. Soil Sci., 37, 29-38.

Wienhold B. J., Andrews S. S., and Karlen D. L. (2004). Soil Quality: A review of the science and experiences in the USA. Environ. Geochem. Hlth. 26: 89-95.

Withers P. J. and Lord E. I. (2002). Agricultural nutrient inputs to rivers and groundwater in the UK: policy, environmental management and research needs. Science of the Total Environment 282, 9-24.

Wymore A.W. (1993). Model-based systems engineering: an introduction to the mathematical theory of discrete systems and to the tricotyledon theory of system design. CRC Press, Inc., Boca Raton, FL.

Yoo G. Y., Nissen T. M., and Wander M. M. (2006). Use of physical properties to predict the effects of tillage practices on organic matter dynamics in three Illinois soils. J. Environ. Qual. 35:1576-1583.

Received on October 27th, 2017 Accepted on July 31st, 2018

FIRST/CORRESPONDING AUTHOR

Dr. Adebayo Oluwole Eludoyin is a Senior Lecturer in Ecohydrology at the Department of Geography, Obafemi Awolowo University, Ile-Ife. Nigeria. His doctoral research was on hydrological pathways at farm-scale at the Rothamsted Research North Wyke was awarded by the University of Exeter, Devon, United Kingdom in 2014. He possesses degrees in the areas of Geography, Geographic Information Systems as well as in Environmental Control and Management. His researches are generally into the interdisciplinary field studying the interactions between water and ecosystems, including the effects of such interactions on streams, atmosphere and land.

AUTHOR GUIDELINES

1. Authors are encouraged to submit high-quality, original work: scientific papers according to the scope of the Journal. reviews (only solicited) and brief articles.

2. Papers are accepted in English. Either British or American English spelling and punctuation may be used.

3. All authors of an article are asked to indicate their names (with one forename in full for each author, other forenames being given as initials followed by the surname) and the name and full postal address (including postal code) of the affiliation where the work was done. If there is more than one institution involved in the work, authors' names should be linked to the appropriate institutions by the use of 1, 2, 3 etc superscript. Telephone and fax numbers and e-mail addresses of the authors could be published as well. One author should be identified as a Corresponding Author. The e-mail address of the corresponding author will be published, unless requested otherwise.

EXAMPLE:

Ivan I. Ivanov[1], **Anton A. Petrov**[1*], **David H. Smith**[2]
[1]University/Organization name, Street, City, ZIP-code, Country
[2]University/Organization name, Street, City, ZIP-code, Country
*** Corresponding author:** example@example.com

4. The GES Journal style is to include information about the author(s) of an article. Therefore we encourage the authors to submit their portrait photos and short CVs (up to 100 words).

5. Article structure should contain further sections:
   - Abstract.
   - Keywords (Immediately after the abstract, provide a maximum of 6 keywords, avoiding general and plural terms and multiple concepts (avoid, for example, 'and', 'of'). Be sparing with abbreviations: only abbreviations firmly established in the field may be eligible. These keywords will be used for indexing purposes.).
   - Introduction (State the objectives of the work and provide an adequate background, avoiding a detailed literature survey or a summary of the results.).
   - Material and methods (Provide sufficient details to allow the work to be reproduced by an independent researcher. Methods that are already published should be summarized, and indicated by a reference. If quoting directly from a previously published method, use quotation marks and also cite the source. Any modifications to existing methods should also be described.
   - Results (Results should be clear and concise.).
   - Discussion (This should explore the significance of the results of the work, not repeat them. A combined Results and Discussion section is often appropriate. Avoid extensive citations and discussion of published literature.).
   - Conclusions (The main conclusions of the study may be presented in a short Conclusions section, which may stand alone or form a subsection of a Discussion or Results and Discussion section.).
   - Acknowledgements (List here those individuals who provided help during the research and funds which provided financial support of your research.).
   - References (Make a list of references according to guidance provided below).
   - Appendices (If there is more than one appendix, they should be identified as A, B, etc.

Formulae and equations in appendices should be given separate numbering: Eq. (A.1), Eq. (A.2), etc.; in a subsequent appendix, Eq. (B.1) and so on. Similarly for tables and figures: Table A.1; Fig. A.1, etc.).

6. Sections and sub-sections shouldn't be numbered, but divided into sub-levels. If you would like to refer to a particular section, name it without any numbers (for example: see "Materials and methods")

7. Math equations should be submitted as editable text and not as images (use appropriate tool in text editor). Present simple formulae in line with normal text where possible and use the solidus (/) instead of a horizontal line for small fractional terms, e.g., X/Y. In principle, variables are to be presented in italics. Number consecutively any equations that have to be displayed separately from the text (if referred to explicitly in the text).

8. Figures and figure captions. Number the illustrations according to their sequence in the text. Regardless of the application used, when your figure is finalized, please 'save as' or convert the images to one of the following formats: TIFF, JPG. Supply files that are optimized for screen use. **The resolution should be at least 300 dpi**. Besides inserting figures into your manuscript, you must also upload appropriate files during paper submission. Ensure that each illustration has a caption. A caption should comprise a brief title (not on the figure itself) and a description of the illustration beginning from "Fig. 1…" (note: no any dots in the end of the capture!). Keep text in the illustrations themselves to a minimum but explain all symbols and abbreviations used.

Example of referring to the figure in text: (Fig. 1)
Example of figure caption: Fig. 1. The distribution of the family Monimiaceae

9. Tables. Please submit tables as editable text and not as images. Tables can be placed either next to the relevant text in the article, or on separate page(s) at the end. Number tables consecutively in accordance with their appearance in the text, place table caption above the table body and place any table notes below the body. Be sparing in the use of tables and ensure that the data presented in them do not duplicate results described elsewhere in the article. Please avoid using vertical rules and shading in table cells.

Example of table caption: Table 1. Case studies and used methods

10. The optimum size of a manuscript is about 3,000–5,000 words. Under the decision (or request) of the Editorial Board methodological and problem articles or reviews up to 8,000–10,000 words long can be accepted.

11. To facilitate the editorial assessment and reviewing process authors should submit "full" electronic version of their manuscript with embedded figures of "screen" quality as a PDF or DOC file.

12. We encourage authors to list three potential expert reviewers in their field. The Editorial Board will view these names as suggestions only.

13. Original reviews of submitted manuscripts remain deposited for 3 years.

SCIENTIFIC AND PRACTICAL PEER-REVIEWED JOURNAL "GEOGRAPHY, ENVIRONMENT, SUSTAINABILITY"

No. 03 (v. 11) 2018

FOUNDERS OF THE MAGAZINE: Russian Geographical Society, Faculty of Geography, Lomonosov Moscow State University and Institute of Geography of the Russian Academy of Sciences

The magazine is published with financial support of the Russian Geographical Society.

The magazine is registered in Federal service on supervision of observance of the legislation in sphere of mass communications and protection of a cultural heritage. The certificate of registration: ПИ № ФС77-67752, 2016, December 21.

PUBLISHER
Russian Geographical Society
Moscow, 109012 Russia
Novaya ploshchad, 10, korp. 2
Phone 8-800-700-18-45
E-mail: press@rgo.ru
www.rgo.ru/en

EDITORIAL OFFICE
Lomonosov Moscow State University
Moscow 119991 Russia
Leninskie Gory,
Faculty of Geography, 1806a
Phone 7-495-9391552
Fax 7-495-9391552
E-mail: ges-journal@geogr.msu.ru
www.ges.rgo.ru

DESIGN & PRINTING
Agency «CONNECT»
Moscow, 117452,
Artekovskaya str., 9, korp. 1
Phone: +7 (495) 955-91-53
E-mail: info@connect-adv.ru

Sent into print 28.09.2018
Order N gi318

Format 70 ½ 100 cm/16
11,4 p. sh.
Digital print
Circulation 130 ex.